ISTANBUL TECHNICAL UNIVERSITY ★ GRADUATE SCHOOL OF SCIENCE ENGINEERING AND TECHNOLOGY

DONOR AND ACCEPTOR CONTAINING MONOMERS

M.Sc. THESIS

Damla GÜLFİDAN

Department of Polymer Science and Technology

Polymer Science and Technology Programme

JANUARY 2012

ISTANBUL TECHNICAL UNIVERSITY ★ GRADUATE SCHOOL OF SCIENCE ENGINEERING AND TECHNOLOGY

DONOR AND ACCEPTOR CONTAINING MONOMERS

M.Sc. THESIS

Damla GÜLFİDAN
515091026

Department of Polymer Science and Technology

Polymer Science and Technology Programme

Thesis Advisor: Prof.Dr. Metin Hayri ACAR

JANUARY 2012

İSTANBUL TEKNİK ÜNİVERSİTESİ ★ FEN BİLİMLERİ ENSTİTÜSÜ

DONÖR VE AKSEPTÖR İÇEREN MONOMERLER

YÜKSEK LİSANS TEZİ

Damla GÜLFİDAN
515091026

Polimer Bilim ve Teknolojisi Anabilim Dalı

Polimer Bilim ve Teknolojisi Programı

Tez Danışmanı: Prof.Dr. Metin Hayri ACAR

OCAK 2012

Damla Gülfidan, a **M.Sc.** student of ITU **Institute of / Graduate School of Science and Technology** student ID **515091026**, successfully defended the **thesis** entitled "**DONOR AND ACCEPTOR CONTAINING MONOMERS**", which she prepared after fulfilling the requirements specified in the associated legislations, before the jury whose signatures are below.

Thesis Advisor :	**Prof.Dr. Metin Hayri ACAR** İstanbul Technical University	.....
Jury Members :	**Prof. Dr. H.Ayşen Önen** İstanbul Technical University	.....
	Prof. Dr. Yusuf Menceloğlu Sabancı University	.....

Date of Submission : 19 December 2011
Date of Defense : 25 January 2012

To my family,

FOREWORD

First, I would like to thank my advisor, Professor Metin Hayri ACAR. When I came to ITU, I did not know about research. I learned every things through Professor Acar. He gave me the encourage in my worry times by saying me "Research is very long process". He taught me how it should be a good researcher. He has supported me all the time. I am grateful to him for his patience and his support. I am sure that I will miss to make discussion about science and life with him.

I would also thank to Assoc. Prof. Sermet Koyuncu for his advices, supports during my thesis and interpretation for results of optical measurements; and I also would like to thank Emre Sefer for synthesizing of acceptor monomer and optical measurements of (co)polymers.

I would like to thank my past and current laboratory group members for all their help, support and excellent friendship. Especially, Dr. Şebnem İnceoğlu, Hamza Kocatürk, Candan Çatlı, Evrim Büyükaslan, Ari Şant Bilal, Atılay Tuzer, Cüneyt Erdinç Taş and Mehmet Başdal.

In addition that I also thank to neighboring the laboratory members Dr. Aydan Dağ, Dr. Hakan Durmaz, Aslı Çapan, İpek Ösken, Timuçin Balkan and Uğur Nazif Kaya for their help and friendship.

I am very lucky to have the world's best family. I want to thank to my mother Nalan Gülfidan, my grandfather Mehmet Ziya Gülfidan and my sister Yağmur Gülfidan for their moral support and encouragement during my education. Especially I owe all my life to my grandfather and my grandmother who died. I am grateful them for everything.

Finally, I would like to thank my private friend Abidin Danış for endless patience, his excellent understanding and importantly for moral support. It is a great feeling to know that he is always with me.

This work was supported by ITU graduate school of science engineering and technology.

December 2011

Damla GÜLFİDAN
Chemist

TABLE OF CONTENTS

Page

ABBREVIATIONS

I	**:** 6-bromo-2-(2-ethylhexyl)-1-H-benzo[de]isoquinoline 1,3(2H)-dione
II	**:** 2-(2-ethylhexyl)-6-((2-hydroxyethyl)(methyl)amino)-1H-benzo [de]isoquinoline-1,3(2H)-dione
A	**:** Acceptor
AIBN	**:** 2,2′-Azobis(isobutyronitrile)
AM	**:** 2-((2-(2-ethylhexyl)-1,3-dioxo-2,3-dihydro-1H-benzo[de]iso quinolin-6-yl)(methyl)amino)ethyl acrylate
ATRP	**:** Atom transfer radical polymerization
CEA	**:** 2-(9H-carbazol-9-yl)ethyl acrylate
CMS	**:** 4-Vinyl benzyl chloride
CV	**:** Cyclic voltammetry
CzMS	**:** 4-(9-Carbazolyl) methylstyrene
D	**:** Donor
DCM	**:** Dichloromethane
DMF	**:** Dimethyl formamide
DSC	**:** Differential scanning calorimeter
FT-IR	**:** Fourier transform infrared spectroscopy
GPC	**:** Gel permation chromatography
HEC	**:** N-(2′-hydroxyethyl) carbazole
HOMO	**:** Highest Occupied Molecular Orbitals
KOH	**:** Potassium hydroxide
LUMO	**:** Lowest Unoccupied Molecular Orbitals
MeOH	**:** Methanol
NMR	**:** Nuclear magnetic resonance
NVK	**:** N-Vinylcarbazole
OLED	**:** Organic light-emitting diodes
PAM	**:** Acceptor polymer
PCEA	**:** Poly(2-(9H-carbazol-9-yl)ethylacrylate)
PCzMS	**:** Poly(4-(9-carbazolyl)methylstyrene)
PDI	**:** Poly dispersity index
PVBEC	**:** Poly(9-(2-(4-vinylbenzyloxy)ethyl)-9H-carbazole)
TEA	**:** Triethyl amine
T_g	**:** Glass transition temperature
THF	**:** Tetrahydrofuran
VBEC	**:** 9-(2-(4-Vinylbenzyloxy)ethyl)-9H-carbazole

LIST OF TABLES

Page

LIST OF FIGURES

Page

DONOR AND ACCEPTOR MONOMERS

SUMMARY

In recent years, energy consumption has been one of the world's problems with the increased of global warming. The world is dependent on the electricity which are produced by the decreased water sources because of the effect of global warming. Hence, energy saving has been raised. Researches to reduce the consumption of the electricity is increasing day by day.

Especially the most of the consumed electricity is a known fact that to be used in lighting and visually (television and bulbs) so production of materials that as well as showing good fluorescence properties and consuming less energy-efficient has become a target of researchers.

The purpose of this thesis that to investigate effect of composition, a good electron transfer properties of copolymers of acceptor and donor monomer in different side chain lengths. Based on these reasons, carbazole and napthlamide side chain containing styrenic and acrylate type monomers with different chain lengths (CzMS, CEA, VBEC, AM) were synthesized according to the literature. Homopolymers of CzMS, CEA, VBEC and AM and also copolymers of AM with CzMS and VBEC were synthesized via free radical polymerization, characterized by ^{1}H NMR, FT-IR, DSC, GPC.

To determined the effect of spacer, electrochemical and optic properties of homopolymers and copolymers were investigated. The energy transfer from donor moiety (carbazole) to acceptor part (napthalimide) on the copolymer structure (poly(VBEC-*r*-AM)) was proved with the all exitations and the band intensifications. The electrochemical and optical HOMO-LUMO band gaps of all the polymers were calculated from the onset of the oxidation/reduction potentials and absorption values, respectively.

The obtained polymers were crosslinked via electropolymerization which posses to forming a good film and were investigated their optical properties by CV, UV-Vis

and fluorescence spectrophotometers. Although carbazol containing polymers were shown similar electrochemical and optical properties, all the electrochromic parameters (i.e. response time, contrast change…) were effected by the differentiated to the spacer groups between carbazole-electroactive moiety and polymer chain.

DONÖR VE AKSEPTÖR MONOMERLER

ÖZET

Son yıllarda küresel ısınmanın artması ve yenilenemeyen enerji kaynaklarının (fosil yakıtlar) kısıtlı, maliyetli olması nedeniyle, enerji tüketimi dünyanın başlıca sorunlarından biri haline gelmiştir. Küresel ısınmanın tehlikeli sonuçlara yol açmasını önlemek için sıcaklık ortalamalarının iki dereceden fazla artmaması gerektiğinin vurgulandığı son zamanlarda, yenilenemeyen enerji kaynaklarının aşırı tüketiminin bir sonucu olarak, CO_2 salınımı artışından dolayı sera etkisi gün geçtikçe artmakta ve küresel ısınmayı tetiklemektedir. Fosil yakıtların çoğunun çevreyi kirlettiği de göz önüne alındığında, hem küresel ısınmanın etkilerini azaltmak hem de çevreyi kirleten yenilenemeyen enerji kaynaklarına alternatif enerji kaynağı üretebilmek için dünyada birçok çalışma yapılmaktadır. Yenilenebilir temiz enerji teknolojileri ve enerji tüketimini azaltmaya yönelik çalışmalar bu anlamda ön plana çıkmaktadır.

Güneş, yenilenebilir ve en önemlisi de hiç bir bedel ödenmeden ulaşılabilen sınırsız bir enerji kaynağı olduğundan; yenilenebilir temiz enerji rönesansından bahsedilen son zamanlarda, güneş ışığından elektrik enerjisi üreten fotovoltaik adı verilen teknoloji, gün geçtikçe araştırmacıların ilgisini daha da çok çekmektedir. Özellikle fotovoltaik paneller ve güneş pilleri bu konuda değer kazanmaktadır.

Dünyanın bağımlı olduğu elektriğin bir kısmının, küresel ısınma nedeniyle azalan su kaynaklarından elde edildiği düşünüldüğünde, enerji tasarrufunun da temiz enerji gibi küresel ısınmayı azaltacağı fikri savunulmaktadır. Bu bağlamda, tüketilen elektriğin aydınlatma ve görsellikte daha çok kullanıldığı göz önüne alındığında, hem daha az enerji tüketen hem de iyi floresans özellik gösteren tasarruflu malzemeleri üretmek, araştırmacıların hedefi haline gelmiştir.

Elektronik sistemlerdeki düşük enerji tüketimine yönelik çalışmalar, özellikle organik ışık yayan diyotlar (OLED) konusunda yoğunlaşmıştır. OLED'ler, geleneksel cihazlara göre; düşük enerji tüketimi, yüksek parlaklık ve kontrast, hızlı

cevap zamanı, geniş görüş açısı ve hafiflik gibi bir çok üstün özelliğe sahiptir. Tris(8-quinolinolato)aluminum (Alq3) yapısına dayalı ilk yüksek verimli, organik ışık yayan cihazların (OLED) 1987 yılında Tang ile Van Slyke tarafından, polimere dayalı elektrolüminesans cihazların ise 1990 yılında Burroughes ve grubu tarafından ispatlanmasından bu yana, OLED konusundaki çalışmalar hız kazanmıştır.

İlk çalışmalar ana zincirde konjuge olan polimerlere dayalı başlamıştır. Konjuge yapıların gösterdiği çözünmeme problemi, konjuge yapıya alkil gruplarının yan zincir olarak eklenmesiyle çözülmüş olsa da, buna alternatif olarak düşünülen ana zincirde konjuge olmayan yapılarla ilgili çalışmalar da gün geçtikçe artmaktadır. Bunun yanında OLED yapısında kullanılan malzemelerin çok tabakalı olması da karışıklığa sebep olmakta ve cihaz üretim maliyetini artırmaktadır. Bu sebepten dolayı, OLED de kullanılacak malzemelerin organik çözücülerde çözülebilen, kolay işlenebilir, yüksek verimli, tek katmanlı özellik göstermesi istenmektedir. Özellikle yan zincirlerinde birbirleriyle etkin bir biçimde etkileşebilecek donor ve akseptör grup içeren polimerler önem kazanmaktadır. Bu etkileşimlerin etkin bir biçimde oluşması için donör ve akseptör grubun polimer zinciri üzerindeki tekrarlanma oranları, birbirine ve ana zincire uzaklığı önemlidir.

Bu çalışmanın amacı; farklı zincir uzunluklarına sahip donör ve akseptör monomerlerinden oluşturulan kopolimerlerin, düşük enerji tüketimiyle iyi elektron transferi vermesini sağlamaktır. Bu konudan yola çıkarak; farklı zincir uzunluklarında, yan zincirinde karbazol ve naftalimit içeren stirene ve akrilata dayalı donör monomerler (CzMS, CEA, VBEC) ve akseptör monomer (AM) literatüre uygun olarak sentezlenmiştir. Sentezlenen monomerler ve bu monomerlerin radikal polimerizasyon yöntemi ile oluşturulan homopolimerleri (PCzMS, PCEA, PVBEC, PAM) ve kopolimerleri (poly(CzMS-*r*-AM) and poly(VBEC-*r*-AM)) enstrümental cihazlarla (^{1}H NMR, FT-IR, DSC, GPC) analiz edilmiştir. Farklı zincir uzunluklarında sentezlenen donör monomerlerin zincir uzunluklarının, maddenin optik özelliğine etkisi incelenmiştir. Sentezlenen monomerler içinde kısa ara zincir uzunluğuna sahip monomer (CzMS) ve uzun ara zincir uzunluğuna sahip monomer (VBEC), akseptör ile kopolimerleştirilmiş (sırasıyla poly(CzMS-*r*-AM) ve poly(VBEC-*r*-AM) olmak üzere) ve elde edilen kopolimerlerin optik özellikleri incelenmiştir. Homopolimer ve kopolimerlerin elektronik ve optik enerji band aralıkları bulunmuştur.

Poly(VBEC-*r*-AM)'in enerji transfer yeteneği araştırılmış, donör gruptan (karbazol) akseptör gruba (naftalimit) enerji aktarıldığı, şiddetlenen floresans bandıyla kanıtlanmıştır.

Homopolimerlerin elektropolimerizasyon yöntemi ile oluşturulan, iyi film oluşturma özelliğine sahip olan çapraz bağlı polimerlerinin optik özellikleri CV, UV-Vis ve floresans spektroskopileri ile incelenmiştir.

Karbazol içeren donör polimerlerin elektrokromik ve optik özellikleri aynı olsa da, elektrokromik parametrelerinin (cevap verme süresi, kontrast değişimi vb.) ara zincir uzunluğuna bağlı olarak farklı olduğu görülmüştür.

1. INTRODUCTION

Today, fossil fuels are running out and are held responsible for the global warming because of the increased concentration of carbon dioxide in the earth's atmosphere. Therefore, developing environmentally friendly, renewable energy is one of the important part in the 21st century. Accordingly, electronic systems running on low energy consumption are highly important. The reduction of energy consumption besides the cheap power generation is another important parameter. In general, although light emitting diode (LED), which is made from inorganic materials and can produce light with a very low amount of energy, had been used for many years, LED production from organic materials (OLED) only started in 1990 and studies on this technology is still being carried out.

An increasing number of polymers is being reported that were used in OLED, electroluminescence devices. Mainly, these polymers can be divided two groups as conjugated and non-conjugated polymers. In addition that, this polymers can be contain donor-acceptor groups in main chain or side chain. This polymers posses lots of advantage and disadvantage.

The conjugated backbone presents problems for synthesis and processing because of rigidity and dissolubility of polymers. This problems were be overcoming with two main approaches. The first is to form a non-conjugated precursor polymer, which can be processed and then converted in situ to the conjugated polymer (which is normally insoluble). The second is to make a conjugated polymer that is soluble by the addition of lipophilic soluble linkers or side groups. There are different advantages and disadvantages of the two approaches. A disadvantage of precursor route polymers is that there is some proof that by-products from the conversion from precursor to conjugated polymer can damage electrodes. The insoluble polymers are generally more difficult to prepare than their soluble counterparts as there are limited routes for the synthesis. In contrast, soluble conjugated polymers are relatively easy to prepare. The advantage of such materials is that they often are highly luminescent, can be prepared via a number of different synthetic routes, and easily processed.

Today, the principle of all the photo-electronic products is based on electron transfer process between the multi-layer systems. The material used in the active layer is very important in photo-electronic systems. Therefore, in contrast to inorganic materials, the use of organic materials is gradually increasing due to such advantages as flexibility, aesthetical look and ductility. In addition, organic layers used in the photo-electronic systems are composed of 2 or 3 layers, which are extremely disadvantageous for electron transfer because they are covered as layer by layer. One of the disadvantages is that it can be more difficult to prepare multilayer devices by solution processing. On the other hand, the need for more than one layer in a device obviously increases the complexity and cost of device manufacture.

Polymers which containing donor-acceptor moities were important for OLED and electroluminescence devices. There are some polymer types which used in this area such as: conjugated donor-acceptor structures (D-A-D-A), in main donor chain bearing acceptor group, polymers which containg side chain donor and acceptor group (copolymers) and in main chain which bear donor-bridge-acceptor moities. Polymers which containing side chain donor and acceptor group have the most changeable properties in these polymer types (Figure 1.1). The other polymer types possess some disadvantages:

Conjugated donor-acceptor polymers show good luminescence properties, but their donor/acceptor composition was not changed unless monomers were not be changed.

In main donor chain bearing acceptor group polymers, in main chain donor groups is always same but only composition of acceptor groups can be changed.

Polymers which bear donor-bridge-acceptor side chain posses a disadvantage, too. Their chain lenght of donor/acceptor moities can not be changed but only the composition was changed.

In contrast to, such parameters, as donor/acceptor (D/A) composition, chain length of polymers which containg side chain donor and acceptor group (copolymers, Figure 1.1) can be changed in order to realize electron transfer on a single layer and with high efficiency by preparing (co)polymers with different chain length, different chain hierarchy.

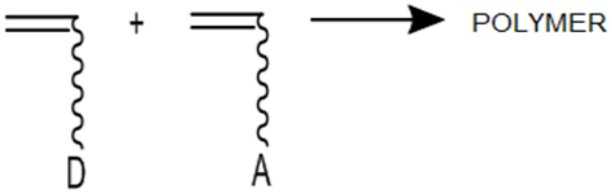

Figure 1.1 : Illustration of copolymers which containg side chain donor and acceptor group.

Based on these reasons, donor and acceptor containing styrenic and acrylate type monomers with different chain lengths were synthesized and characterized. After characterization of obtained polymer and copolymer by free radical polymerization, especially, spacer effect in the monomer and donor/acceptor composition in the copolymer were investigated.

2. THEORETICAL PART

Nowadays, researches are focused on low energy consumption and renewable energy. One of the subject is renewable energy technologies which is photovoltaics (PV), the technology that directly converts daylight into electricity. One of the other subject is the low energy consumption which is important for electronics devices. Especially, an increasing number of polymers which were used in OLED were attractted attention. Some of the synthesized polymers include conjugated or non-congugated backbone which are contained donor and acceptor group as main chain or side chain. Between the effect of donor and acceptor moities are dependent on energy transfer.

2.1 Energy Transfer in Donor-Acceptor Molecule

An electronic transition consists of the promotion of an electron from an orbital of a molecule in the ground state to an unoccupied orbital by absorption of a photon [1]. The molecule is then said to be in an excited state. A σ orbital can be formed either from two s atomic orbitals, or from one s and one p atomic orbital, or from two p atomic orbitals having a collinear axis of symmetry. The bond formed in this way is called a σ bond. A π orbital is formed from two p atomic orbitals overlapping laterally. The resulting bond is called a π bond. Absorption of a photon of appropriate energy can promote one of the π electrons to an antibonding orbital denoted by π*. The transition is then called $\pi \rightarrow \pi^*$. The promotion of a σ electron requires a much higher energy (absorption in the far UV). A molecule may also possess non-bonding electrons located on heteroatoms such as oxygen or nitrogen. The corresponding molecular orbitals are called n orbitals. Promotion of a non-bonding electron to an antibonding orbital is possible and the associated transition is denoted by $n \rightarrow \pi^*$.

The energy of these electronic transitions is generally in the following order:

$$n \rightarrow \pi^* < \pi \rightarrow \pi^* < n \rightarrow \sigma^* < \sigma \rightarrow \pi^* < \sigma \rightarrow \sigma^*$$

To illustrate these energy levels, Figure 2.1 shows formaldehyde as an example, with all the possible transitions. In absorption and fluorescence spectroscopy, two important types of orbitals are considered: the Highest Occupied Molecular Orbitals (HOMO) and the Lowest Unoccupied Molecular Orbitals (LUMO). Both of these refer to the ground state of the molecule. For instance, in formaldehyde, the HOMO is the n orbital and the LUMO is the π^*orbital (Figure 2.1)

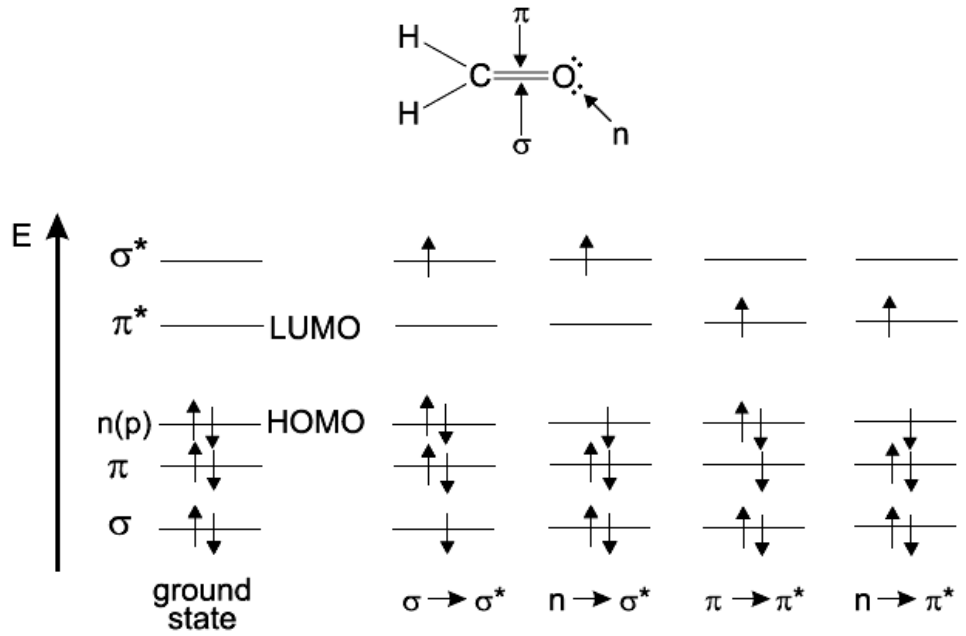

Figure 2.1 : Energy levels of molecular orbitals in formaldehyde (HOMO: Highest Occupied Molecular Orbitals; LUMO: Lowest Unoccupied Molecular Orbitals) and possible electronic transitions.

When one of the two electrons of opposite spins (belonging to a molecular orbital of a molecule in the ground state) is promoted to a molecular orbital of higher energy, its spin is in principle unchanged so that the total spin quantum number remains equal to zero. Because the multiplicities of both the ground and excited states (M = 2S+1) is equal to 1, both are called singlet state (usually denoted S_o for the ground state, and S_1, S_2, ... for the excited states) (Figure 2.2). The corresponding transition is called a singlet–singlet transition. A molecule in a singlet excited state may undergo conversion into a state where the promoted electron has changed its spin; because there are then two electrons with parallel spins, the total spin quantum number is 1 and the multiplicity is 3. Such a state is called a triplet state because it corresponds to three states of equal energy.

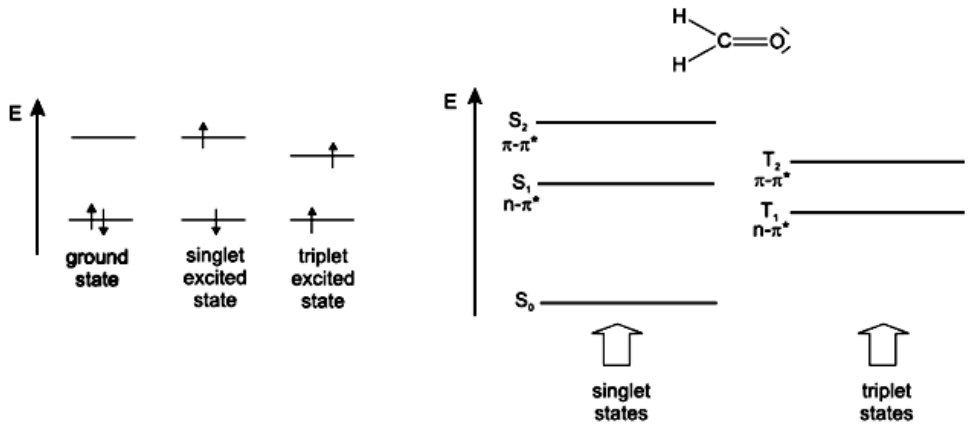

Figure 2.2 : Distinction between singlet and triplet states, using formaldehyde as an example.

The Perrin–Jablonski diagram (Figure 2.3) is convenient for visualizing in a simple way the possible processes: photon absorption, internal conversion, fluorescence, intersystem crossing, phosphorescence, delayed fluorescence and triplet–triplet transitions. The singlet electronic states are denoted S_o (fundamental electronic state), S_1, S_2, ... and the triplet states, T_1, T_2, ... Vibrational levels are associated with each electronic state. It is important to note that absorption is very fast ($\approx 10^{-15}$ s) with respect to all other processes. The vertical arrows corresponding to absorption start from the 0 (lowest) vibrational energy level of S_o because the majority of molecules are in this level at room temperature. Absorption of a photon can bring a molecule to one of the vibrational levels of S_1, S_2 and so on.

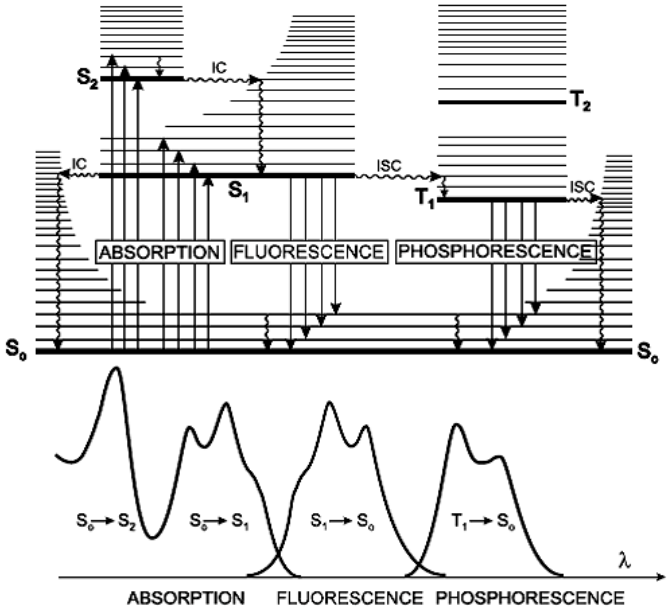

Figure 2.3 : Perrin–Jablonski diagram and illustration of the relative positions of absorption, fluorescence and phosphorescence spectra from references [1].

All photochemical and photophysical processes are initiated by the absorption of a photon of visible or ultraviolet radiation leading to the formation of an electronically-excited state [2].

$$R + h\nu \rightarrow R^* \qquad \textbf{(2.1)}$$

Electronically-excited states of molecules are endowed with excess energy due to their formation by photon absorption. These excited states are short-lived, losing their excess energy within a very short period of time through a variety of deactivation processes and returning to a ground-state configuration. If the excited molecule returns to its original ground state then the dissipative process is a physical process, but if a new molecular species is formed then the dissipative process is accompanied by chemical change.

Physical relaxation processes may be classified as (Figure 2.4):

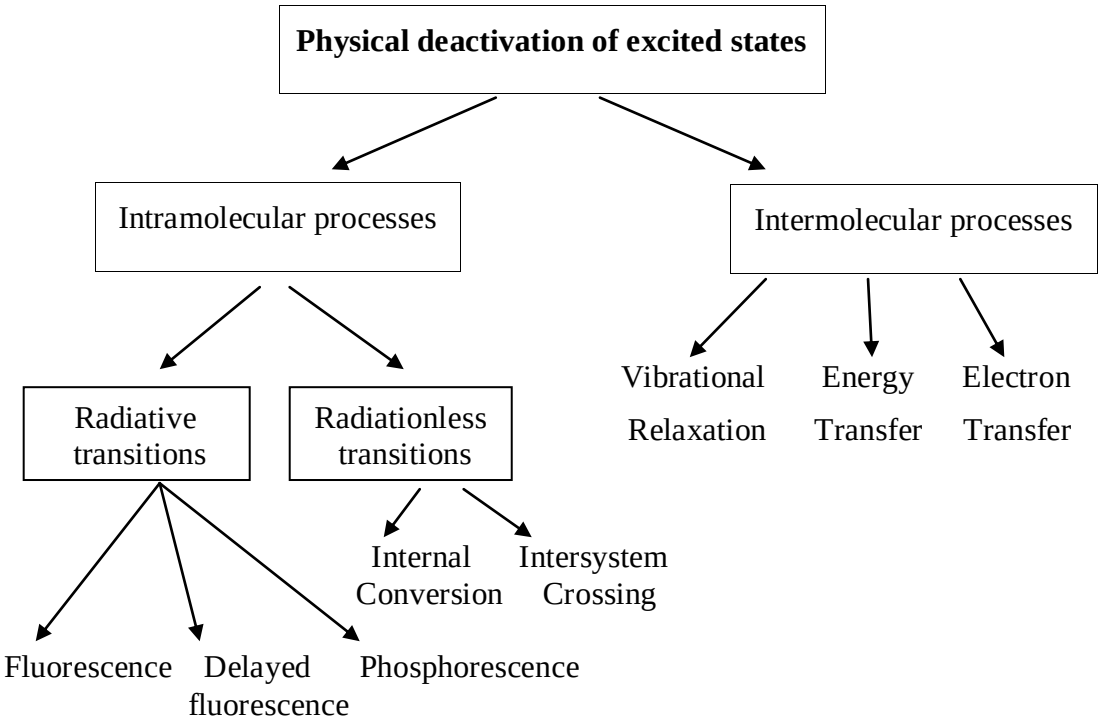

Figure 2.4 : Physical deactivation of excited states from [2].

1. Intramolecular processes

• **Radiative transitions**, which involve the emission of electromagnetic radiation as the excited molecule relaxes to the ground state. Fluorescence and phosphorescence are known collectively as luminescence.

Fluorescence involves a radiative transition (photon emission) between states of the same multiplicity (spin-allowed), usually from the lowest vibrational level of the lowest excited singlet state, $S_1(v = 0)$.

$$S_1 \rightarrow S_0 + h\nu \qquad \textbf{(2.2)}$$

Typical timescales for fluorescence emission are $10^{-12} - 10^{-6}$ s.

Phosphorescence is a spin-forbidden radiative transition between states of different multiplicity, usually from the lowest vibrational level of the lowest excited triplet state, $T_1(v = 0)$. Thus phosphorescence emission is less intense and less rapid than fluorescence.

$$T_1 \rightarrow S_0 + h\nu \qquad \textbf{(2.3)}$$

Typical timescales for photon emission by phosphorescence are $10^{-3} - 10^{2}$ s.

Delayed Fluorescence

Thermally activated delayed fluorescence: Reverse intersystem crossing $T_1 \rightarrow S_1$ can occur when the energy difference between S_1 and T_1 is small and when the lifetime of T_1 is long enough [1]. This results in emission with the same spectral distribution as normal fluorescence but with a much longer decay time constant because the molecules stay in the triplet state before emitting from S_1. This fluorescence emission is thermally activated; consequently, its efficiency increases with increasing temperature. It is also called delayed fluorescence of E-type because it was observed for the first time with eosin.

Triplet–triplet annihilation: In concentrated solutions, a collision between two molecules in the T_1 state can provide enough energy to allow one of them to return to the S_1 state. Such a triplet–triplet annihilation thus leads to a delayed fluorescence emission (also called delayed fluorescence of P-type because it was observed for the first time with pyrene).

• **Radiationless transitions**, where no emission of electromagnetic radiation accompanies the deactivation process [2]. As shown in Figure 2.5, a radiative transition occurs between vibronic states which differ in energy, whereas a radiationless transition occurs between vibronic states of the same energy.

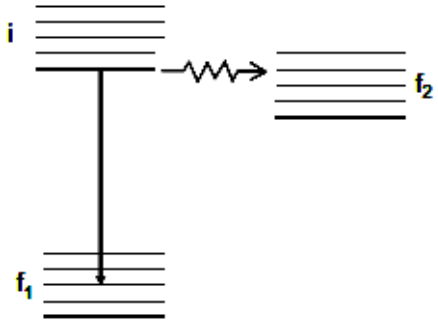

Figure 2.5 : Competing radiative (vertical straight arrow) and radiationless (horizontal wavy arrow) processes between initial (i) and final (f) electronic states.

Internal conversion involves intramolecular radiationless transitions between vibronic states of the same total energy (isoenergetic states) and the same multiplicity for example $S_2(v = 0) \rightsquigarrow S_1(v = n)$ and $T_2(v = 0) \rightsquigarrow T_1(v = n)$. Typical timescales are $10^{-14} – 10^{-11}$ s (internal conversion between excited states) and $10^{-9} – 10^{-7}$ s (internal conversion between S_1 and S_o). Internal conversion between excited states, e.g. $S_2 \rightsquigarrow S_1$ is much faster than internal conversion between S_1 and S_o.

Intersystem crossing involves intramolecular spin-forbidden radiationless transitions between isoenergetic states of different multiplicity, for example $S_1(v = 0) \rightsquigarrow T_1(v = n)$. $S_1 \rightsquigarrow T_1$ intersystem crossing has a timescale of $10^{-11} – 10^{-8}$ s.

2. Intermolecular processes

• **Vibrational relaxation**, where molecules having excess vibrational energy undergo rapid collision with one another other and with solvent molecules to produce molecules in the lowest vibrational level of a particular electronic energy level. e.g. $S_2 (v = 3) \rightsquigarrow S_2 (v = 0)$. Typical timescales for the process are of the order of $10^{-13} – 10^{-9}$ s in condensed phases, and the excess vibrational energy is dissipated as heat.

• Energy transfer

Radiative mechanism of energy transfer

A molecule in an excited electronic state, which is called a '**donor**', may transfer its energy to another molecule, which is called an '**acceptor**' [3]. After this process, the donor molecule returns to its ground electronic state and the acceptor molecule is promoted to a higher state, which can be represented as:

$$D^* + A \rightarrow D + A^* \quad \textbf{(2.4)}$$

where D and A are the donor and acceptor, respectively. The asterisk denotes the excited state. Energy transfer can be a two-step process without direct interaction between the donor and acceptor molecules as follows:

$$D^* \rightarrow D + h\nu \quad \textbf{(2.5)}$$

$$h\nu + A \rightarrow A^* \quad \textbf{(2.6)}$$

Photons from the radiative recombination of donor are absorbed by the acceptor and promote the acceptor to an excited state. This is called radiative energy transfer since photons are involved in this process. The strength of this energy transfer only depends on the emission efficiency of the donor and the absorption efficiency of the acceptor at this wavelength. A single process without the intermediation of photons is also possible when donor and acceptor molecules are close (less than 10 nm), which is called nonradiative energy transfer, through the energetic resonance of two molecules.

Nonradiative energy transfer

- **Dexter mechanism: Energy transfer by radiative emission**

The Dexter mechanism describes electron exchange from the excited state of the donor to the excited state of the acceptor, accompanied by a simultaneous exchange of an electron of the ground state from the acceptor to the donor (Figure 2.6) [4]. This electron exchange necessitates overlapping of the donor- and acceptor orbitals, yet no spectral overlapping is required. This is a short-range interaction (over a distance of less than 10 Å) which decreases exponentially with increasing distance.

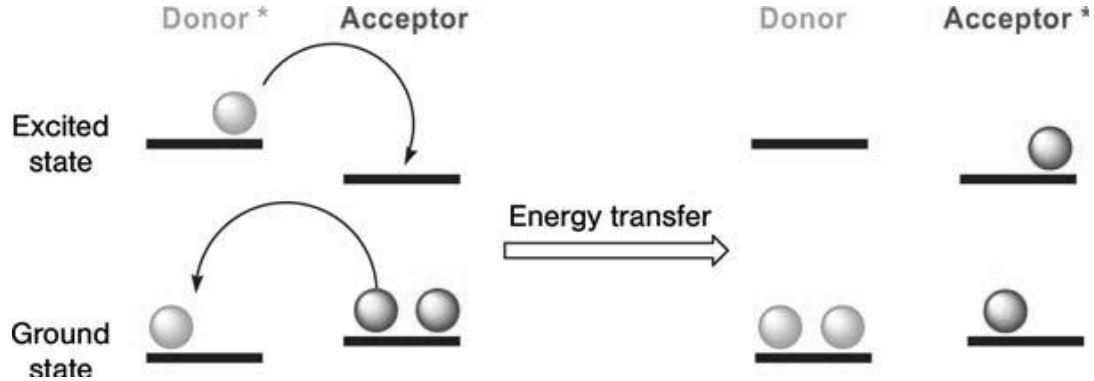

Figure 2.6 : Energy transfer according to the Dexter mechanism (schematic).

- **Förster mechanism: Energy transfer by dipole-dipole interactions**

A non-radiative energy transfer solely by dipole-dipole interactions–without recourse to electron exchange–from energy donor to an acceptor (Figure 2.7) is described by the Förster mechanism.

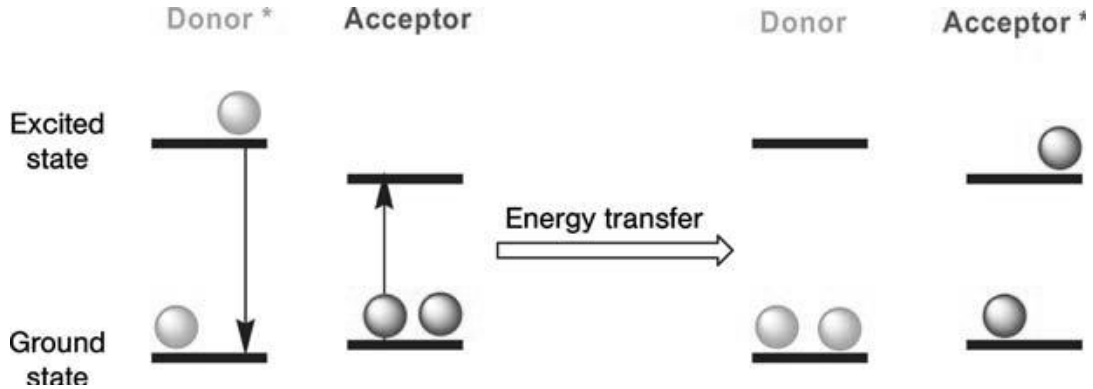

Figure 2.7 : Energy transfer according to the Förster mechanism (schematic).

An important condition for energy transfer in this manner is an overlapping of the fluorescence emission spectrum of the donor with the absorption spectrum of the acceptor (Figure 2.8).

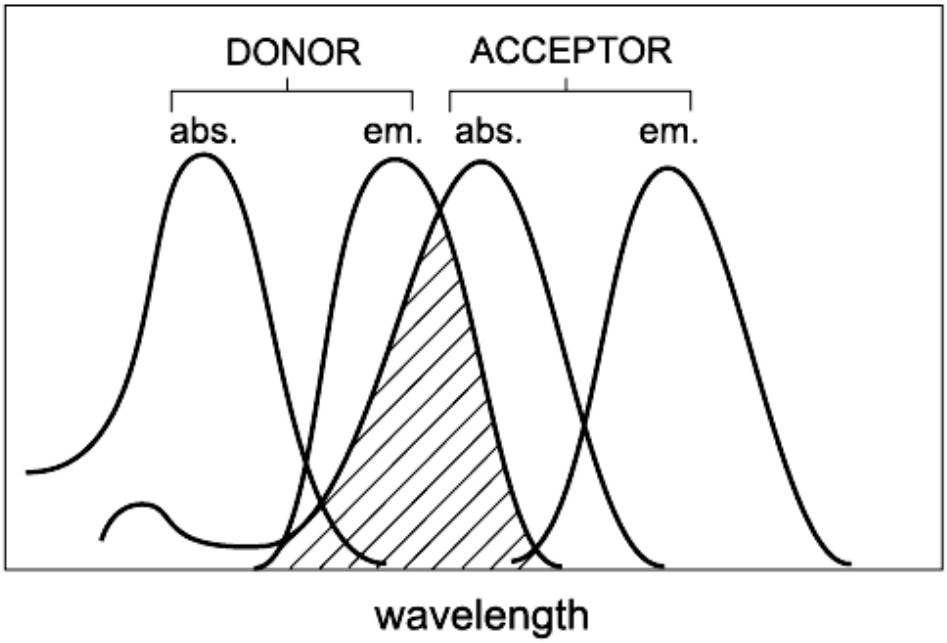

Figure 2.8 : Illustration of the integral overlap between the emission spectrum of the donor and the absorption of the acceptor from.

A small distance (less than 10 nm) between donor and acceptor is likewise important because according to Förster the efficiency of energy transfer decreases with the inverse sixth power of the distance between donor and acceptor:

$$E = 1 / [1 + (r / R_o)^6] \quad \textbf{(2.7)}$$

r = distance between donor and acceptor

R_o = Förster radius

Here the chromophores can be farther apart (10–100 Å; long-range interactions) since this mechanism does not require any overlapping of orbitals. The Förster radius designates the distance between donor and acceptor at which the efficiency of energy transfer amounts to exactly 50%. Half of the excited donor molecules are then deactivated by fluorescence resonance energy transfer and the other 50% by fluorescence or phosphorescence.

• **Electron transfer**, considered as a photophysical process, involves a photoexcited donor molecule interacting with a ground-state acceptor molecule [2]. An ion pair is formed, which may undergo back electron transfer, resulting in quenching of the excited donor.

Fluorescence Quenching

The intermolecular deactivation of an excited molecule by another molecule (of the same or different type) is a process which called as quenching . Any substance that increases the rate of deactivation of an electronically - excited state is known as a quencher and is said to quench the excited state.

2.2 Donor-Acceptor Containing Polymers

An increasing number of polymers is being reported that contain donor and acceptor moieties incorporated in the main chain, as endgroups, pendant groups, or as block copolymers [5]. These donor-acceptor polymers are designed to enable energy and electron transfer in the electronically excited state of the polymer and the donor–acceptor (D–A) type polymers have been widely explored for electronic and optoelectronic device applications, including light emitting diodes, photovoltaic cells, field-effect transistors, and polymer memory devices.

There are different donor-acceptor types polymers which some of them are shown in Tablo 2.1.

Table 2.1: Illustritaion of type of donor-acceptor polymers.

TYPE OF DONOR-ACCEPTOR POLYMERS	REFERENCES
	[6]
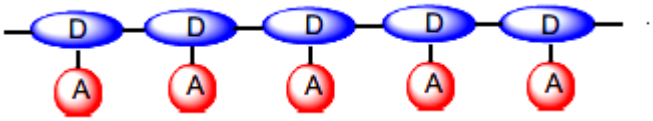	[7], [8]
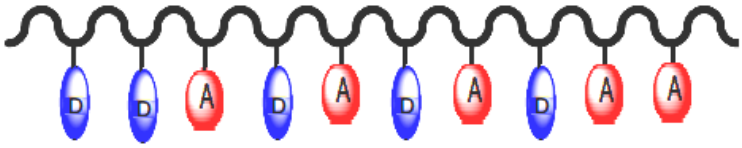	[9], [10]
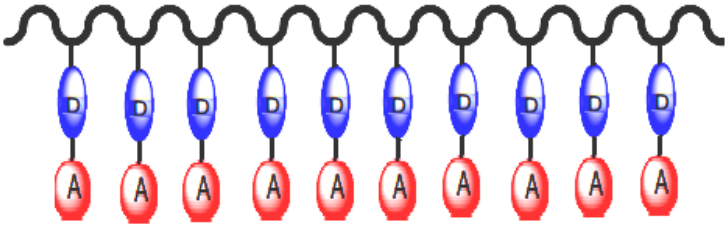	[11]

Wang et al. [6] reported that a new donor–acceptor alternating copolymer PDDTBT based on DTT (dithieno[3,2-b:2’,3’-d]thiophene) as donor unit and BT units (5,6-bis(tetradecyloxy)benzo-2,1,3-thiadiazole) as acceptor has been synthesized (Figure 2.9). Since the BT unit has long alkyoxyl side chains, the polymer was soluble in common organic solvents. Optoelectronic properties of the copolymer (PDTTBT) were investigated and observed by UV–vis, photoluminescence (PL) spectra, and cyclic voltammogram (CV). Based on the ITO/PEDOT:PSS/PDTTBT:PCBM/Al device structure, the power conversion efficiency (PCE) under the illumination of AM 1.5 (100 mW/cm^2) was 0.113%. It was found that PCE of 0.301% could be acquired under the annealing condition at 150 ^{o}C for 30 min. In addition, solar cells fabricated with the 1,8-octanedithiol (OT) additive in the mixture solvent or adding TiOx optical spacer show efficiencies significantly improved over 15%.

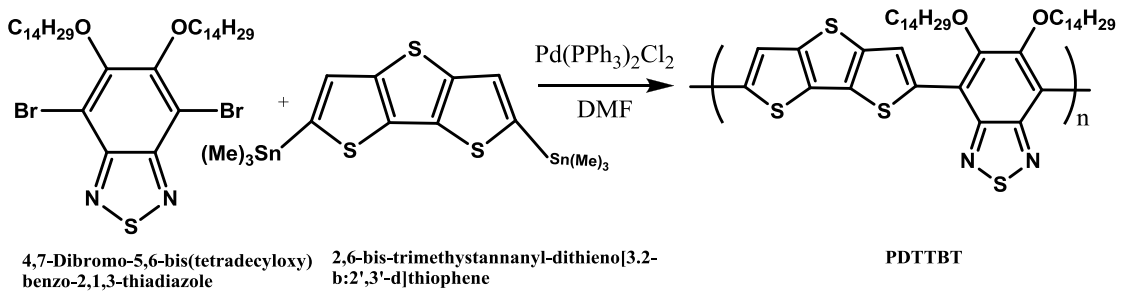

Figure 2.9 : Synthesis of PDTTBT copolymer.

Advincula et al. [9] reported that synthesis of precursor polymers in different ratio via free radical polymerization used in AIBN as initiator that contain two pendent electro-active monomer units (terthiophene and carbazole) by design were investigated for their copolymerization phenomena in forming conjugated polymer network films (Figure 2.10).

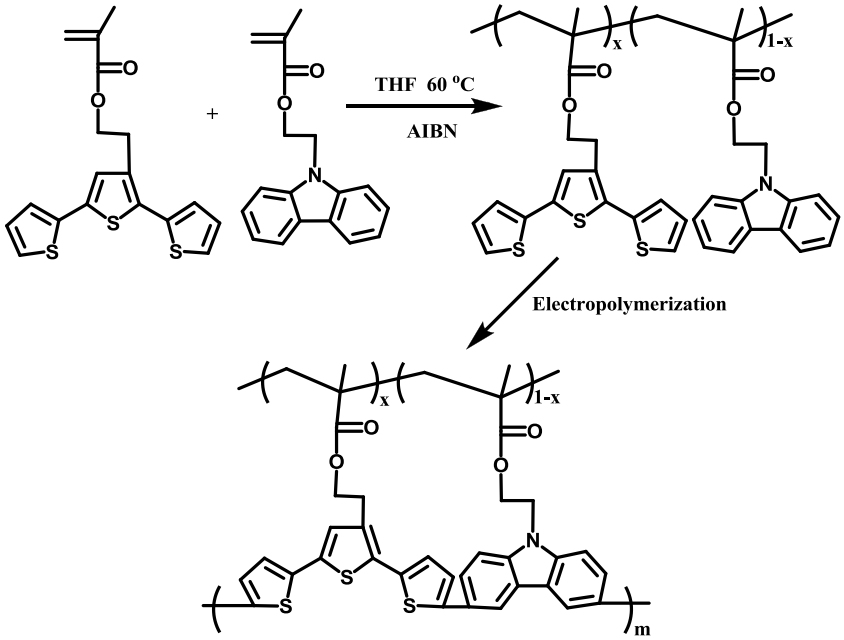

Figure 2.10 : Synthesis of precursor copolymer and their electropolymerization.

Fang et al. [10] reported synthesis new non-conjugated random copolymers containing pendant electron-donating carbazole and electron-accepting 1,3,4-oxadiazole by nitroxide-mediated free radical polymerization (Figure 2.11). The thermal, optical, and electrochemical properties of the prepared copolymers were characterized. Due to Fang, the present study suggested the high performance polymer memory devices could be achieved by changing the donor/acceptor ratio or chemical structure.

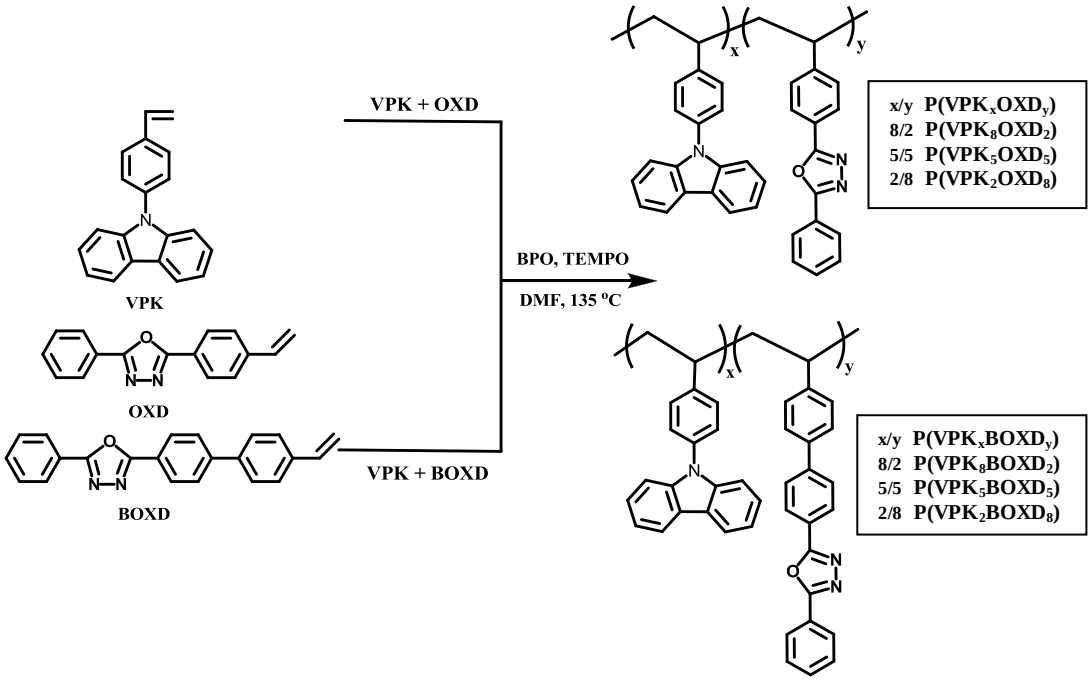

Figure 2.11 : Synthesis of $P(VPK_xOXD_y)$ and $P(VPK_xBOXD_y)$ random copolymers.

Li et al. [7] reported that polymers, two kinds of side chains were designed: one was the repeating units similar to that of P3HT, with the aim to increase the compatible with $PC_{61}BM$ and the hole mobility; another one was the acceptor groups connected with the electron-rich backbone through the conjugated 3,4-ethylenedioxythiophene bridge, in order to broaden the absorption and lower the LUMO level (Figure 2.12). UV-vis absorption, energy levels, and photovoltaic performances of these polymers were investigated.

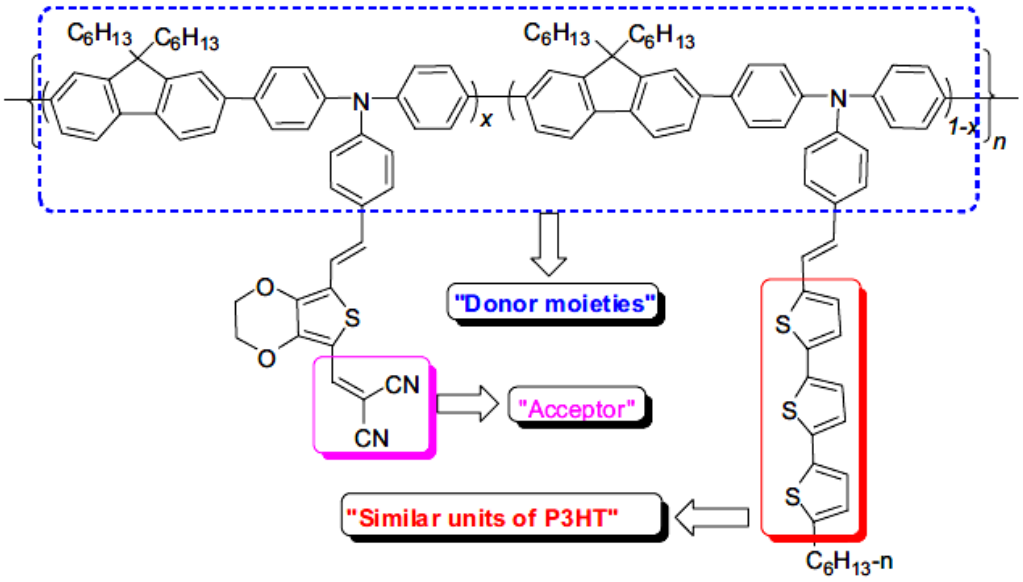

Figure 2.12 : Illustration of polymer.

Zhong et al. [8] reported the synthesis of three novel donor-acceptor polymeric metal complexes based on polycarbazole (as the electron donor) containing complexes of 1,10-phenanthroline with Zn(II), Cd(II) and Ni(II) as the electron acceptor and the optical, thermal and photovoltaic properties of the resulting polymers were investigated (Figure 2.13). The application of these organometallic polymers in fabricated dye-sensitized solar cells has been studied. According to Zhong, the solar cells exhibited good device performance with a power conversion efficiency of up to 0.44%, under simulated air mass 1.5 G solar irradiation.

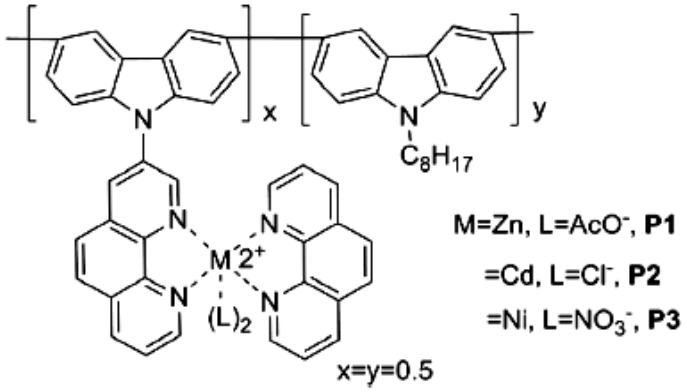

Figure 2.13 : Illustration of donor-acceptor copolymer.

Entazami et al. [11] reported that the synthesis of methacrylate monomers 4-(ω-methacryloyloxyalcyloxy)-N-(5-nitro-2-trienylmetylene)aniline, (nitro thienyl group as acceptor, oxyphenyl group as donor), with alkylene groups of different length by two different routes and polymerization using a free radical initiator to produce low molecular weight polymers useful for nonlinear optics (Figure 2.14). Conventional spectroscopic methods of the resulting polymers were investigated. These compounds with electron donor and acceptor groups can be considered as nonlinear optics (NLO) materials with potential application in nonlinear optic devices.

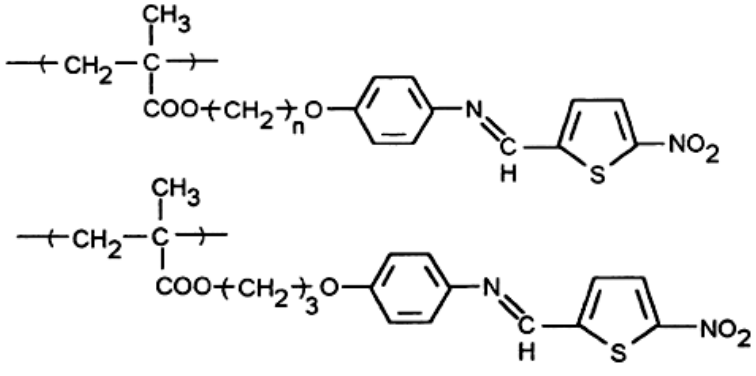

Figure 2.14 : Illustration of copolymer.

2.3 Carbazole Side Chain Polymers

Carbazole and other carbazole-related polymers attract attention because of their unusual physical properties such as electrophotographic micro filming, electro photographic printing plates, laser printing, light emitting fluorescent material, and photovoltaic devices. Carbazole based polymers are most frequently used as polymeric hosts because of hole transporting properties and large band gap [12]. In general, the carbazole-containing polymers can be divided into two groups: polymers containing carbazole moieties in the main chain or side chain [13]. Poly(*N*-vinylcarbazole) belongs to polymers having carbazolyl groups in the side chains. A variety of polymers with pendant carbazolyl groups have been reported, including polyacrylate, polymethacrylate and polystyrene derivatives. Many factors, such as chemical structures, polymer architectures, conformation, location, and stacking of the carbazole units, play a crucial role in manipulation of the properties and in several practical applications.

Simionescu [14] also reported on a series of carbazole-based polymers in early 1980's and investigated their thermal properties.

Bottle et al. [15] demonstrated the mechanism of initiation in the free radical polymerization of NVK. However, the polymer obtained by conventional free radical polymerization does not provide control over the molecular weight and the polydispersity index (PDI) values.

Mori et al. [13] reported the synthesis of poly (N-ethyl-3-vinylcarbazole) and its block copolymers with styrene via RAFT. These polymerizations were performed at higher temperature and no control in molecular weight distribution was reported.

Endo et al. [13] reported the synthesis of well-defined polymers with pendant carbazolyl groups (in which the carbazole unit is directly bound to the polymer main chain) by RAFT polymerization of N-ethyl-3-vinylcarbazole (E3VC) with 2,2′-azobis(isobutyronitrile) (AIBN) as an initiator using benzyl 1-pyrrolecarbodithioate as a chain transfer agent (CTA), where the homopolymers with controlled molecular weights and low polydispersities (M_w/M_n = 1.15-1.29) were obtained (Figure 2.15).

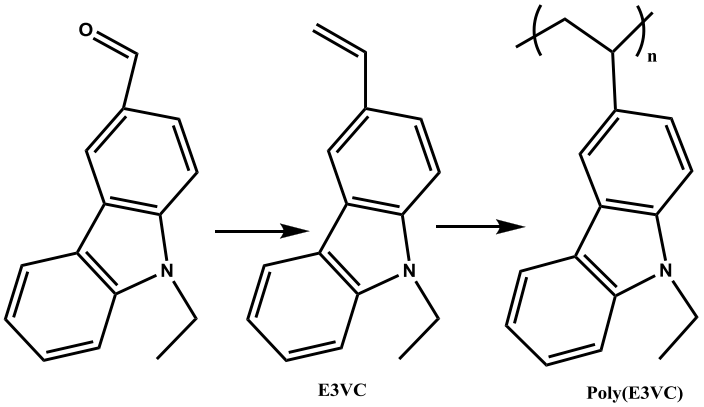

Figure 2.15 : Homopolymer of N-ethyl-3-vinylcarbazole.

Recently, Brar and Kour [16] reported the polymerization of NVK by ATRP at 90 ^{o}C using N-2-bromoethyl carbazole as the initiator to produce polymers with control over molecular weight and polydispersity (Figure 2.16)

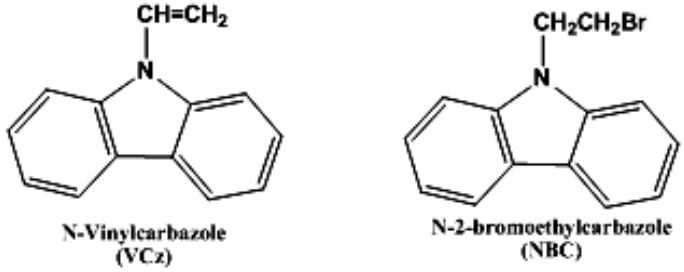

Figure 2.16 : Illustration of N-2-bromoethylcarbazole.

Babazadeh [17] reported the synthesis of 4-(N-carbazolyl) methyl styrene (CzMS) that was homo and copolymerized with some methacrylic and acrylic monomers by the free radical polymerization method. In addition, Babazadeh reported that the molecular weight of the samples increased with increasing polymerization time in experimental conditions (Figure 2.17).

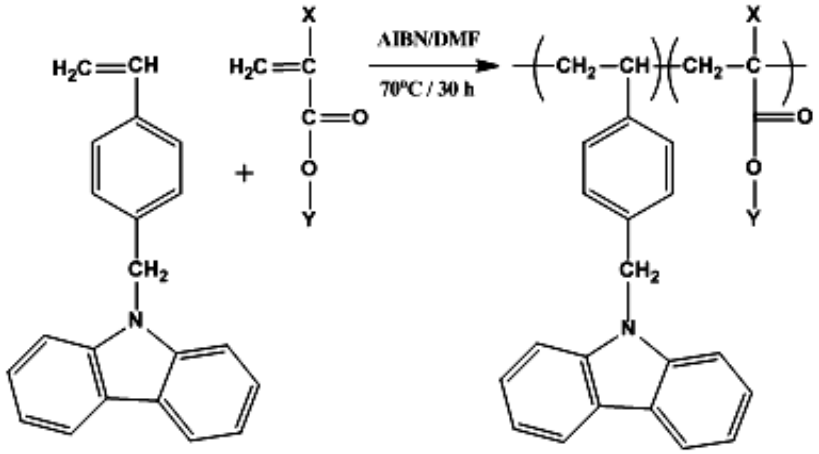

Figure 2.17 : Copolymer of CzMS with acrylic and metacrylic monomers.

Zhu et al. [18] reported the synthesis of the well-defined homopolymer with pendant carbazolyl groups [poly(9-(4-vinylbenzyl)-9H-carbazole), (PVBK)] and the block copolymer PVBK-b-PS via nitroxide-mediated free radical polymerization (Figure 2.18).

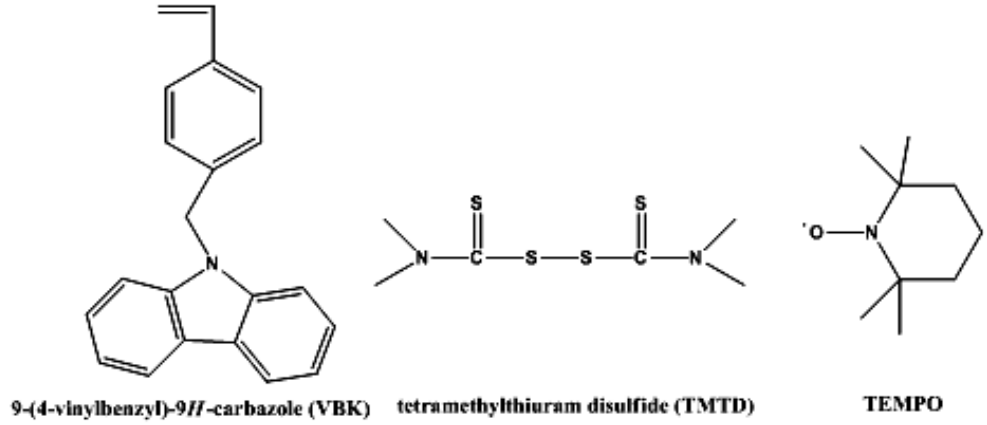

Figure 2.18 : The illustration of (9-(4-vinylbenzyl)-9H-carbazole).

Uryu et al. [19] reported that stereoregular polymerization of 2-N-carbazolylethyl acrylate by use of an anionic catalyst, producing the completely isotactic polyacrylate which has good film-forming properties. According to Uryu, yields of the anionically polymerized polymers were low, and molecular weight distributions were broad. The reason for these results may be attributed to the poor solubility of poly-(2-N-carbazolylethyl acrylate) in the polymerization solvent.

North et al. [20] reported that the polymerization of 2-(9-carbazoly1) ethyl methacrylate initiated by AIBN (free-radical polymerization) produces polymers with broader PDI values of >2.0.

Strohriegl et al. [21] reported that the synthesis of polyacrylates and polymethacrylates with pendant carbazole by two different methods (Figure 2.19). These methods were free radical polymerization of the corresponding (meth)acrylates and the polymer-analogous reaction of ω-hydroxyl carbazoles with poly(meth)acryloylchloride. According to Strohriegl, the molecular weights of the polymers obtained by free-radical polymerization with AIBN in toluene solution were rather low and all polymers exhibited a broad molecular weight distribution because of low solubility of these polymers in the polymerization solvent-toluene. In more polar solvents like tetrahydrofuran, the molecular weight is limited by chain transfer reactions. Highmolecular weight poly(meth)acrylates (M_n=50000–70000,

M_w=100000–150000) were obtained by polymer-analogous reaction of ω-hydroxyalkylcarbazoles with poly(meth)acryloylchloride.

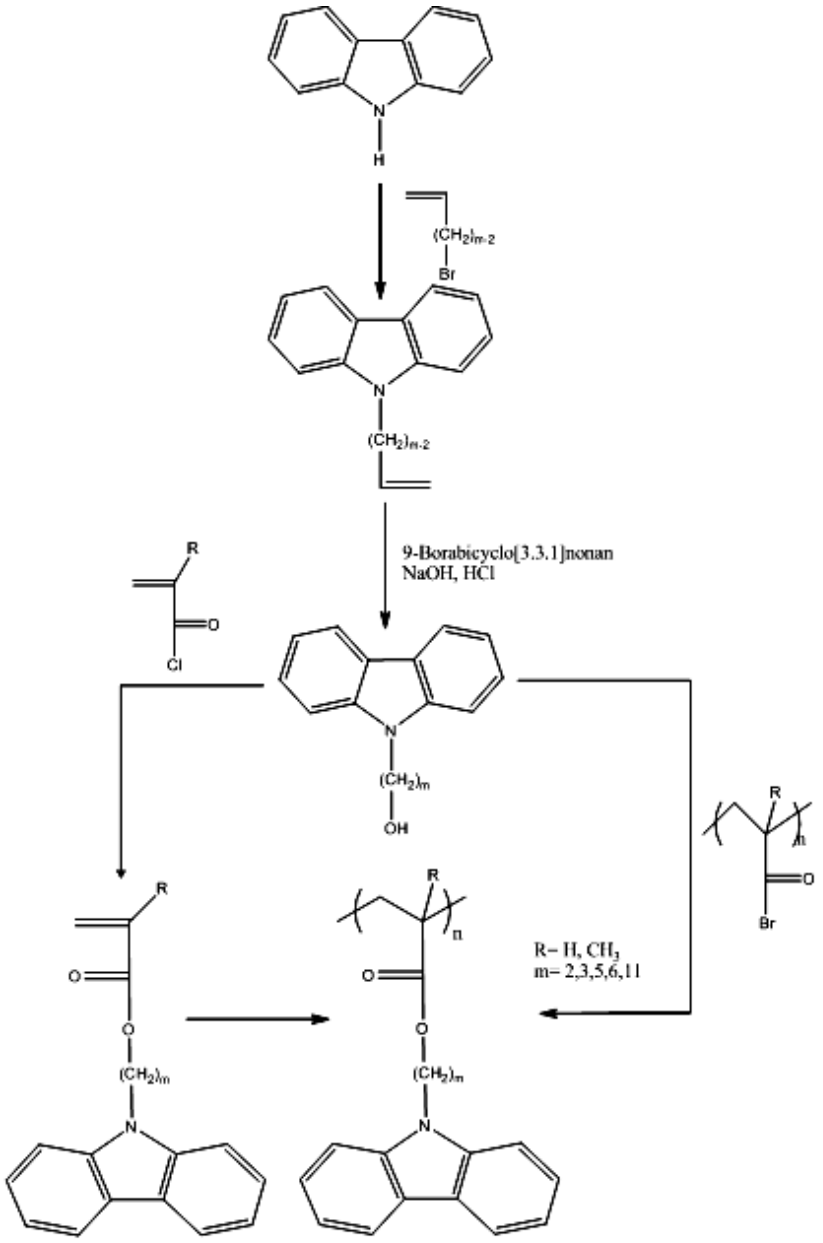

Figure 2.19 : Synthesis of polyacrylates and polymethacrylates with pendant carbazole.

Sato et al. [22] reported the synthesis of the homopolymer with carbazoyl groups poly(2-(N-carbazolyl)ethyl methacrylate) via ATRP.

Haridharan et al. [12] reported that the polymerization of N-vinylcarbazole (NVK) and carbazole methacrylate (CMA, 3-(9H-carbazol-9-yl)propyl methacrylate) was carried out using controlled radical polymerization methods such as atom transfer radical polymerization (ATRP), single electron transfer (SET)-LRP, and single

electron transfer initiation followed by reversible addition fragmentation chain transfer (SET-RAFT) (Figure 2.20).

Li et al.[23] reported polymer brushes containing pendant carbazole, (Poly(9-(2-(4-vinyl(benzyloxy)ethyl)-9H-carbazole))) tethered directly on the Si surface, have been prepared by surfaceinitiated ATRP and the memory behaviors are first observed in the polymer brushes.

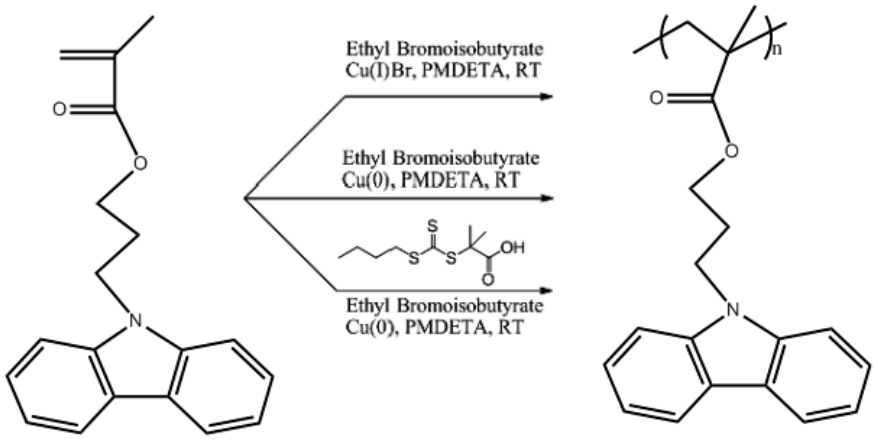

Figure 2.20 : The polymerization methods of 3-(9H-carbazol-9-yl)propyl methacrylate.

2.4 Naphthalamide Side Chain Containing Polymers

1,8-Naphthalimide derivatives are a well known class of compounds that have wide range of applications. Besides their uses as fluorescent dyes for coloring synthetic polymers and textile materials, they are also used in fluorescent solar energy collectors, as liquid-crystal additives, as electrooptically sensitive materials, in laser technology and as fluorescent markers in medicine and biology. They can also be used as yellow components for daylight fluorescent pigments, as fluorescent dichroic dyes in liquid-crystal displays and as fluorescent brighteners in detergents, textiles, paper, plastics and paints. Also the use of 1,8-naphthalimide derivatives as DNA intercalators [24].

Bouche et al. [25] reported that synthesis of homopolymers derived from the naphthalimide emitting moiety which differ either by the nature of the backbone (poly(methyl methacrylate) (PMMA) or polystyrene (PS)) or by the N-substituent and characterized by UV-visible absorption and photoluminescence (PL) (Figure 2.21). According to Bouche et al., reported that all the polymers show a green

electroluminescence (EL) and a bilayer diode emitted a maximum luminance as high as 7100 cd/m^2 and exhibited a maximum external quantum yield of 1%.

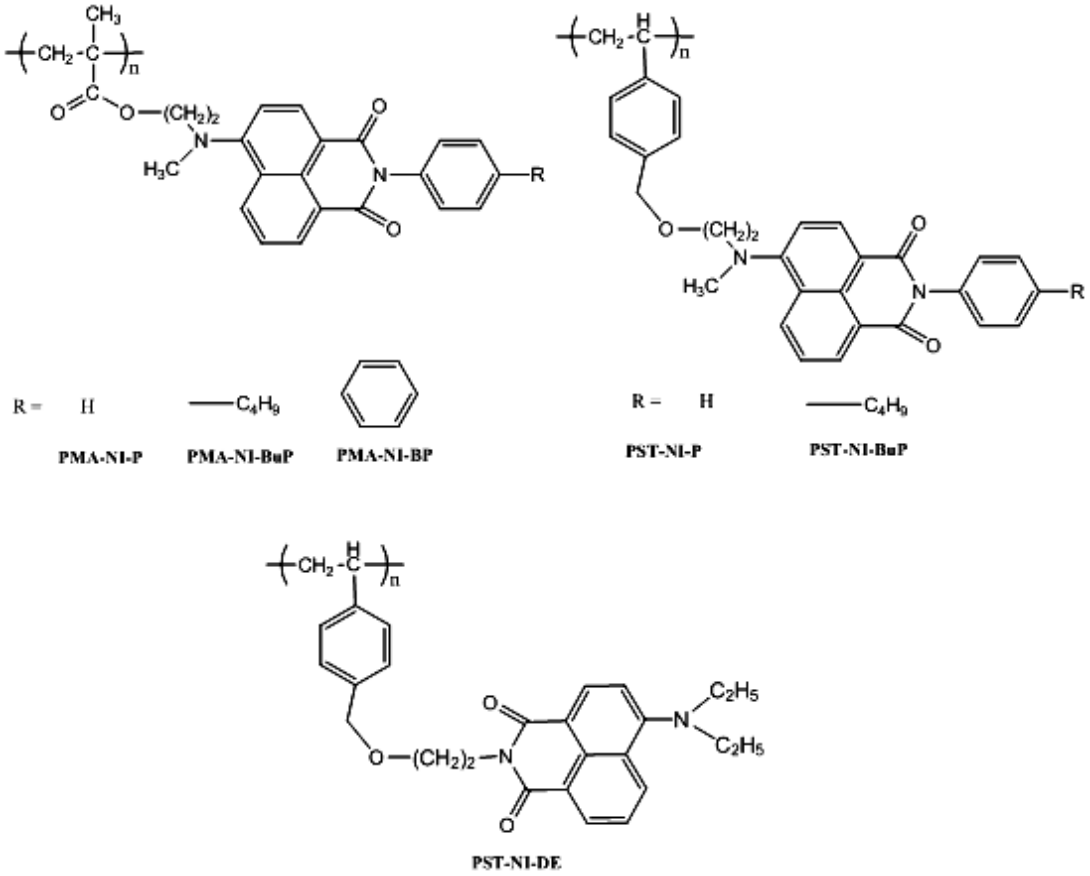

Figure 2.21 : Chemical structure of the naphthalimide containing side-chain polymers.

2.5 Carbazole and 1,8-naphthalimide Side Chain Containing Polymers

Tian et al. [26] reported that the characterization of novel copolymers P(NA-VC) used for EL devices via free radical polymerization used in benzoyl peroxide as initiator. In such copolymers, the electron transporting unit (oxadiazole moiety, OX), hole-transporting unit (carbazole, VC) and emitter (naphthalimide, NA) are incorporated into one copolymer thus these copolymers can be single-layer structure because the single-layer has already three functions and has good film-forming property by spin-coating (Figure 2.22). Electroluminescence properties of copolymer was investigated and it was demonstrated that the EL spectra of single-layer structure device made by these copolymers has a broad luminescent spectrum, which shows a nearly white light.

Kukhta et al. [27] proposed the synthesis of a novel copolymer with moieties capable of charge transport and light emission on the basis of polyvinylcarbazole and 1,8-naphthalimide which both carbazole and naphthalimide moieties are side bonded (Figure 2.23). This polymer is capable of luminescence and both hole (carbazole moiety) and electron (naphthalimide moiety) transport. According to Kukhta, a strong energy transfer from carbazole to naphthalimide moieties is occurred. In addition, a bright and stable electroluminescence from single layered structure is observed.

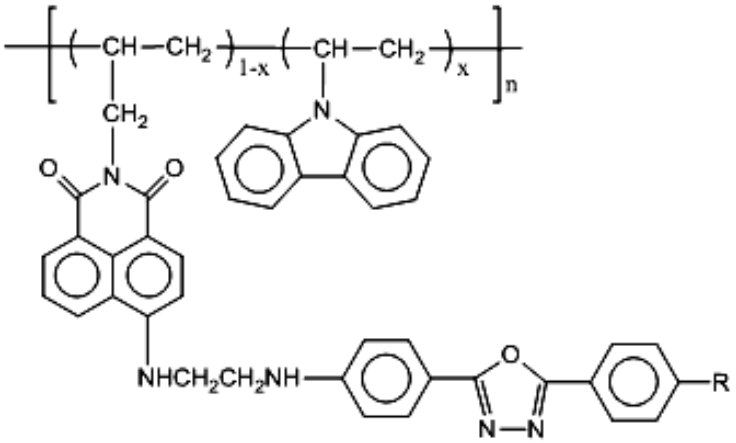

Figure 2.22 : Chemical structures of copolymers P(NA-VC).

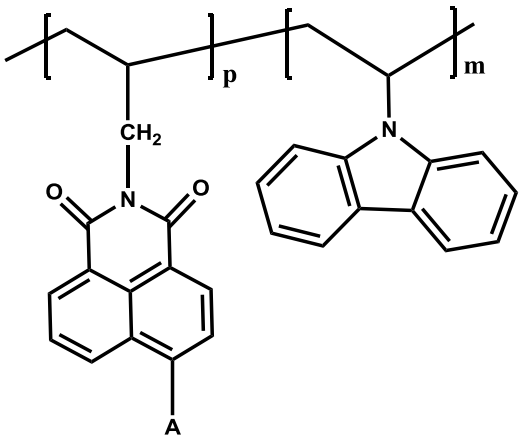

Figure 2.23 : The structure of copolymer containing carbazol and naphthalimide.

Chen et al. [28] reported that a novel copolymer, HT-1 (Figure 2.24), with moieties capable of charge transport and luminescence. A high-efficiency electroluminescent device with a bi-layer structure of ITO/copolymer HT1/2-(4-biphenylyl)-5-(4-tertbutylphenl)-1,3,4,-oxadiazole (PBD)/LiF/Al was fabricated (Figure 2.25). According to Che et al., the device was observed to emit a bright blue-green light

peaking at a wavelength of 496 nm, originating from the copolymer with a maximum current efficiency of 10 cd/A, and a maximum luminescence efficiency of 2.9 lm/W at a DC drive voltage of 12 V.

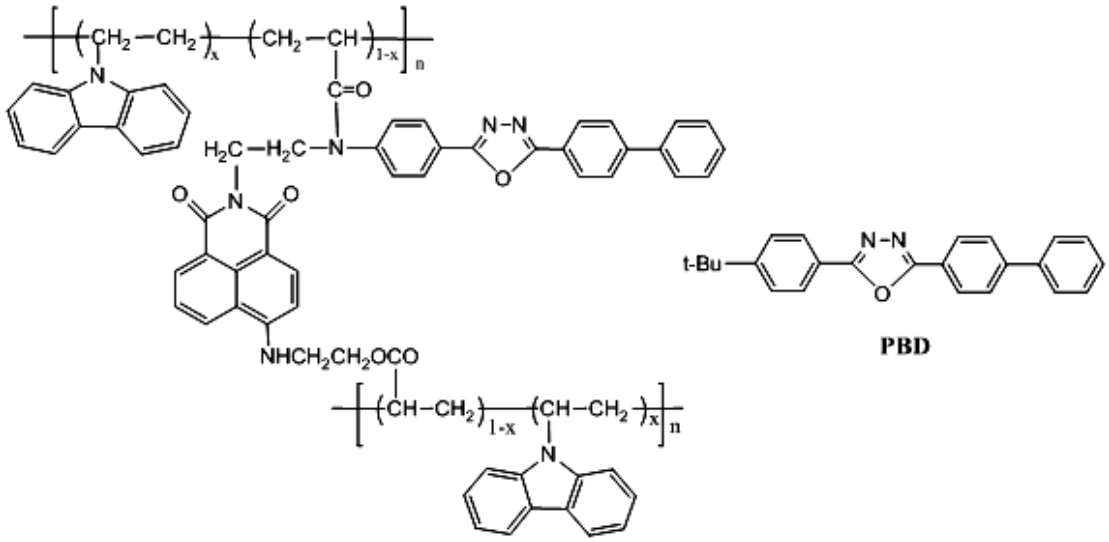

Figure 2.24 : Chemical structures of copolymer HT-1.

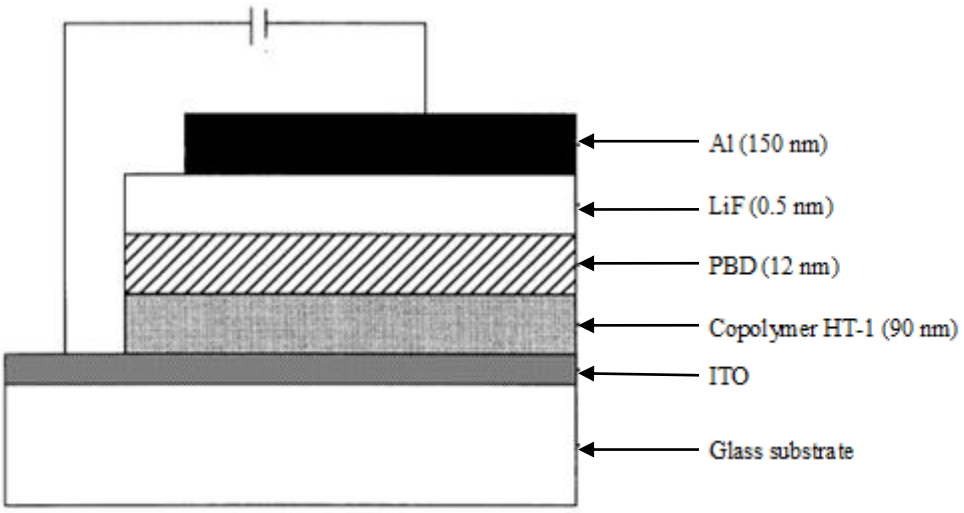

Figure 2.25 : Schematic diagram of the device configuration.

Tian et al. [29] reported synthesis four novel dyad monomers containing two copolymerizable groups which copolymerized with N-vinyl carbazole (Figure 2.26). This structures would be used as electroluminescent materials in which there are three functional segments: 1,8-naphthalimide as emitter, oxadiazole as electron transporting unit and carbazole as hole-transporting segments. The effective intramolecular singlet energy transfer from oxadiazole or carbazole to naphthalimide was observed from the emission spectra of the dyad monomers and copolymers.

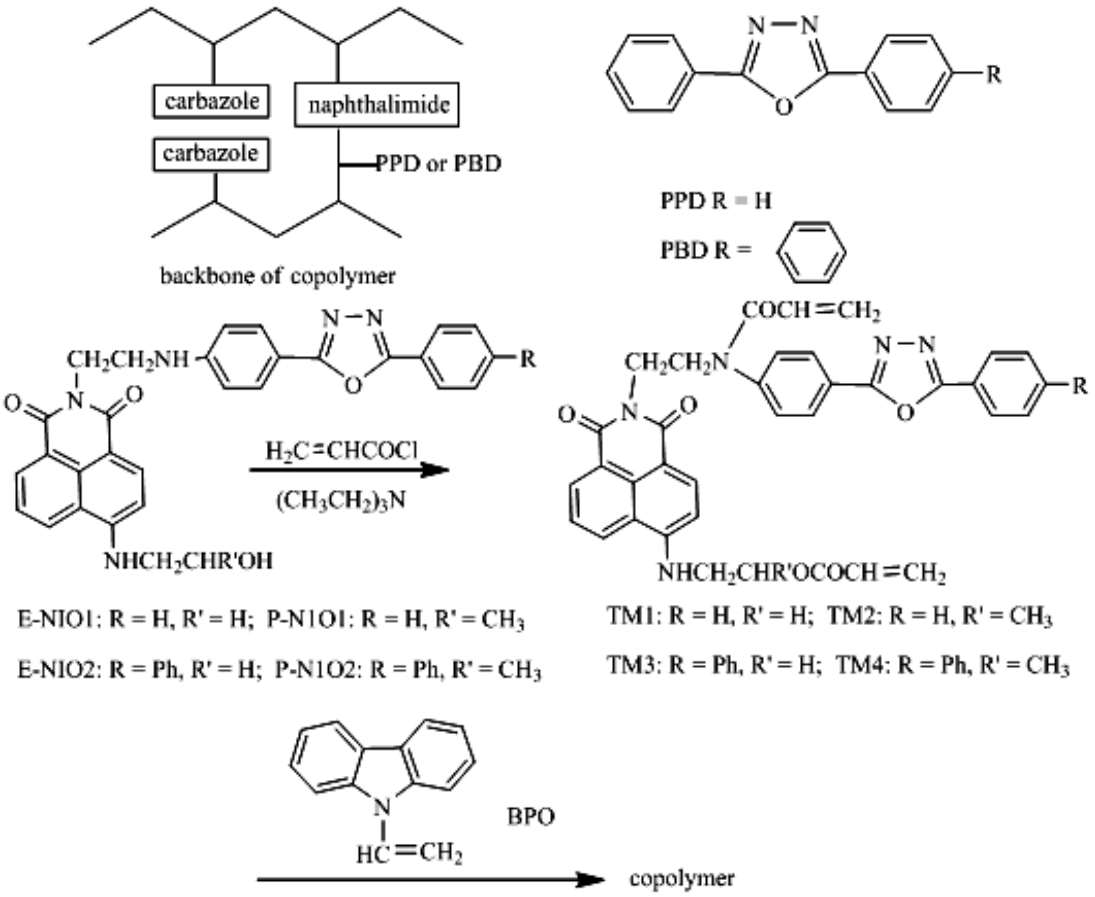

Figure 2.26 : Synthetic routes of copolymer.

2.6 Methods of Polymerization

There are basically two methods by which polymers can be synthesized, namely chain (addition) polymerization and condensation (step-growth) polymerization [30]. When molecules just add on to form the polymer, the process is called chain (addition) polymerization. The monomer in this case retains its structural identity, even after it is converted into the polymer, i.e. the chemical repeat unit in the polymer is the same as the monomer. When molecules react with each other (with the elimination of small molecules such as water), instead of simply adding together, the process is called step-growth polymerization. In this case, the chemical repeat unit is different from the monomer.

Compounds containing a reactive double bond usually undergo chain polymerization. In this type of polymerization process, a low-molecular-weight monomer molecule with a double bond breaks the double bond so that the resulting free valencies will be able to bond to other similar molecules to form the polymer.

This polymerization takes place in three steps, namely, initiation, propagation and termination. Depending on the mechanism, there are therefore three types of chain polymerization, namely, free radical, ionic (cationic and anionic) and coordination polymerization.

2.6.1 Free radical polymerization

Free-radical polymerization is one of the most common ways of preparing polymers. This method involves the use of a free-radical initiator and is applicable for the polymerization of a number of vinyl monomers. A number of small molecules containing carbon-carbon double bonds such as ethylene (CH_2=CH_2) and related derivatives such as CH_2=CHR can be readily polymerized by free-radical polymerization. Free-radical polymerization implies that the polymerization proceeds by the generation of a free radical, which rapidly adds other monomer molecules to afford a polymer. Free radicals are generated by heat, radiation or by chemical initiators.

Typical chemical initiators are benzoyl peroxide, 2,2'-azobisisobutyronitrile (AIBN) and redox initiators. Benzoyl peroxide or AIBN decompose when heated to moderate temperatures of 60-80°C. AIBN decomposes by the elimination of nitrogen molecule to generate the isobutyronitrile radical (Figure 2.27)

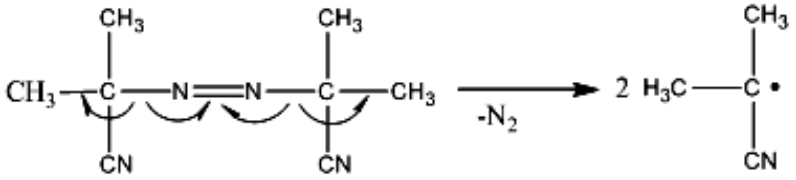

Figure 2.27 : Decomposition of AIBN.

2.6.2 Electropolymeriation

Electrochemical polymerization of such polymers is seemingly a very simple process: it is enough to impose a sufficiently positive potential, E_{polym} (for potentiostatic regime), or to cycle with a sufficiently high anodic limit (generally, it should exceed E_{polym} by 100–200 mV), or to pass an anodic current through the solution of a monomer, and the film of the corresponding polymer progressively grows at the electrode surface [31]. For most monomers representing conjugated molecules, their electrooxidation results in linear polymer chains, with chemical bonds between neighboring monomer units formed in the way that the chain also

corresponds to a conjugated structure, for example, in positions 2 and 5 for Py and Th rings, or in para position for benzene and aniline.

For each monomer the potential, E_{polym} and the deposition rate depend on the concentration of the monomer: the higher the concentration, the faster the film growth (at fixed E_{polym}) or E_{polym} may be lowered (for the same growth rate). The process is influenced strongly by the choice of the solvent. The process may also be affected by the type of the ''background'' electrolyte (the term background means the absence of its redox transformation) since its components are trapped by the film, thus affecting its properties. The polymerization rate and properties of the film may also depend on temperature, pH, convective motion of solution (with or without stirring) and other factors.

The polymer may be deposited usually on any electrode surface stable to its oxidation up to E_{polym}: Pt, glassy carbon, highly oriented pyrolytic graphite (HOPG), indium tin oxide (ITO) or SnO_2 coated glass, Au (for monomers with relatively low oxidation potentials), stainless steel and so on. It is technically much easier to obtain a uniform and well-adhered film at the electrode with a small surface area (below 0.1 cm^2 or so). For the deposition of the film with similarly advantageous properties at the electrode with a size of about 1 cm or greater, it is required to deal carefully with significant ohmic potential losses (preferably, by making the potential drop inside the solution identical for all points at the electrode surface, by the proper geometrical configuration of electrodes), with variation of convective-diffusion transport conditions along the surface (which affects the distribution of the limiting diffusion current), with specific transport conditions near the solution/air surface (such as meniscus, capillary waves, etc.). In general, a slower deposition rate results in a more uniform film formation.

Electrochemical route to synthesize conjugated polymers possesses both merits and shortcomings, compared to alternative polymerization routes: by reaction of the monomer with an oxidative agent or via organometallic catalysis. The electrochemical method, besides its simplicity to realize, allows one to avoid extra chemical agents (from the oxidant, extra agents, or catalyst) inside the polymer. It gives the polymer in the form of a film at the electrode surface, or a free-standing film (e.g., for membrane applications) while the chemical routes result in a powder. The powder form of the polymer is less advantageous for most applications, for

example, in catalysis because of the necessity for the postreaction separation of the powder from products. The drawback of electrochemically deposited polymers is their insolubility in solvents (there may be exceptions) and their decomposition before melting (expectedly, due to the chemical bond formation between polymer chains), which does not permit their redeposition at another (in particular, insulating) substrate.

3. EXPERIMENTAL PART

3.1 Chemicals and purification

Carbazole (≥ 95%), ethylene carbonate (98%), 2,2′-Azobis(isobutyronitrile) (AIBN, 98%), 2-Ethylhexylamine (98%), 4-bromo-1,8-naphtalic anhydride (95%) were purchased from Sigma-Aldrich. Acryloyl chloride (≥ 96%) and crown ethers (18-crown-6, 15-crown-5 for synthesis) were purchased from Merck; CMS (4-vinyl benzyl chloride, 90%) and triethylamine (TEA, 99%) from Across Organics; 2-aminoethanol (≥ 95%) from Fluka; Potassium hydroxide (KOH pellets) from J.T. Baker; NaH (60% in oil) from ABCR GmbH & Co; Sodium sulphate anhydrous from C. ERBA. They were used as received.

Acetone, ethylacetate, n-hexane, MEOH (used for the precipitation) that were technical and were used without purification. Cyclohexanone (≥ 99%), DMF (dimethyl formamide, ≥ 99.8%) and diethyl ether (≥ 99.7%) were purchased from Merck. THF (tetrahdyrofuran, HPLC grade) and chloroform (99-99.4%) were purchased from Sigma-Aldrich. Silica gel 60 (0.063-0.200 nm) were used as received.

Dichloromethane (DCM, technical) was dried $CaCl_2$ and molecular sieves (4A), respectively, then distilled over NaH. DMF was dried Na_2SO_4 and molecular sieves. THF was distilled over benzophenone/sodium.

3.2 Monomer Synthesis

3.2.1 Carbazole side chain monomers

Side-chain carbazole containing precursor N-(2′-hydroxyethyl) carbazole and its acrylic derivative [2-(9H-carbazol-9-yl)ethyl acrylate] and its styrenic derivative [9-(2-(4-vinylbenzyloxy)ethyl)-9H-carbazole] were synthesized with some modifications to the literature procedures. In addition that, carbazole containing styrene derivative [4-(9-carbazolyl)methyl styrene] was also synthesized with some modifications to the literature procedure.

3.2.1.1 Synthesis of 4-(9-carbazolyl) methylstyrene

According to the literature procedure [17], 0.86 g sodium hydride (36 mmol) was slowly added to 3 g (18 mmol) of carbazole dissolved in 100 ml of DMF at room temperature in a round bottom flask (250 mL). After addition of NaH, 3.1 ml (3.3 g 21.6 mmol) of CMS (4-vinyl benzyl chloride) was added to the reaction mixture. The reaction was stirred at 60 ^{o}C (in an oil bath) for 16 h. After cooling the reaction mixture to room temperature, it was poured into aqueous NH_4Cl solution then white precipitate was collected by filtration and washed with water and acetone several times to remove the unreacted carbazole. The final white product was dried in a vacuum oven at 40 ^{o}C to give 3.3 g of CzMS (yield: 65%, m.p. 175.3 ^{o}C).

3.2.1.2 Synthesis of N-(2′-hydroxyethyl) carbazole

N-(2′-hydroxyethyl) carbazole (precursor, HEC) was synthesized according to the literature procedure [32]. A mixture composed of 4.1 g (24.5 mmol) of carbazole, 3.17 g (36 mmol) of ethylene carbonate, and 0.68 g (12.2 mmol) of potassium hydroxide in 30 mL of DMF was left refluxing under vigorous stirring for 8 h in a round bottom flask (100 mL). After cooling the reaction mixture to room temperature, it was poured into 200 mL of water under vigorous stirring to remove ethylene carbonate. The resulting white precipitate was filtered, air-dried and purified by column chromatography (silica) using chloroform as an eluent. The solvent was removed under reduced pressure using rotary evaporation. The resulting off-white precipitate was dissolved in boiling DCM then the mixture was precipitated from n-hexane to give 3.31 g white precipitate HEC (yield: 64%, m.p. 78.6 ^{o}C).

3.2.1.3 Synthesis of 2-(9H-carbazol-9-yl)ethyl acrylate

2-(9H-carbazol-9-yl)ethyl acrylate (CEA) was synthesized according to the literature procedure [33]. 1.2 g of HEC (5.7 mmol) was dissolved in 30 mL of dichloromethane in a round bottom flask (100 mL). Triethylamine (1.03 mL, 7.4 mmol) was added and the reaction mixture was allowed to stir in an ice bath for 30 min. Acryloyl chloride (0.6 mL, 7.4 mmol) solution in 10 ml of DCM was slowly added over a period of 10 min. Afterwards, the ice bath was removed and the mixture was allowed to stir at room temperature overnight. The precipitated salt Et_3NHC1 was filtered off. Organic layer was extracted with water (4x20 ml) and 10% $NaHCO_3$ solution in water (2x20 ml). The resulting organic phase was dried over anhydrous sodium

sulfate. The organic layer was purified by column chromatography (silica) using DCM as an eluent. The solvent was removed under reduced pressure using rotary evaporation. The product was then reprecipitated in methanol 2 times, the precipitate was filtered and air dried to give 1.04 g of CEA (yield: 69%, m.p. 77.3 ^{o}C).

3.2.1.4 Synthesis of 9-(2-(4-vinylbenzyloxy)ethyl)-9H-carbazole

1.5 g of HEC (7.1 mmol) was added to the mixture of sodium hydride (23.7 mmol, 0.57 g) and 45 ml of dry THF in a round bottom flask (100 mL) at 0 ^{o}C under a nitrogen atmosphere then 15-crown-5 (0.26 g, 1.19 mmol) was added to the reaction. When the colour of the reaction mixture was turn from white to red, the mixture of CMS (2 ml, 14.2 mmol), 18-crown-6 (0.31 g, 1.18 mmol) and potassium iodide (0.2 g, 1.2 mmol) in 10 ml of dry THF was added dropwise to the reaction mixture at 0 ^{o}C under a nitrogen atmosphere. The reaction mixture was allowed to stir overnight. The reaction was monitored with thin layer chromotography (TLC). When the complete conversion observed, 0.1 mL of methanol was dropped to the reaction mixture, then 100 ml of water was added. The mixture was extracted with diethylether (4x65 ml). The organic layer was combined then solvent was evaporated to dryness. The crude product was purified by column chromatography (silica) using mixture of ethylacetate/hexane (1/8, v/v) as an eluent. The solvent was removed under reduced pressure using rotary evaporation. The resulting white precipitate was dissolved in boiling DCM then the mixture was precipitated from n-hexane to give 2 g white precipitate of VBEC (yield: 87.6%, m.p. 94.9 ^{o}C).

3.2.2 1,8-Naphtalamide Side Chain Monomers

Side-chain 1,8-Naphtalamide containing acceptor monomer was synthesized with some modifications to the literature procedure [24].

3.2.2.1 Synthesis of 6-bromo-2-(2-ethylhexyl)-1-H-benzo[de]isoquinoline 1,3(2H)-dione (I)

2-Ethylhexylamine (6 ml, 36 mmol) and 4-bromo-1,8-naphtalic anhydride (10 g, 36 mmol) were added into 60 ml dry pyridine and refluxed under argon atmosphere for 5 hours in a round bottom flask (250 mL). Then the mixture was cooled to room temperature and poured into 3 M of HCl solution (250 ml). The resulting precipitate

was collected by filtration, washed with $NaHCO_3$ solution (100 mL) and water (100 mL) and then the residue was crystallized from chloroform-hexane (1/1, v/v) to give 1.1 g of **I** (yield: 78%).

3.2.2.2 Synthesis of 2-(2-ethylhexyl)-6-((2-hydroxyethyl)(methyl)amino)-1H-benzo[de]isoquinoline-1,3(2H)-dione (II)

3.83 g of **I** (10 mmol) was dissolved in 10 ml of pyridine at room temperature in a round-bottomed flask equipped with a magnet and condenser and then 2-aminoethanol (6 mL, 100 mmol) were added to the reaction mixture. The reaction mixture was refluxed and the course of the reaction was monitored with thin layer chromatography (TLC). After 24 h, the reaction was completed. The solvent was evaporated under vacuum and the product was prufied by column chromatography (second fraction) on silica gel using chloroform as an eluent. The solvent was removed under reduced pressure using rotary evaporation. The crystals were dried under vacuum at 40 ^{o}C for 10 h to obtain **II** (yield 72%).

3.2.2.3 Synthesis of 2-((2-(2-ethylhexyl)-1,3-dioxo-2,3-dihydro-1H-benzo [de]isoquinolin-6-yl)(methyl)amino)ethyl acrylate (AM, acceptor monomer)

II (3.77 g, 10 mmol), triethylamine (4.1 mL, 30 mmol) and anhydrous dichloromethane (100 mL) and were added to a three-neck 250 mL round-bottomed flask equipped with a condenser, magnet and a gas inlet. Acryloyl chloride (2 mL, 20 mmol) solution in dichloromethane (50 mL) was slowly added dropwise into the mixture at 0 °C and stirred for 30 min. It was then warmed to room temperature and stirred for 24 hours. The completion of the reaction was monitored with TLC using mixture of n-hexane-chloroform (1/1, v/v) as eluent. When the complete conversion observed, 10 mL of water was dropped to quench to the reaction mixture then the reaction washed with saturated $NaHCO_3$ (3x10 mL) and water (10 mL). The resulting organic layer was dried over anhydrous $MgSO_4$, filtered and evaporated under vacuum. Purification by column chromatography on silica gel (first fraction) gave the desired product (**AM, acceptor monomer**) as a yellowish green oil (yield: 68%).

3.3 Donor-acceptor Type Polymer Synthesis

3.3.1 Carbazole side-chain polymers synthesis

3.3.1.1 Synthesis of poly(4-(9-carbazolyl)methyl styrene)

Poly(4-(9-carbazolyl)methyl styrene) (**PCzMS**) was synthesized according to the literature [34]. 0.5 g CzMS ($1.77x10^{-3}$ mol), AIBN (2.9 mg, $1.77x10^{-5}$ mol) and cyclohexanone (5 ml) were added to a 48 ml of flask, which contains a side arm with a teflon valve sealed with a teflon stopper and the flask was degassed by nitrogen atmosphere for 15 min. Afterwards, the reaction mixture was stirred in thermostatically controlled oil bath at 80 ℃ with 400 rpm stirring rate for 196 h. After that, reaction was stopped with 0.1 mL MeOH then it was diluted with 1 ml of DCM and it was poured into 50 mL of methanol. The white precipitated poly(4-(9-carbazolyl) methyl styrene) was collected by filtration. This purification process was repeated twice in order to remove the residual monomer. The purified polymer (**PCzMS**) was then dried in a vacuum oven at 40 ^{o}C (yield: 0.35 g, conversion: 70%).

3.3.1.2 Synthesis of poly(9-(2-(4-vinylbenzyloxy)ethyl)-9H-carbazole)

0.26 g of VBEC ($7.94x10^{-4}$ mol), AIBN (1.3 mg, $7.94x10^{-6}$ mol) and cyclohexanone (4 ml) were added to a 48 ml of flask, which contains a side arm with a teflon valve sealed with a teflon stopper and the flask was degassed by nitrogen atmosphere for 15 min. Afterwards, the reaction mixture was stirred in thermostatically controlled oil bath at 80 ℃ with 400 rpm stirring rate for 93 h. After applying same purification methot with PCzMS by addition of 0.1 mL of concentrated HCl in order to remove the residual monomer, the purified polymer (**PVBEC)** was obtained (yield: 0.12 g, conversion: 44%).

3.3.1.3 Synthesis of poly(2-(9H-carbazol-9-yl)ethylacrylate)

0.26 g CEA ($9.8x10^{-4}$ mol), AIBN (0.8 mg, $4.9x10^{-6}$ mol) and cyclohexanone (4 ml) were added to a 48 ml of flask, which contains a side arm with a teflon valve sealed with a teflon stopper and the flask was degassed by nitrogen atmosphere for 17 min. Afterwards, the reaction mixture was stirred in thermostatically controlled oil bath at 80 ℃ with 400 rpm stirring rate for 65 h. After applying same purification methot

with PVBEC, the purified polymer (**PCEA)** was obtained (yield: 0.184 g, conversion: 70.8%).

3.3.2 The synthesis of 1,8-naphtalamide side-chain containing polymer

0.25 g of AM ($5.73x10^{-4}$ mol), AIBN (0.94 mg, $5.73x10^{-6}$ mol) and cyclohexanone (5 ml) were added to a 48 ml of flask, which contains a side arm with a teflon valve sealed with a teflon stopper and the flask was degassed by nitrogen atmosphere for 15 min. Afterwards, the reaction mixture was stirred in thermostatically controlled oil bath at 80 ℃ with 400 rpm stirring rate for 46 h. After applying same purification methot with PVBEC, the purified acceptor polymer (**PAM**) was obtained (yield: 0.036 g, conversion: 14.5%).

3.3.3 The synthesis of donor-acceptor side chain containing copolymer

3.3.3.1 Synthesis of poly(CzMS-*r*-AM)

0.2 g of AM ($4.58x10^{-4}$ mol) and cyclohexanone (10 ml) monomer were added to a 48 ml of flask, which contains a side arm with a teflon valve sealed with a teflon stopper. The mixture was stirred in thermostatically controlled oil bath at 50 °C with 400 rpm stirring rate for 20 h. Then mixture was cooled to room temperature. CzMS (0.39 g, $1.374x10^{-3}$ mol) and AIBN (3 mg, $1.832\ x10^{-5}$ mol) were added to the flask, and then mixture was degassed by nitrogen atmosphere for 25 min. Afterwards, the reaction mixture was stirred in thermostatically controlled oil bath at 80 ℃ with 400 rpm stirring rate for 116 h. After applying same purification methot with PVBEC, the purified polymer was obtained (yield: 0.18 g, conversion: 31%).

3.3.3.2 Synthesis of poly(VBEC-*r*-AM)

0.25 g of AM ($5.73x10^{-4}$ mol), VBEC (0.188 g, $5.73x10^{-4}$ mol), AIBN (1.88 mg, $11.46x10^{-6}$ mol) and cyclohexanone (5 ml) were added to a 48 ml of flask, which contains a side arm with a teflon valve sealed with a teflon stopper and the flask was degassed by nitrogen atmosphere for 15 min. Afterwards the mixture was stirred in thermostatically controlled oil bath at 80 ℃ with 400 rpm stirring rate for 46 h. After applying same purification methot with PVBEC, the purified copolymer was obtained (yield: 0.14 g, conversion: 32%).

3.4 Characterization Methods

3.4.1 Nuclear magnetic resonance spectroscopy

The monomers, homopolymers and copolymers were characterized by ^{1}H NMR (250 MHz Bruker AC250) using deuterated chloroform ($CDCl_3$).

3.4.2 Fourier transform infrared spectrometer

To identify the structure of the monomers and polymers, FT-IR Spectrometer (Nicolet 6700, Thermo Electron Corporation and Perkin Elmer, spectrum One, with a Universal ATR attachment with a diamond and Znse crystal) with attenuated total reflectance (ATR) accessories was used in.

3.4.3 Gel permation chromatography

The molecular weights and polydisperties were measured by a gel permeation chromatography (GPC) system consisting of an Agilent 1200 series pump, three Waters Styragel HR columns (guard, 4, 3) and a BI-DNDC differential refractometer (Brookhaven Instruments Corporation, 620 nm) with a THF flow rate of 1 ml/min. Poly(methyl methacrylate) or polystyrene were used in calibration standarts.

3.4.4 Differential scanning calorimetry

Differential scanning calorimetry measurements using Q1000 (TA Instruments) were evaluated from second heating run from ambient up to 300 ^{o}C with a ramp rate of 10 ^{o}C/min. Cooling ramp is not specified and equilibrate command was used. All tests were carried out under 50 ml/min rate of nitrogen purge.

3.4.5 UV-Vis spectrophotometer

UV-Vis spectra were recorded on a Perkin Elmer Lamb 35 UV-Vis spectrophotometer.

3.4.6 Fluorescence spectrophotometer

Fluorescence spectra were recorded on a HITACHI F-4500 Fluorescence spectrophotometer.

3.5.7 Cyclic voltammeter (CV)

Cyclic voltammogram were recorded on a CH Instruments Electrochemical Analyzer 400 A.

4. RESULTS AND DISCUSSION

4.1 Synthesis of Monomers

The synthesized monomers were divided into two group as carbazole side chain monomers (donor) and naphthalamide side chain containing monomer (acceptor).

4.1.1 Carbazole side chain monomers

The synthesized monomers, 4-(9-carbazolyl) methylstyrene (**CzMS**); 2-(9H-carbazol-9-yl)ethyl acrylate (**CEA**); 9-(2-(4-vinylbenzyloxy)ethyl)-9H-carbazole (**VBEC**) were characterized by FT-IR, ^{1}H NMR, DSC.

4.1.1.1 Synthesis of 4-(9-carbazolyl) methylstyrene

Carbazole and 4-vinyl benzyl chloride were reacted with NaH to synthesize 4-(9-carbazolyl) methylstyrene (CzMS) according to the Figure 4.1. The presence of aromatic protons that belongs to carbazole molecule at 8.13-7.03 (Figure 4.2) and the vinyl protons at 6.95-6.56, 5.72-5.63 and 5.26-5.16 ppm in the ^{1}H NMR of the monomer were proved to the formation of CzMS (Figure 4.3). In addition that, the formation of CzMS was supported with absence of N-H peak at 3415 cm^{-1} and the presence of vinyl group (–CH=CH_2) peak at 904 cm^{-1} in FT-IR spectrum (Figure 4.4). Moreover, the melting point and purity of CzMS were determined as 175.3 ^{o}C (melting point of carbazole is measured as 246.1 ^{o}C, Figure 4.5) and 98.15 mol% by DSC, respectively (Figure 4.6).

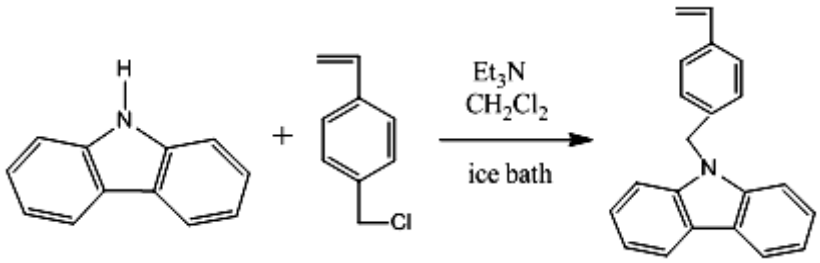

Figure 4.1 : Procedure of 4-(9-carbazolyl) methylstyrene.

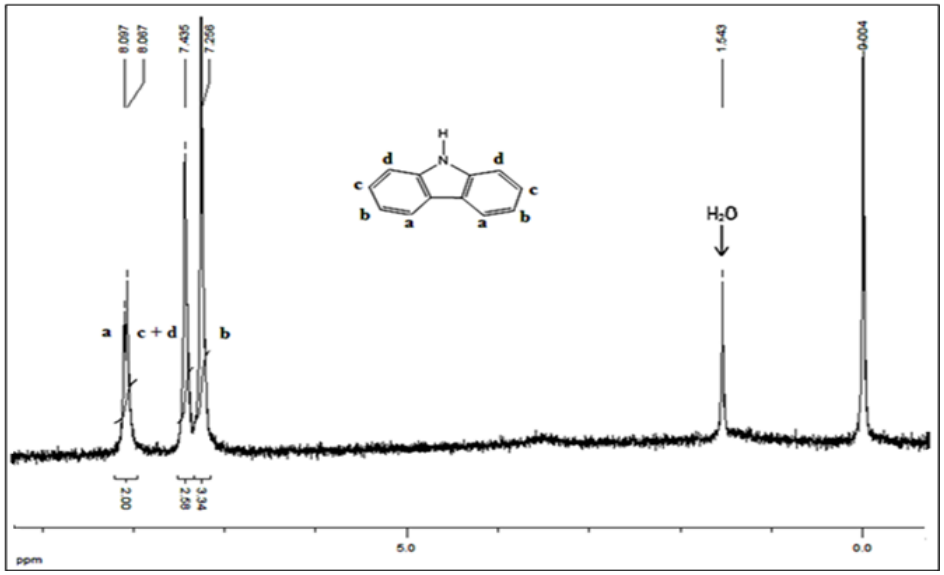

Figure 4.2 : ^{1}H NMR spectrum of carbazole.

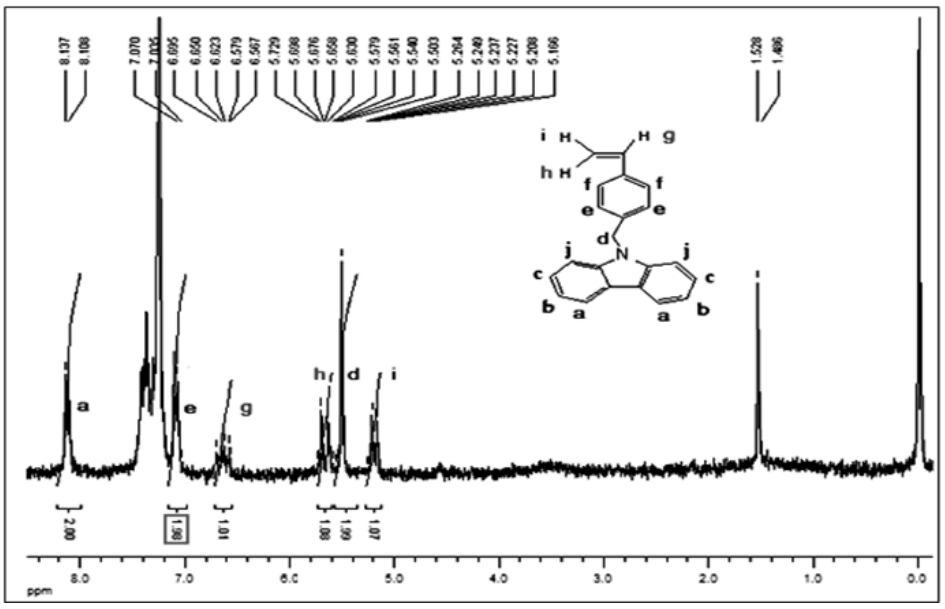

Figure 4.3 : ^{1}H NMR spectrum of CzMS.

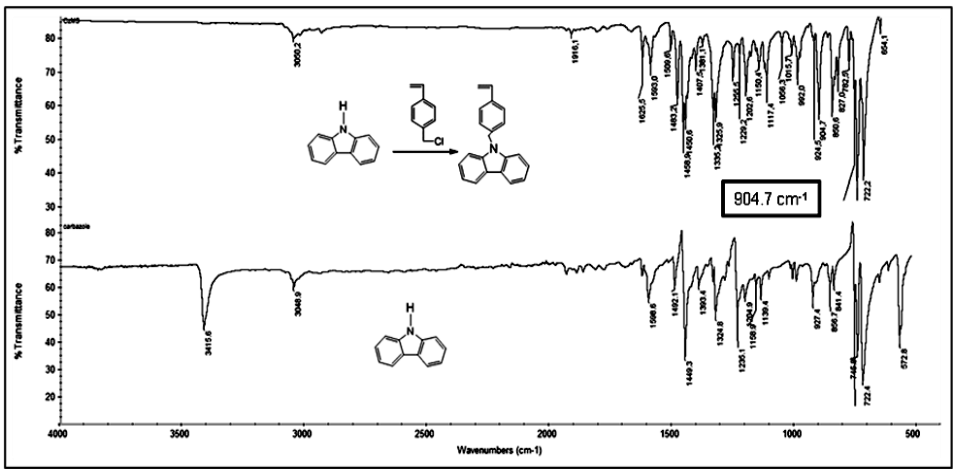

Figure 4.4 : FT-IR spectrum of CzMS.

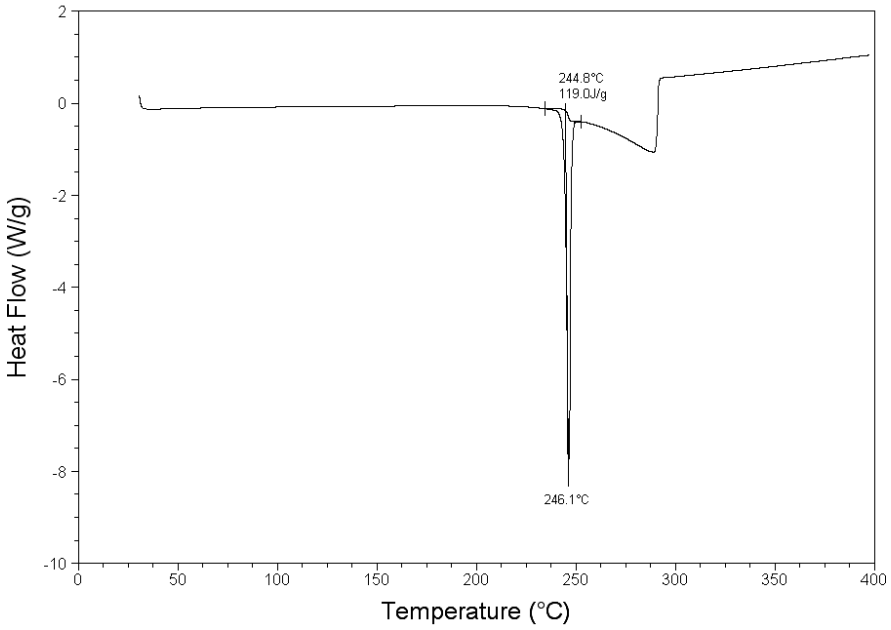

Figure 4.5 : DSC thermodiagram of carbazole.

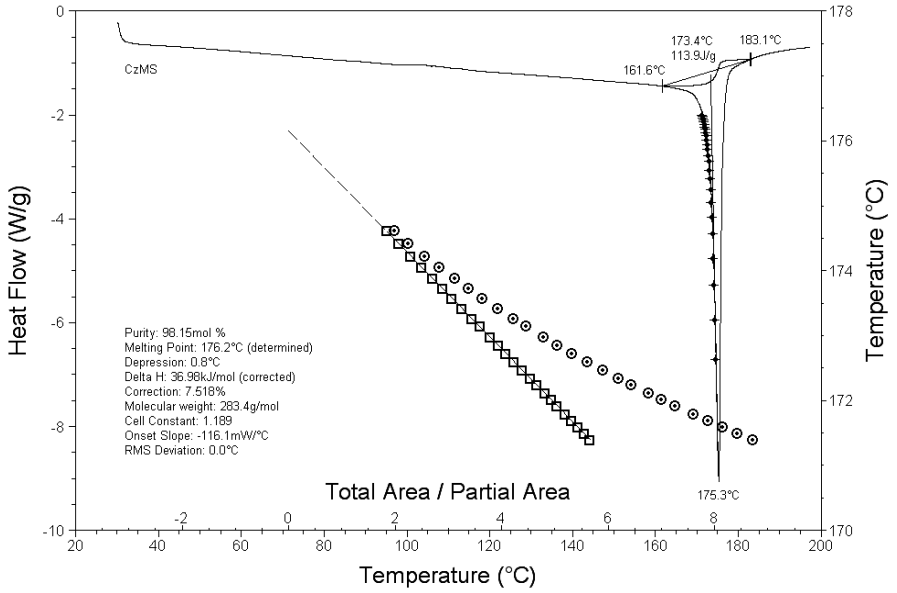

Figure 4.6 : Illustration of melting point of CzMS with DSC.

4.1.1.2 Synthesis of N-(2′-hydroxyethyl) carbazole

Carbazole, ethylene carbonate and KOH were reacted to synthesize N-(2′-hydroxyethyl) carbazole (precursor, HEC) according the Figure 4.7. HEC were used for the synthesis of CEA and VBEC. The presence of aromatic protons at 8.11-7.25 of carbazole protons of alkyl groups (-O-CH_2) and (-N-CH_2) at 4.52-4.48 ppm and at 4.09-4.05 ppm, respectively, in the ^{1}H NMR of the monomer were proved the formation of precursor (Figure 4.8). The presence of hydroxy (–OH) peak at 3198 cm^{-1} and absence of N-H peak at 3415 cm^{-1} in FT-IR spectrum of precursor, were

also supported the formation of the precursor (Figure 4.9). In addition, the melting point and purity of precursor were determined as 78.6 ^{o}C and 98.16 mol% by DSC, respectively (Figure 4.10).

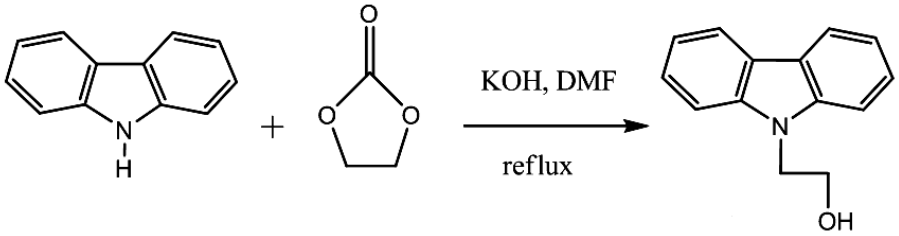

Figure 4.7 : Synthesis of N-(2′-hydroxyethyl) carbazole (precursor, HEC).

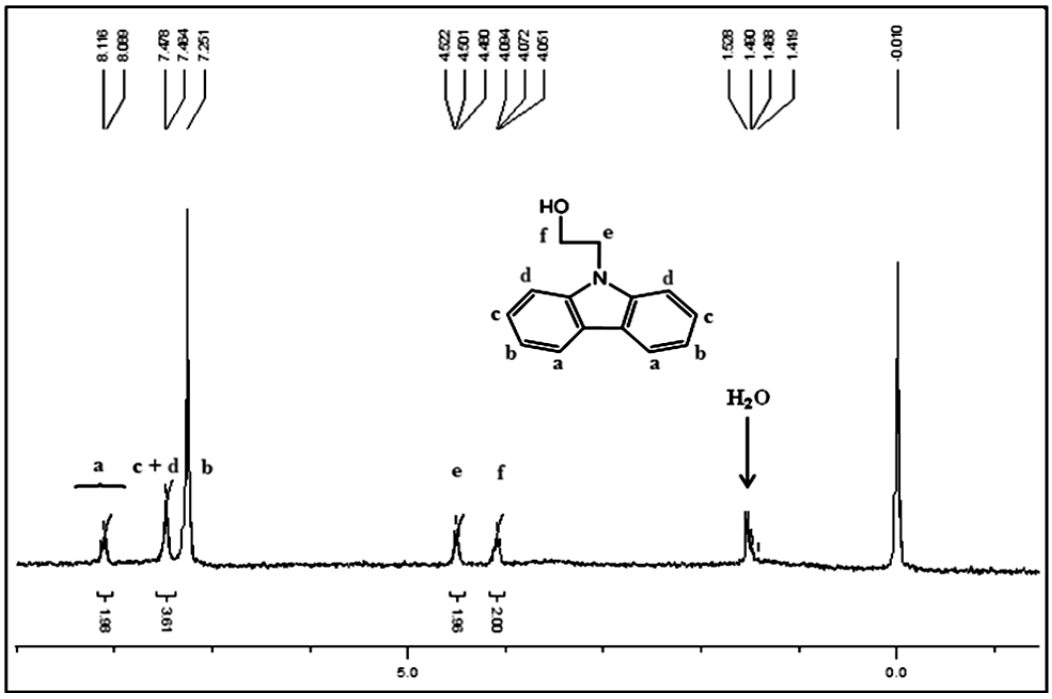

Figure 4.8 : ^{1}H NMR spectrum of precursor.

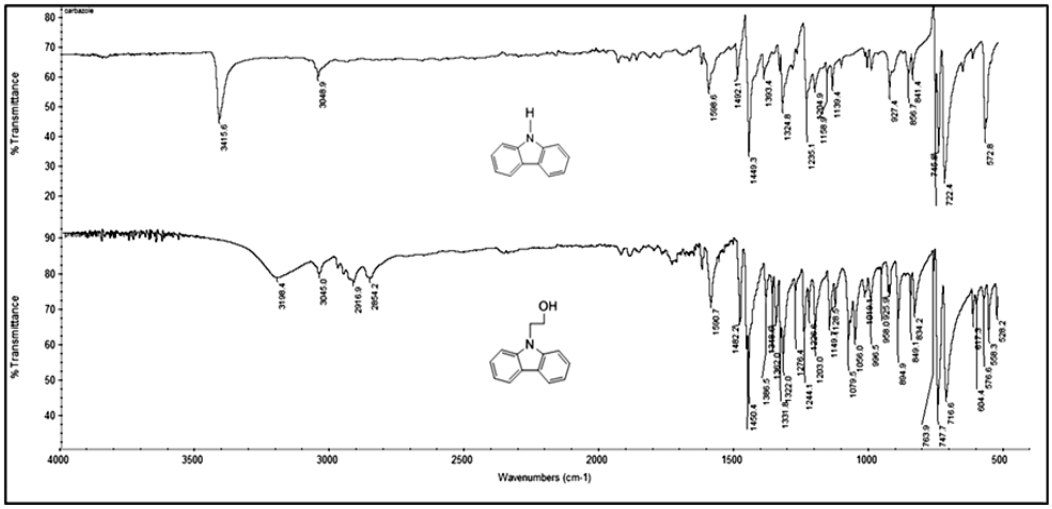

Figure 4.9 : FT-IR spectrum of precursor.

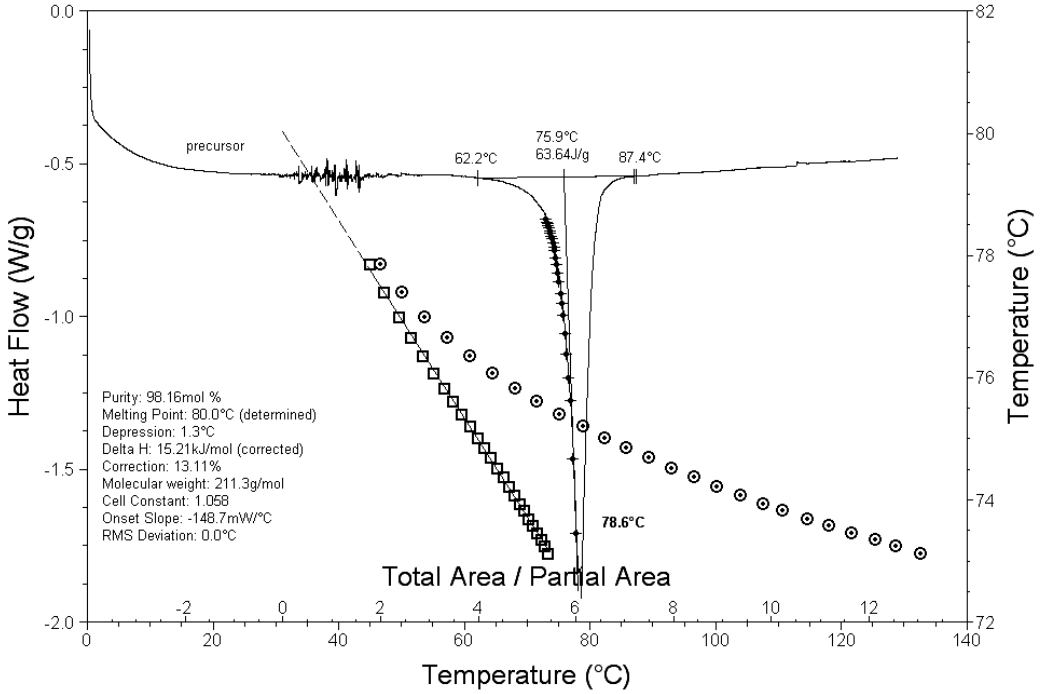

Figure 4.10 : DSC thermodiagram of precursor.

4.1.1.3 Synthesis of 2-(9H-carbazol-9-yl)ethyl acrylate

To synthesize 2-(9H-carbazol-9-yl)ethyl acrylate (CEA), precursor (HEC) and acryloyl chloride were reacted according to the reaction depicted in Figure 4.11. The presence of aromatic protons of carbazole about 8.16-7.00 ppm and vinyl protons at 6.33-5.74 ppm the ^{1}H NMR were an evidence for the formation of CEA (Figure 4.12). In addition, the absence of O-H peak at 3198 cm^{-1} and the presence of ester carbonyl stretching peak at 1720 cm^{-1} (Figure 4.13) in FT-IR spectrum also supported the formation of the CEA. The melting point and purity of CEA were determined as 77.3 ^{o}C and 98.35 mol% by DSC, respectively (Figure 4.14). According to DSC result, the melting point of CEA (77.3 ^{o}C) was different from the melting of precursor (78.6 ^{o}C).

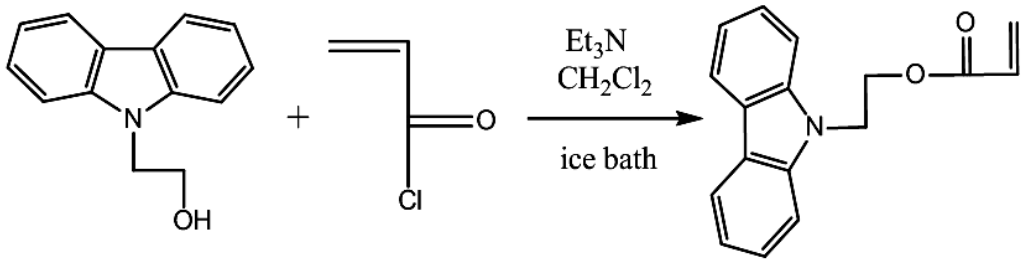

Figure 4.11 : Synthesis of CEA.

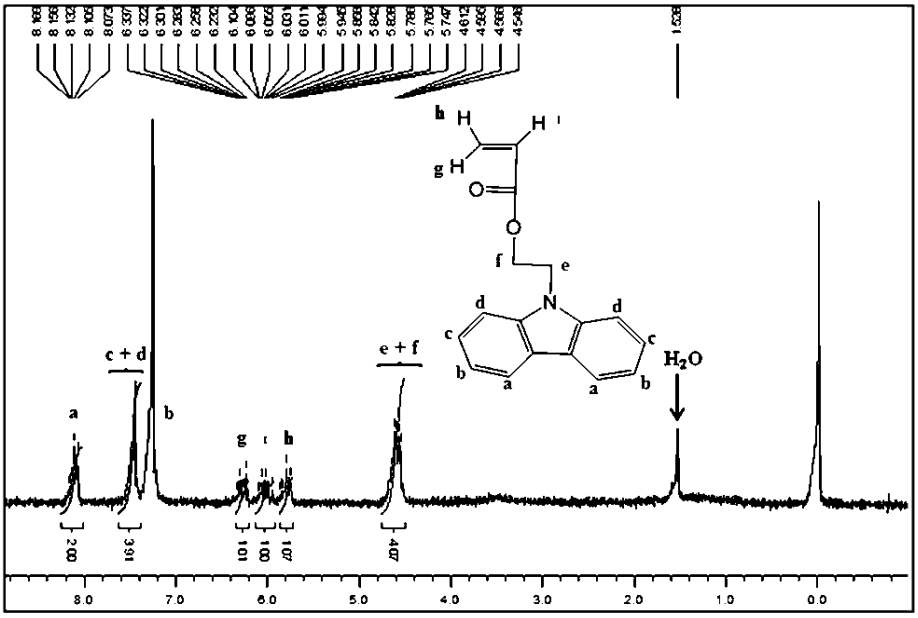

Figure 4.12 : ^{1}H NMR spectrum of CEA.

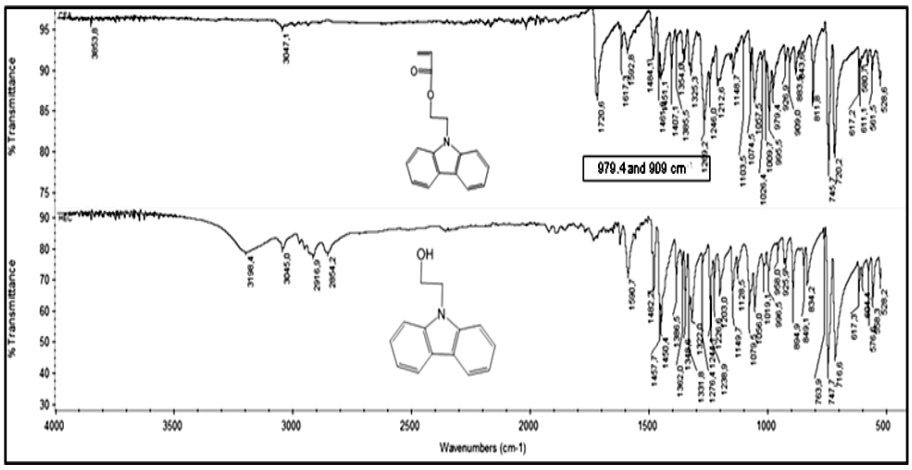

Figure 4.13 : FT-IR spectrum of CEA.

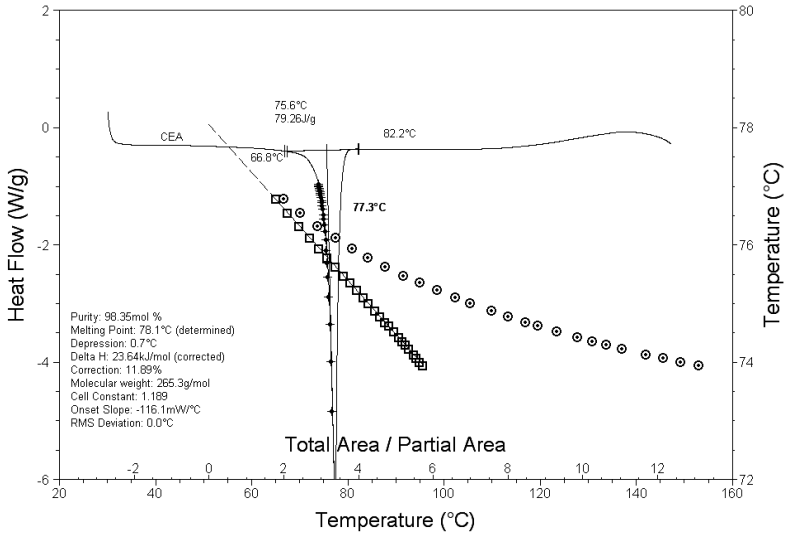

Figure 4.14 : DSC thermodiagram of CEA.

4.1.1.4 Synthesis of 9-(2-(4-vinylbenzyloxy)ethyl)-9H-carbazole

By comparison with condensation reaction of alkoxyamine diol and 4-(chloromethyl)-styrene [35] and reaction of glycidol and 4-vinylbenzyl chloride, the reaction of precursor and 4-chloromethylstyrene in the presence of NaH, KI and crown ethers was carried out to form 9-(2-(4-vinylbenzyloxy)ethyl)-9H-carbazole (VBEC) (Figure 4.15). The presence of aromatic protons of carbazole and vinyl protons at 6.75-5.14 ppm in the ^{1}H NMR were an evidence for the formation of VBEC (Figure 4.16). Moreover, the formation of VBEC was proved by observing the disapperance of O-H peak at 3198 cm^{-1} of HEC and the appearence of the asymmetrical ether stretching (C-O-C) at 1107 cm^{-1} by FT-IR spectrum (Figure 4.17). The melting point and purity of VBEC were determined as 94.9 ^{o}C and 97.42 mol% by DSC, respectively (Figure 4.18). According to DSC result, the melting point of VBEC (94.9 ^{o}C) was different from the melting of precursor (78.6 ^{o}C).

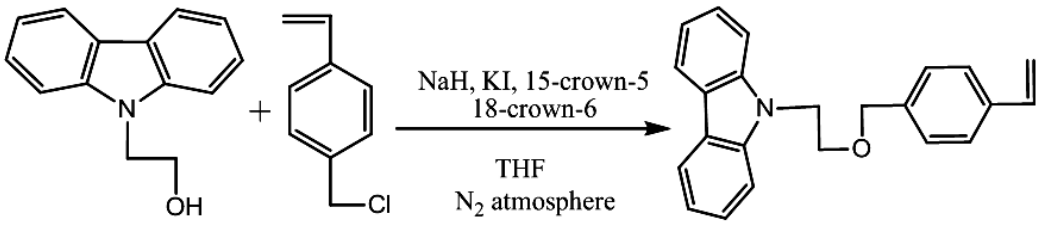

Figure 4.15 : Synthesis of VBEC.

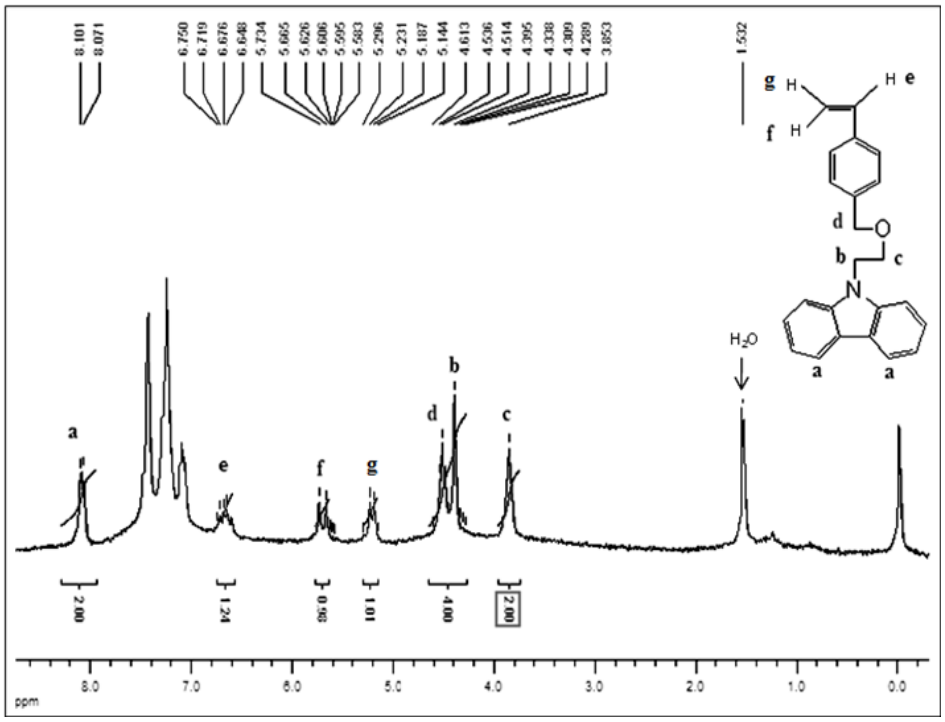

Figure 4.16 : ^{1}H NMR spectrum of VBEC.

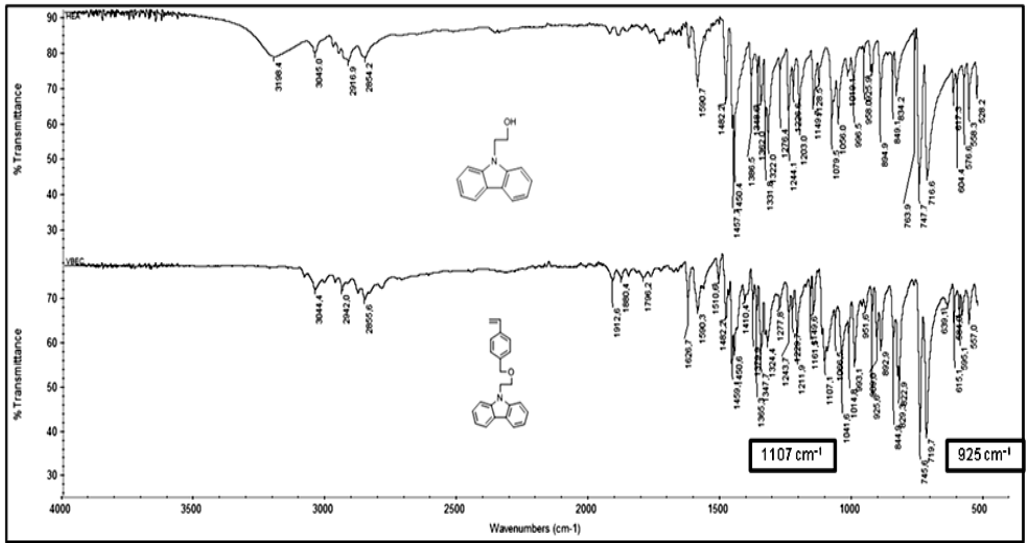

Figure 4.17 : FT-IR spectrum of VBEC.

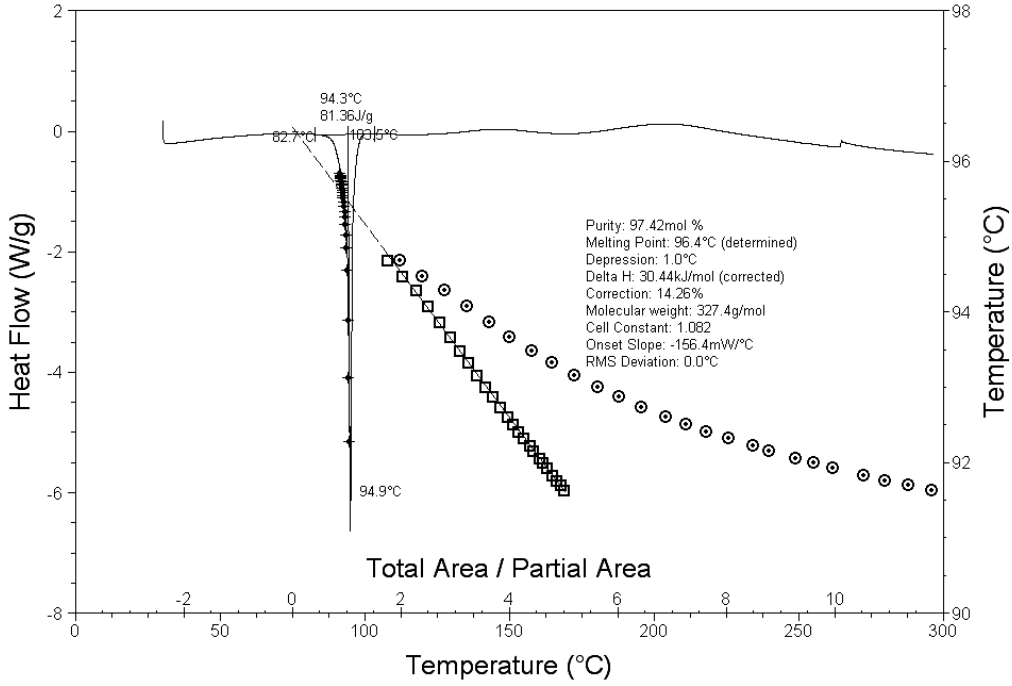

Figure 4.18 : DSC thermodiagram of VBEC.

4.1.2 Naphthalamide side chain containing monomers

4.1.2.1 Synthesis of 6-bromo-2-(2-ethylhexyl)-1-H-benzo[de]isoquinoline 1,3(2H)-dione (I)

2-Ethylhexylamine and 4-bromo-1,8-naphtalic anhydride were reacted to synthesize **I** according to the reaction depicted in Figure 4.19. The presence of 3 aromatic protons of napthalimide (a,c,e) at 8.63-8.39 ppm, 2 protons (b,d) at 8.05-7.84 ppm and -N-$\underline{CH_2}$- signal at 4.09 ppm in the ^{1}H NMR were an evidence for the formation

of **I** (Figure 4.20). The absence of asymmetrical stretching aryl anhyride peak (-CO-O-C-) at 1757-1732 cm^{-1} (Figure 4.21) and the presence of peak of -CO-N-CO- at 1691-1648 cm^{-1} in FT-IR spectrum also supported the formation of **I** (Figure 4.22).

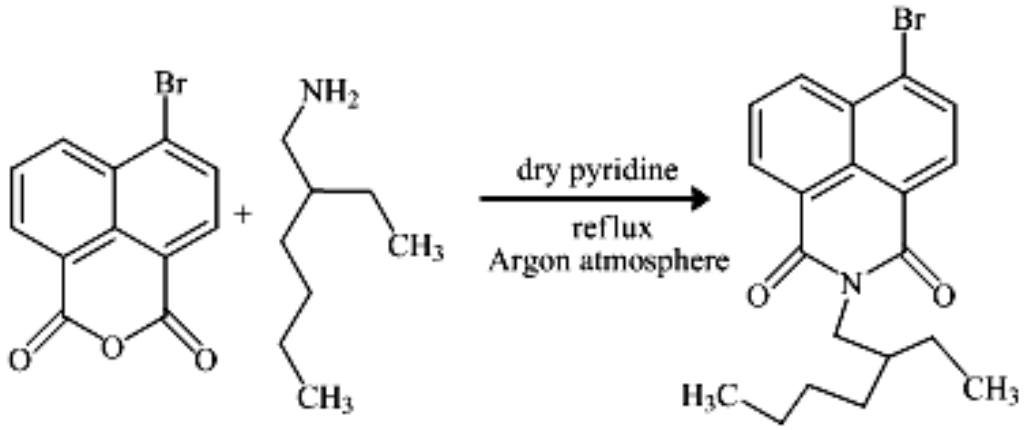

Figure 4.19 : Synthesis of I.

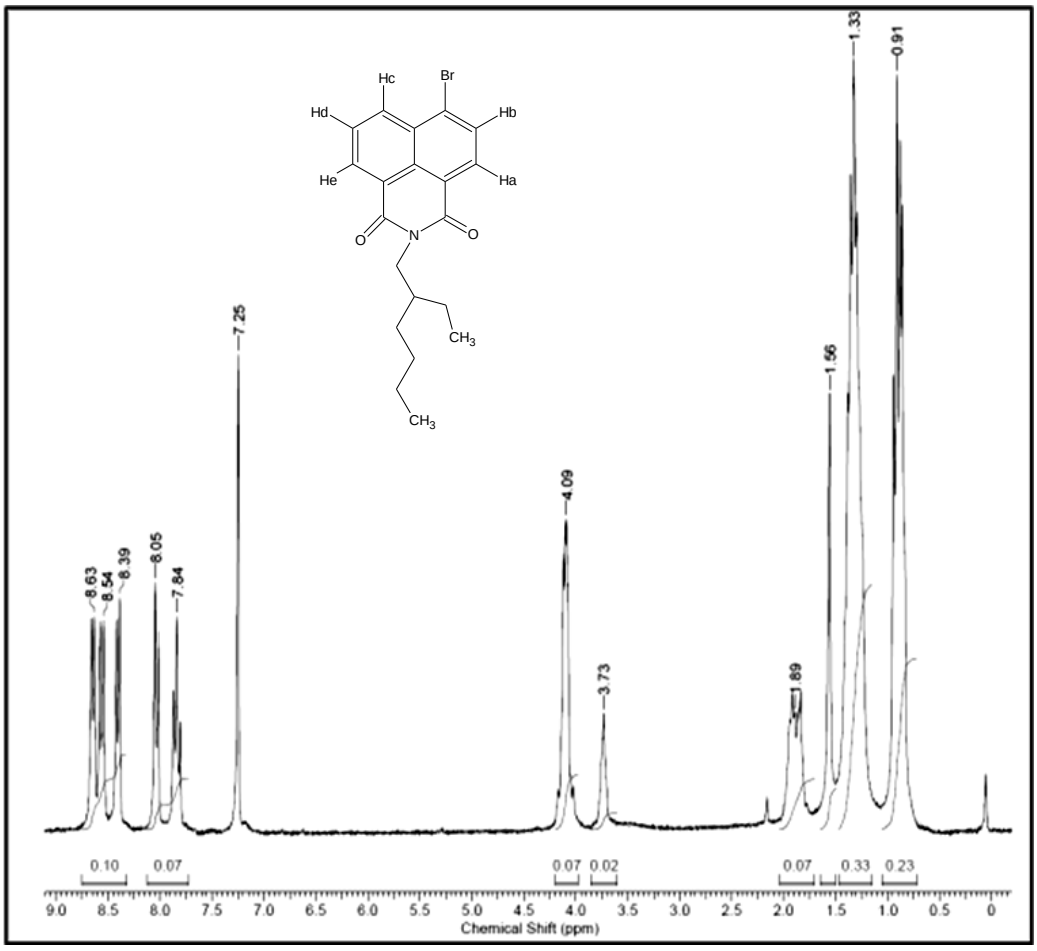

Figure 4.20 : ^{1}H NMR spectrum of I.

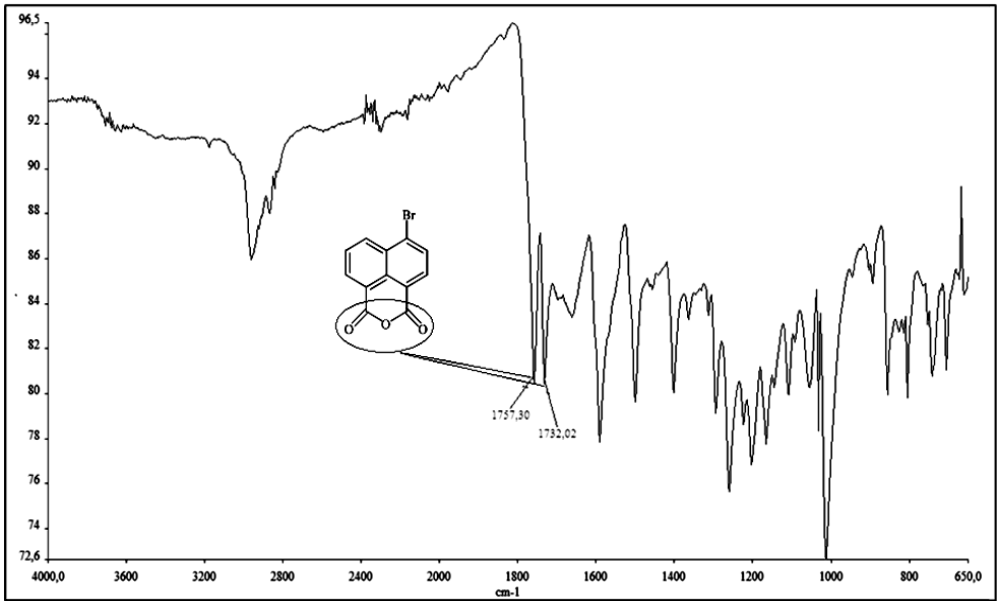

Figure 4.21 : FT-IR spectrum of 4-bromo-1,8-naphtalic anhydride.

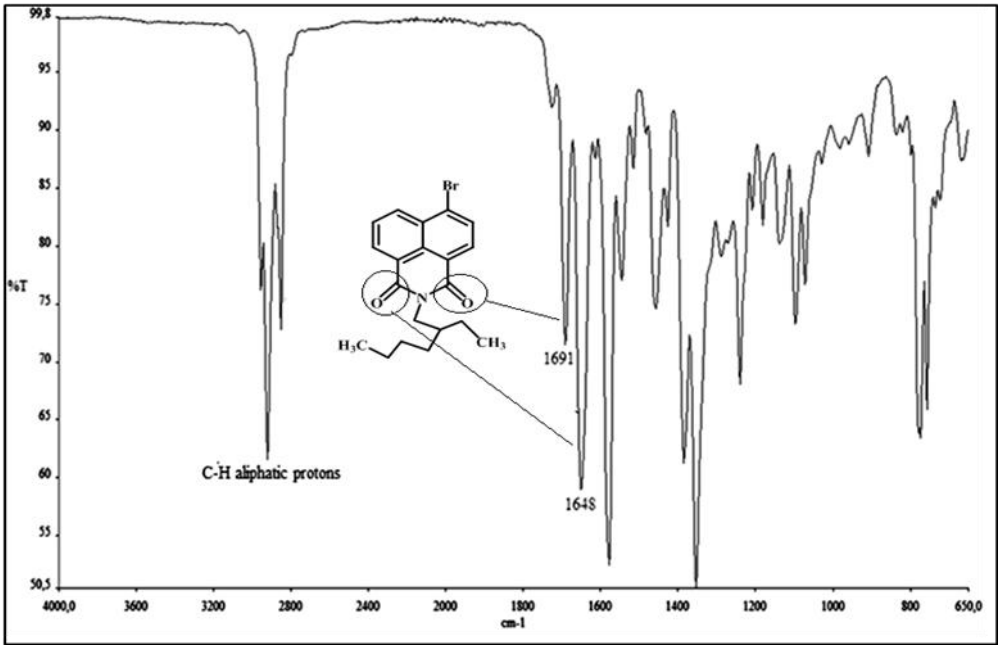

Figure 4.22 : FT-IR spectrum of I.

4.1.2.2 Synthesis of 2-(2-ethylhexyl)-6-((2-hydroxyethyl)(methyl)amino)-1H-benzo[de]isoquinoline-1,3(2H)-dione (II)

I and 2-aminoethanol were reacted to synthesize **II** according to the Figure 4.23. The presence of 3 aromatic protons of napthalimide (a,b,d) at 8.62-8.47 ppm and -O$\underline{CH_2}$- (o), -N-$\underline{CH_2}$- (n+ f), -N-$\underline{CH_3}$ (l) protons at 4.11-2.87 ppm in the ^{1}H NMR were an evidence for the formation of **II** (Figure 4.24). The presence of peak of -CO-N-CO- at 1689-1643 cm^{-1} and the hydroxy peak (-OH) at 3412 cm^{-1} in FT-IR spectrum also supported the formation of **II** (Figure 4.25).

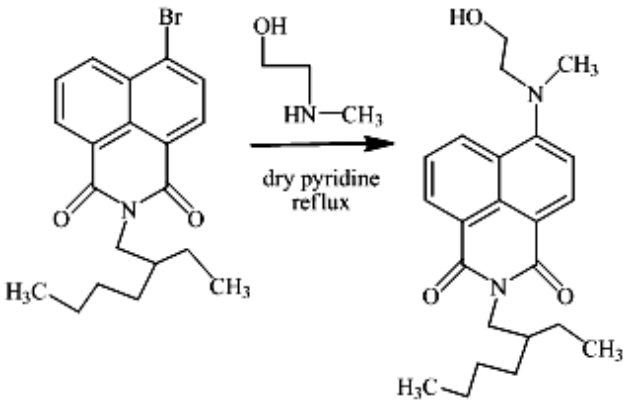

Figure 4.23 : Synthesis of II.

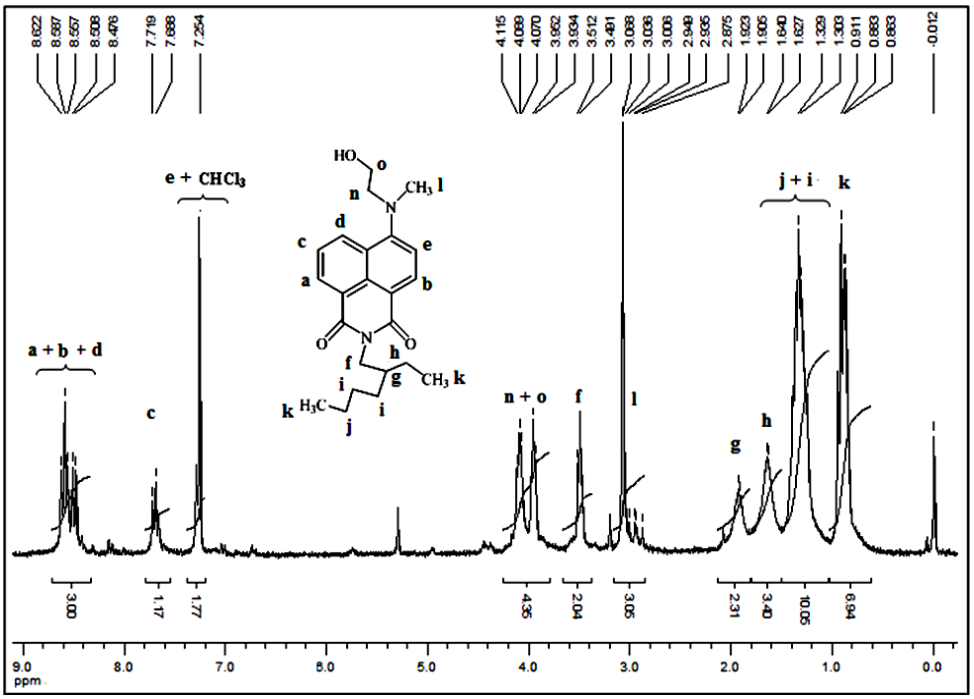

Figure 4.24 : ^{1}H NMR spectrum of II.

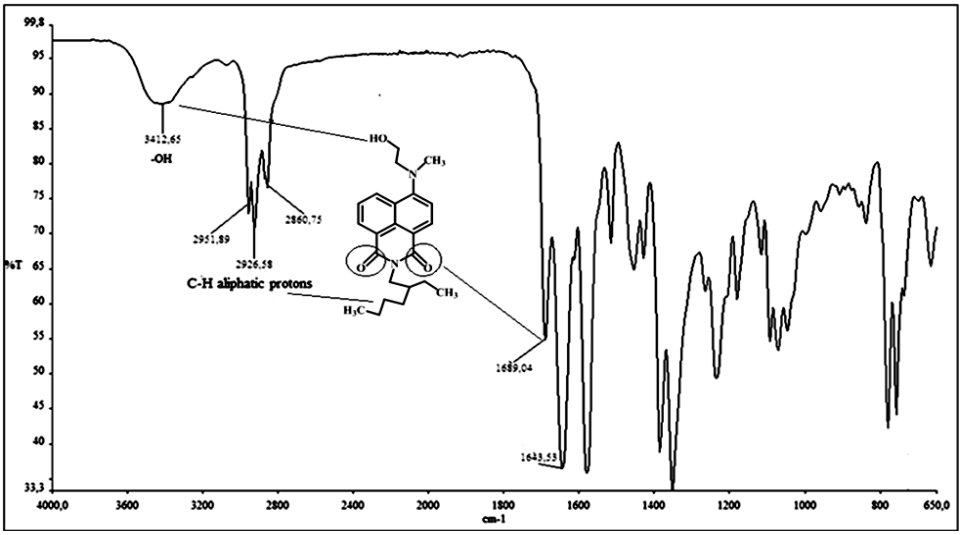

Figure 4.25 : FT-IR spectrum of II.

4.1.2.3 Synthesis of 2-((2-(2-ethylhexyl)-1,3-dioxo-2,3-dihydro-1H-benzo[de]isoquinolin-6-yl)(methyl)amino)ethyl acrylate (AM, acceptor monomer)

II and acryloyl chloride were reacted to synthesize AM according to the reaction depicted in Figure 4.26. The presence of 3 aromatic protons of napthalimide (a, b, e) at 8.58-8.46 ppm, –O$\underline{CH_2}$- (h), -N-$\underline{CH_2}$- (o+ı), -N-$\underline{CH_3}$ (r) protons at 4.49-3.09 ppm and vinyl group (j, f, g) at 6.34-5.78 ppm in the ^{1}H NMR were an evidence for the formation of **AM** (Figure 4.27). Moreover, the formation of **AM** was supported by FT-IR spectrum which shows disapperance of O-H peak of **II** at 3412 cm^{-1}, the presence of ester carbonyl stretching peak at 1723 cm^{-1} and the -CO-N-CO- peak of at 1689 and 1650 cm^{-1} (Figure 4.28). The melting point and purity of AM were determined as 47 ^{o}C and 96.73 mol% by DSC, respectively (Figure 4.29).

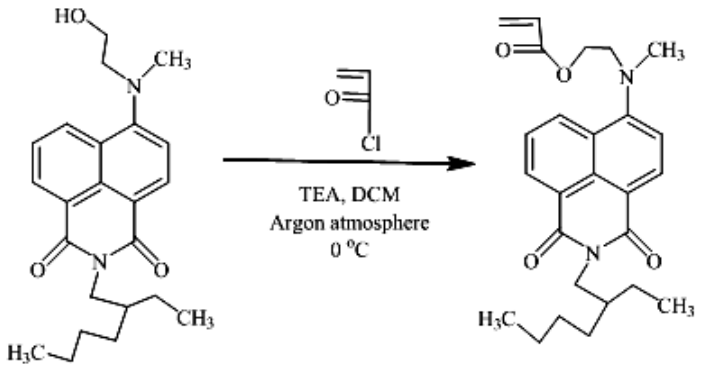

Figure 4.26 : Synthesis of **AM.**

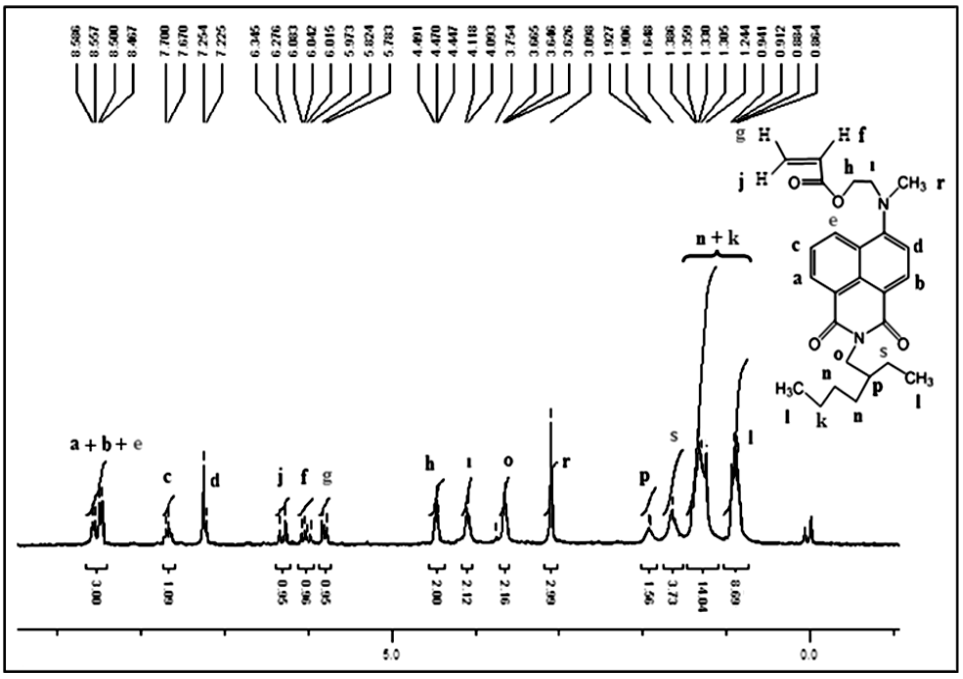

Figure 4.27 : ^{1}H NMR spectrum of **AM.**

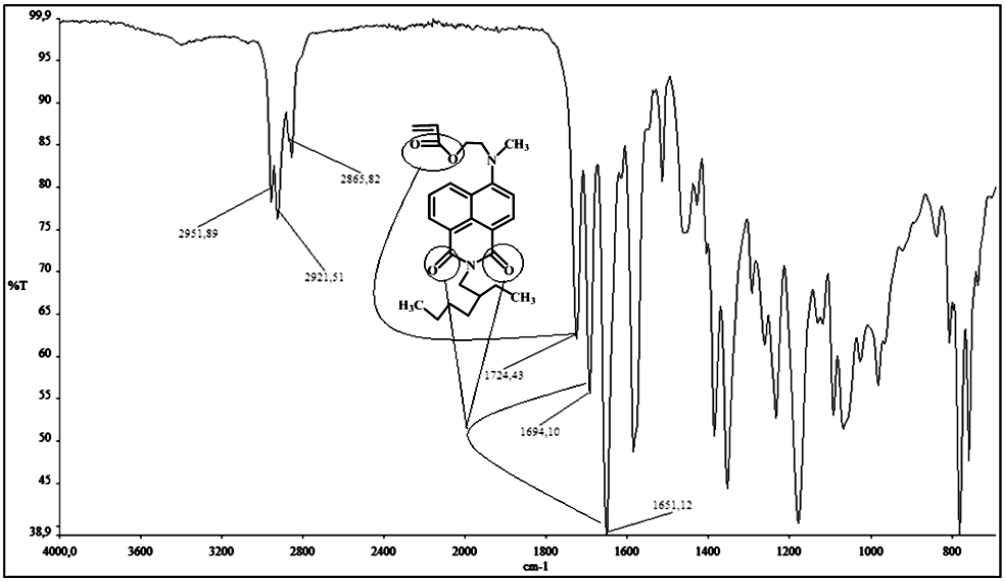

Figure 4.28 : FT-IR spectrum of **AM.**

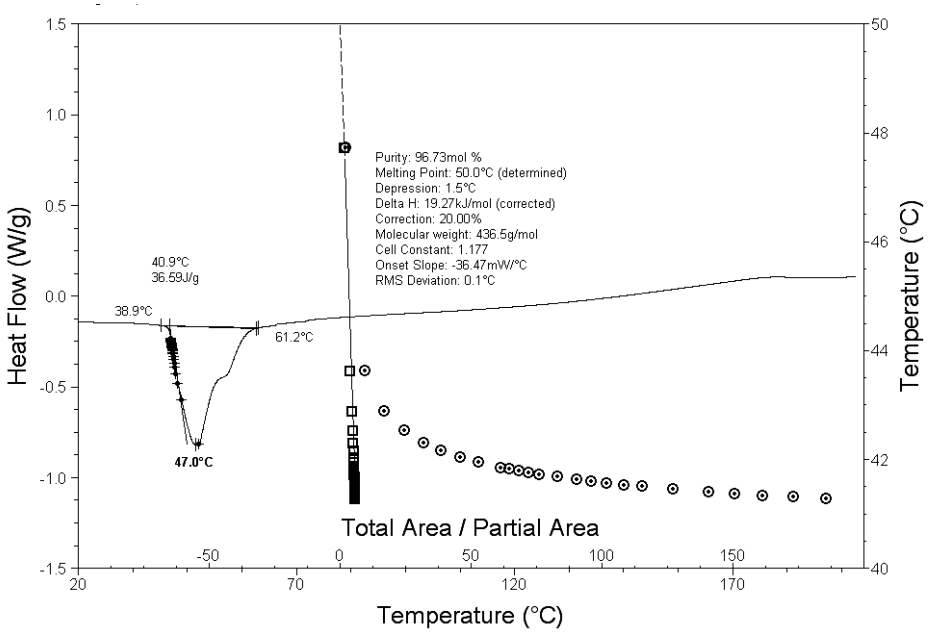

Figure 4.29 : DSC thermodiagram of **AM.**

4.2 Donor-Acceptor Type Polymer Synthesis

4.2.1 Carbazole side-chain polymers synthesis

4.2.1.1 Synthesis of poly(4-(9-carbazolyl)methylstyrene)

Monomer CzMS was polymerized by using AIBN as an initiator in cyclohexanone (Figure 4.30). The signals at 8.05-8.00 and 7.24-7.02 ppm in ^{1}H NMR spectrum of PCzMS were attributed to aromatic peaks of carbazole. The observation of the broad peaks and the absence of protons of vinyl group in the ^{1}H NMR were an evidence for

the formation of poly(4-(9-carbazolyl)methyl styrene) (PCzMS) (Figure 4.31). Absence of vinyl group of CzMS at 904.7 cm^{-1} in FT-IR of the PCzMS was an evidence for the formation of PCzMS (Figure 4.32). The numberaverage molecular weights and polydispersity were measured by GPC against PS standarts and found as M_n=3420 g/mol and PDI=2.04 (Figure 4.33). According to DSC results, the glass transition temperature (T_g) of PCzMS was measured as 155 ^oC (Figure 4.34). The melting point peak of CzMS was not seen in DSC thermogram of PCzMS which is proved that unreacted monomer is not exist in the polymer.

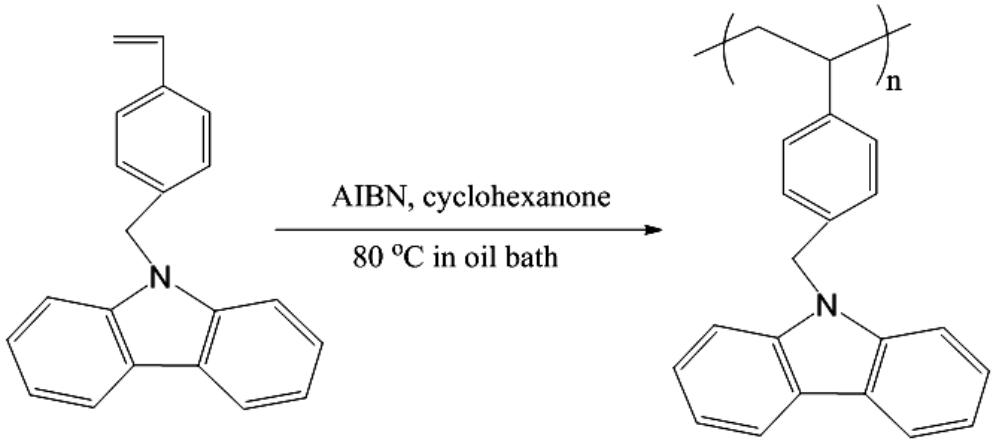

Figure 4.30 : Synthesis of PCzMS.

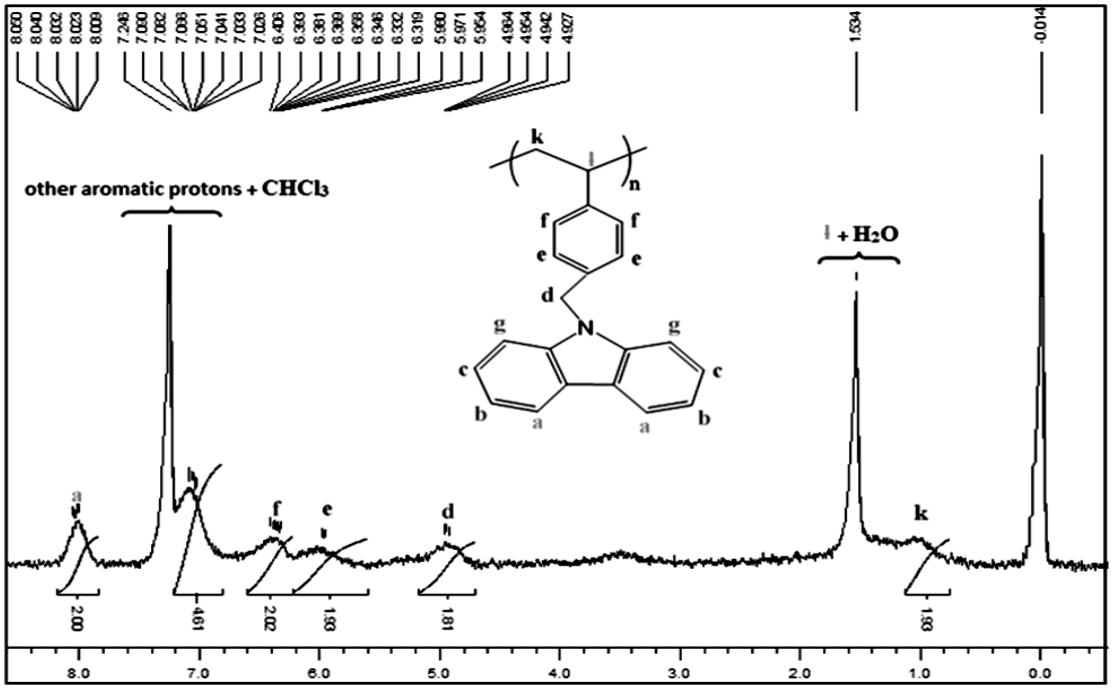

Figure 4.31 : ^1H NMR spectrum of PCzMS.

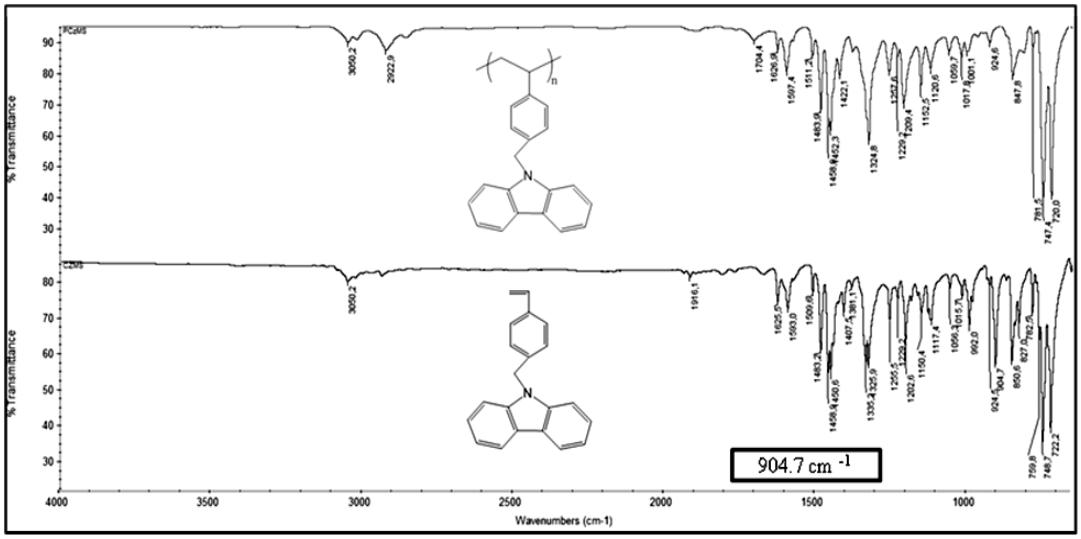

Figure 4.32 : FT-IR spectrum of PCzMS.

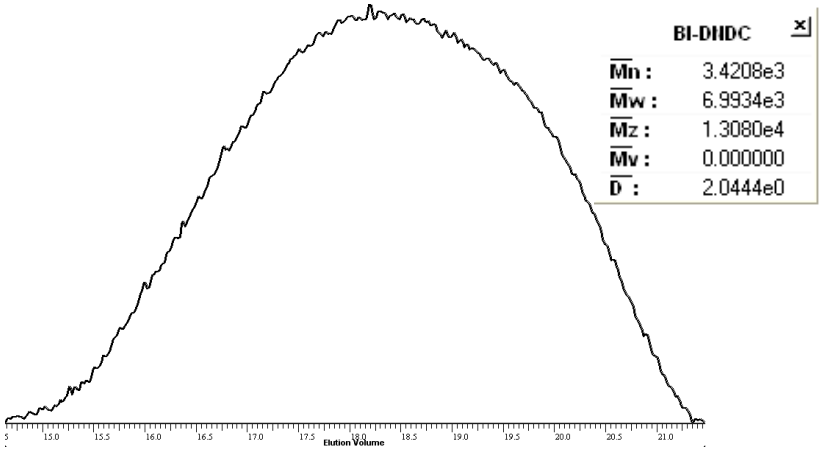

Figure 4.33 : GPC trace of PCzMS.

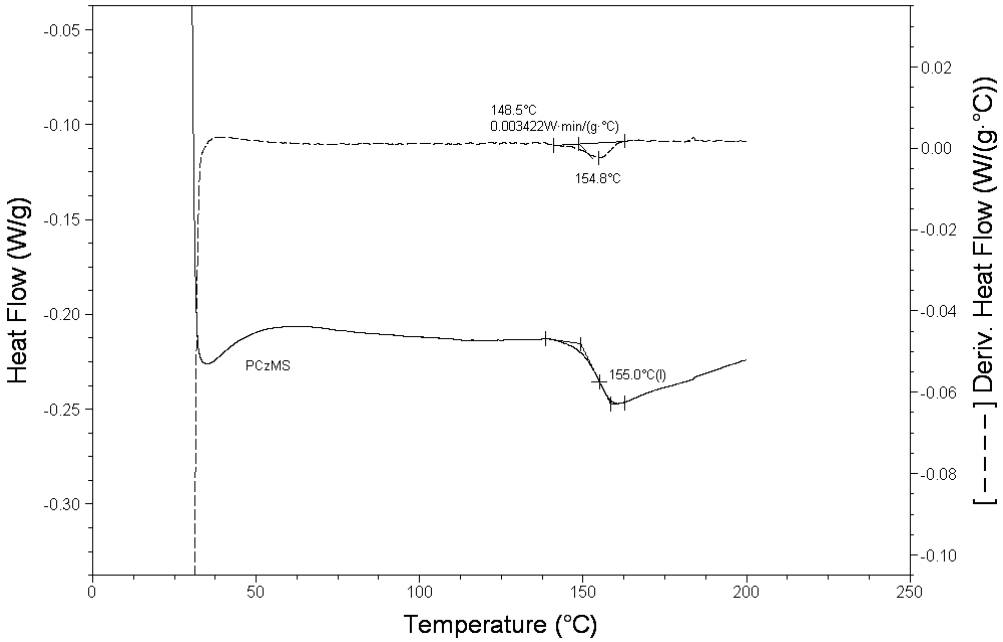

Figure 4.34 : DSC thermodiagram of PCzMS.

4.2.1.2 Synthesis of poly(9-(2-(4-vinylbenzyloxy)ethyl)-9H-carbazole)

Monomer VBEC was polymerized by using AIBN as an initiator in cyclohexanone (Figure 4.35). The signals at 7.99-7.95 and 7.35-7.12 ppm in ^{1}H NMR spectrum of poly(9-(2-(4-vinylbenzyloxy)ethyl)-9H-carbazole) (PVBEC) were attributed to aromatic peaks of carbazole. The broad peaks and the absence of protons of vinyl group in the ^{1}H NMR were an evidence for the formation of PVBEC (Figure 4.36). Absence of vinyl group of VBEC at 925.6 cm^{-1} in FT-IR was also evidenced the formation of PVBEC (Figure 4.37). The numberaverage molecular weights and polydispersity were measured by GPC against PS standarts and found as M_n= 4480 g/mol and PDI=1.88 (Figure 4.38). The glass transition temperature (T_g) of PVBEC was determined as 74.8 °C by DSC (Figure 4.39). The melting point of VBEC (94.9 °C) was not seen in DSC thermogram of PVBEC which proves that there is no monomer residue in the polymer.

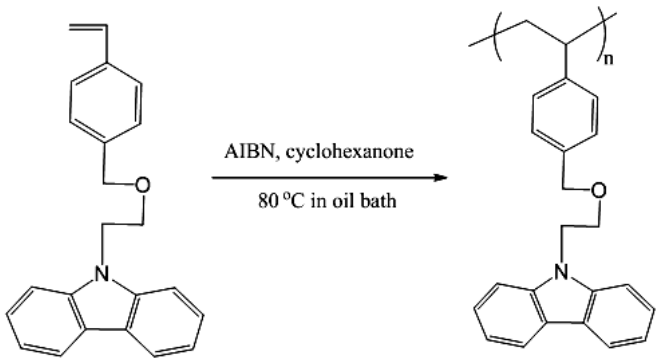

Figure 4.35 : Synthesis of PVBEC.

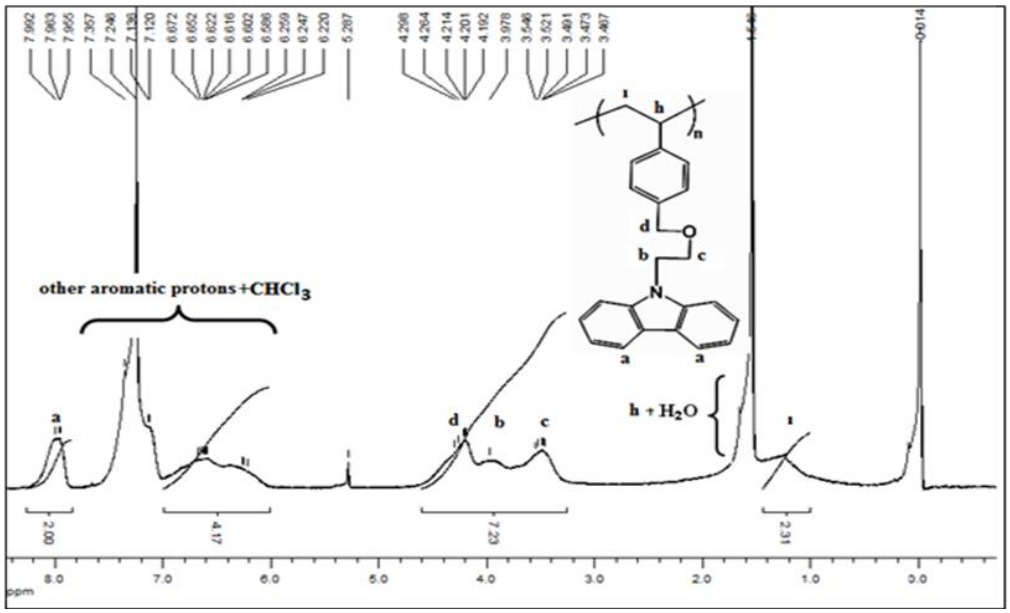

Figure 4.36 : ^{1}H NMR spectrum of PVBEC.

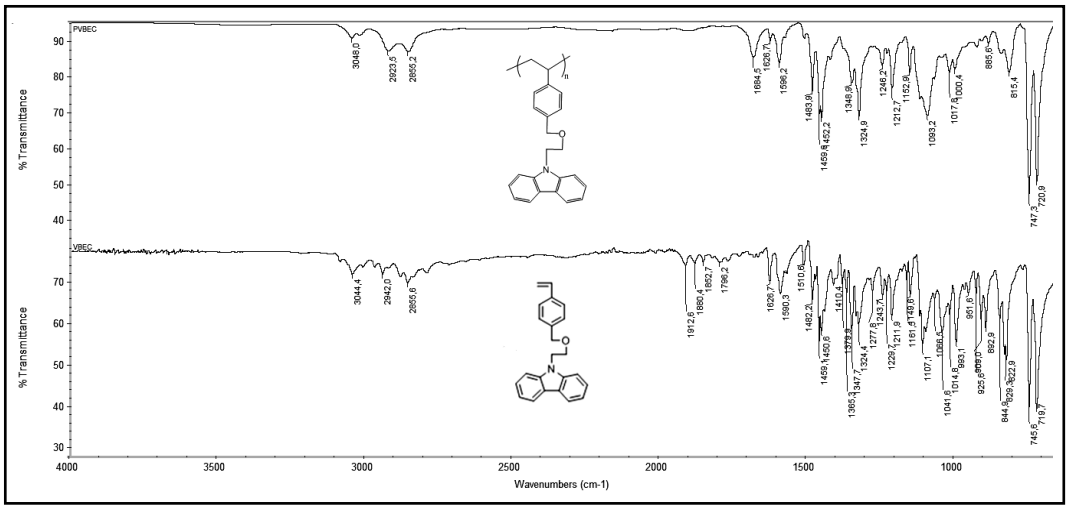

Figure 4.37 : FT-IR spectrum of PVBEC and VBEC.

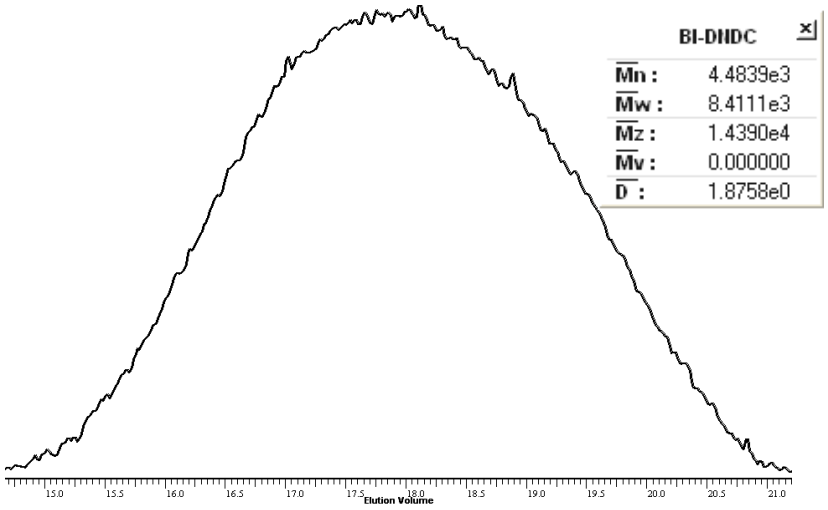

Figure 4.38 : GPC trace of PVBEC.

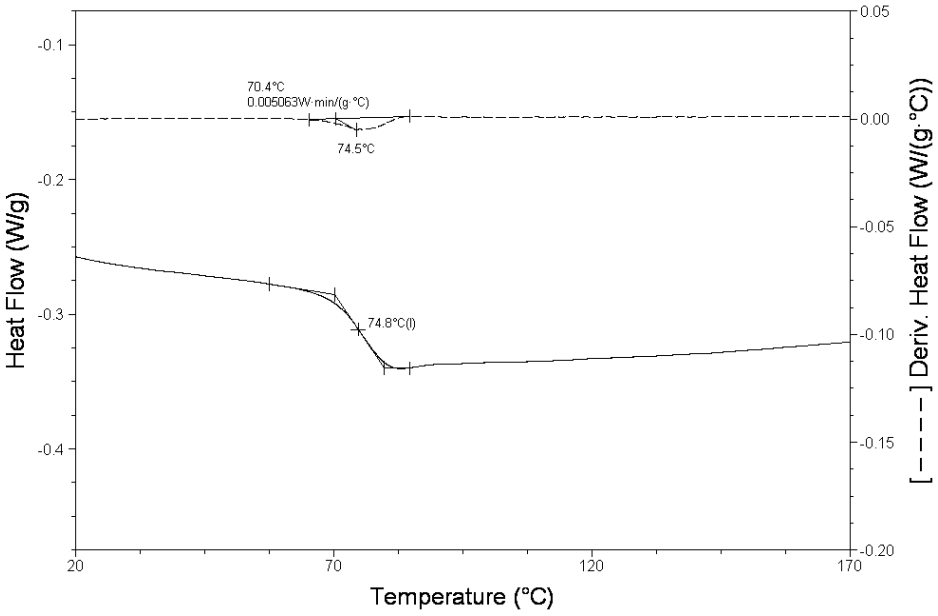

Figure 4.39 : DSC thermodiagram of PVBEC.

4.2.1.3 Synthesis of poly(2-(9H-carbazol-9-yl)ethylacrylate)

Monomer CEA was polymerized by using AIBN as an initiator in cyclohexanone (Figure 4.40). The signals at 7.94-7.92 and 7.24-7.10 ppm in ^{1}H NMR spectrum of poly(2-(9H-carbazol-9-yl)ethylacrylate) (PCEA) were attributed to aromatic peaks of carbazole. The broad peaks and the absence of protons of vinyl group in the ^{1}H NMR were an evidence for the formation of PCEA (Figure 4.41). Absence of vinyl group of CEA at 979.4 and 909 cm^{-1} in FT-IR was an evidence for the formation of PCEA (Figure 4.42). The numberaverage molecular weights and polydispersity were measured by GPC against PMMA standarts and found as M_n=1810 g/mol and PDI=1.38 (Figure 4.43). The glass transition temperature (T_g) of PCEA was determined as 81.2 °C by DSC (Figure 4.44). The melting point of CEA (77.3 °C) was not seen in DSC thermogram of PCEA which proves that there is no monomer residue in the polymer.

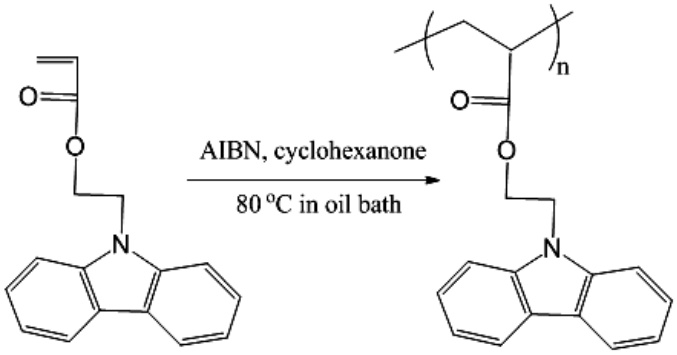

Figure 4.40 : Synthesis of PCEA.

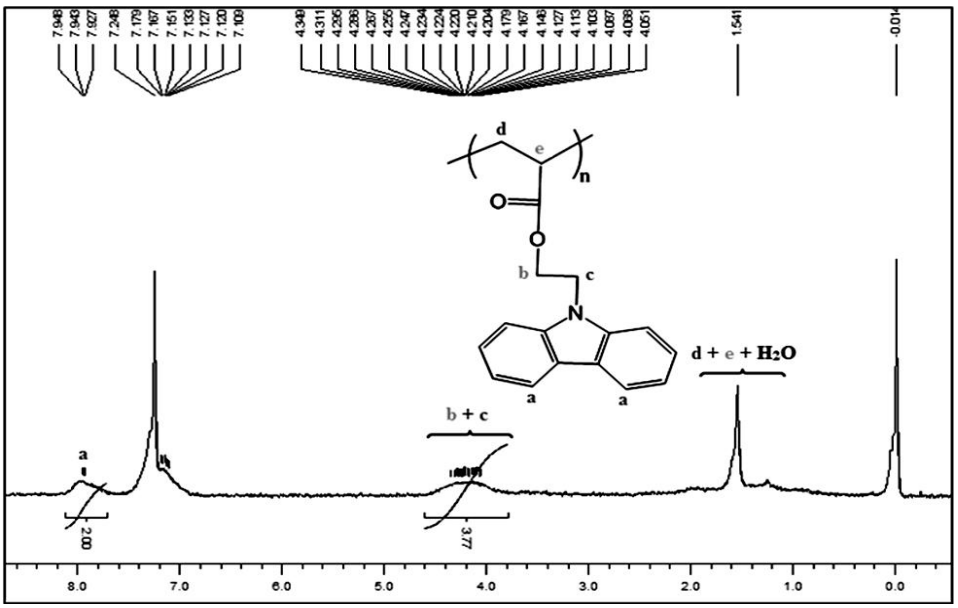

Figure 4.41 : ^{1}H NMR spectrum of PCEA.

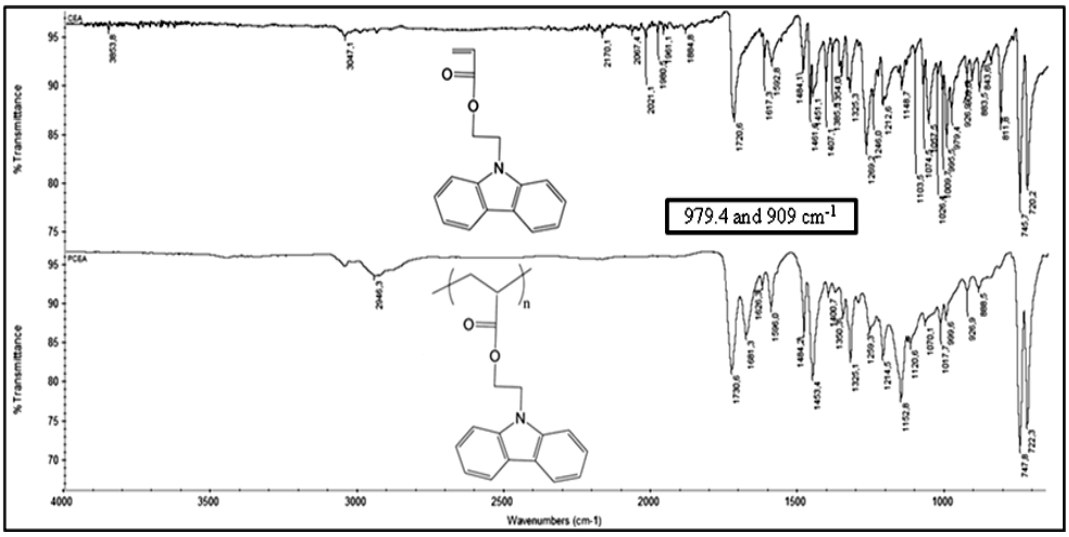

Figure 4.42 : FT-IR spectrum of PCEA and CEA.

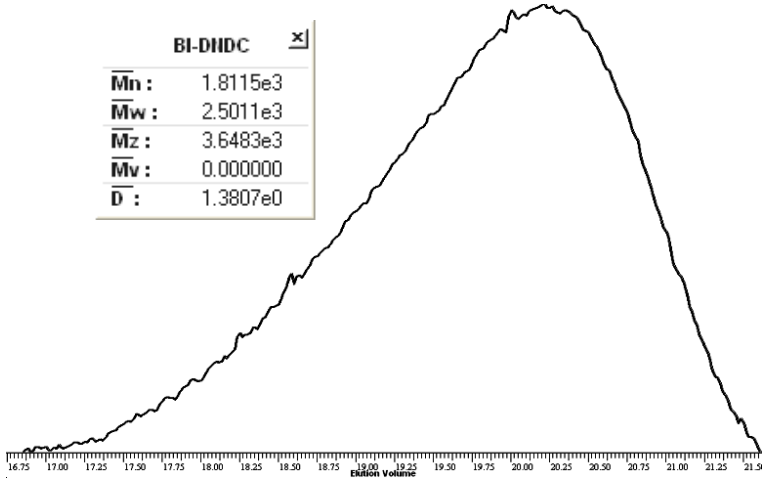

Figure 4.43 : GPC trace of PCEA.

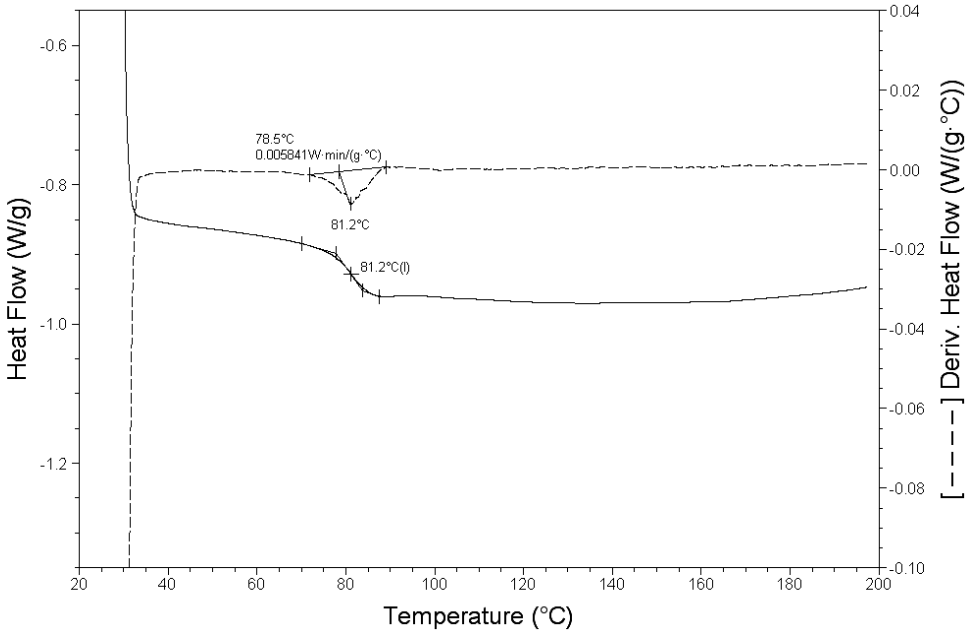

Figure 4.44 : DSC thermodiagram of T_g of PCEA.

4.2.2 The synthesis of 1,8-naphtalamide side-chain containing polymer

AM was polymerized by using AIBN as an initiator in cyclohexanone (Figure 4.45). The signals at 8.54-8.35, 7.36-7.62 and 7.25 ppm in ^{1}H NMR spectrum of acceptor polymer (PAM) were attributed to aromatic peaks of naphtalamide. The broad peaks and the absence of protons of vinyl group in the ^{1}H NMR were an evidence for the formation of PAM (Figure 4.46). The presence of broad peaks and the absence of vinyl group at 977 cm^{-1} in FT-IR spectrum of PAM were a proof for the formation of PAM (Figure 4.47). The glass transition temperature (T_g) of PAM was determined as 33.1 ^{o}C by DSC (Figure 4.48). The melting point of AM (47 ^{o}C) was not seen in DSC thermogram of PAM which proves that there is no monomer residue in the polymer.

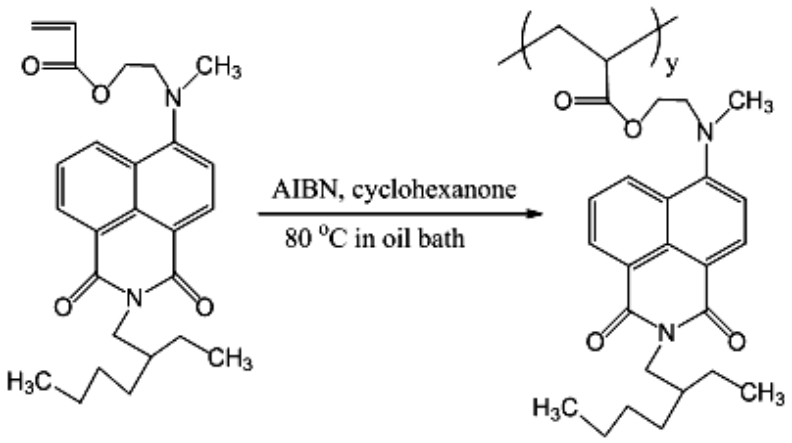

Figure 4.45 : Synthesis of PAM.

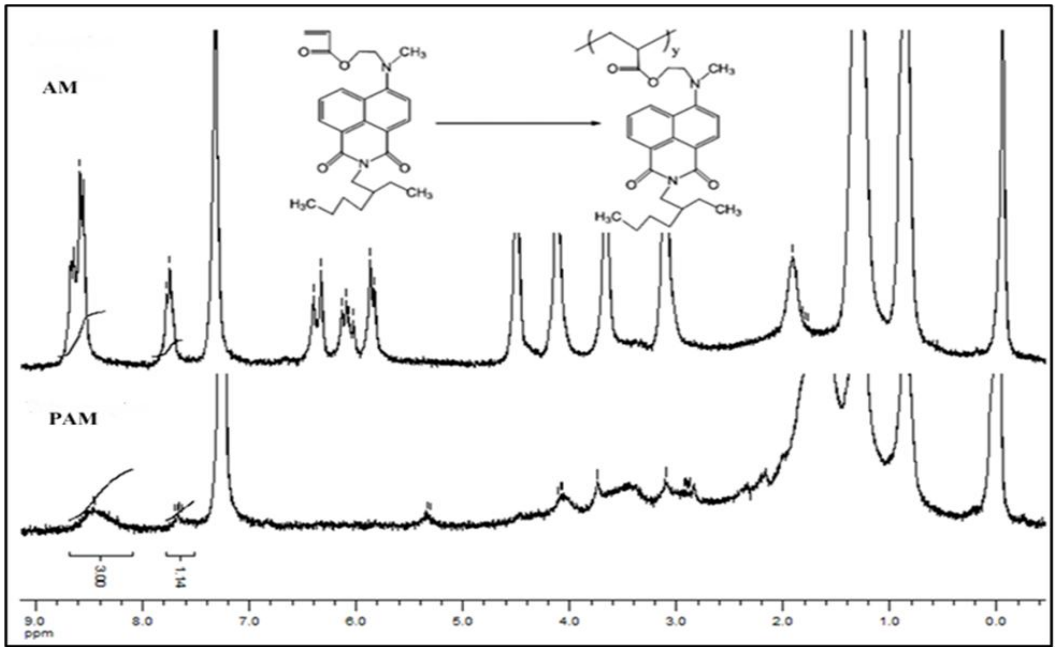

Figure 4.46 : ^{1}H NMR spectrum of PAM.

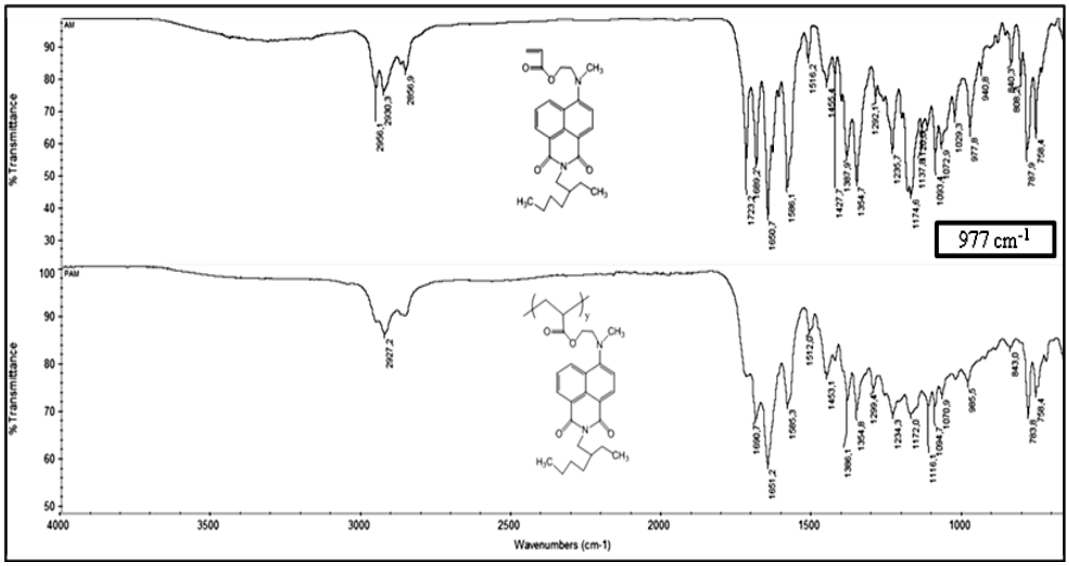

Figure 4.47 : FT-IR spectrum of AM and PAM.

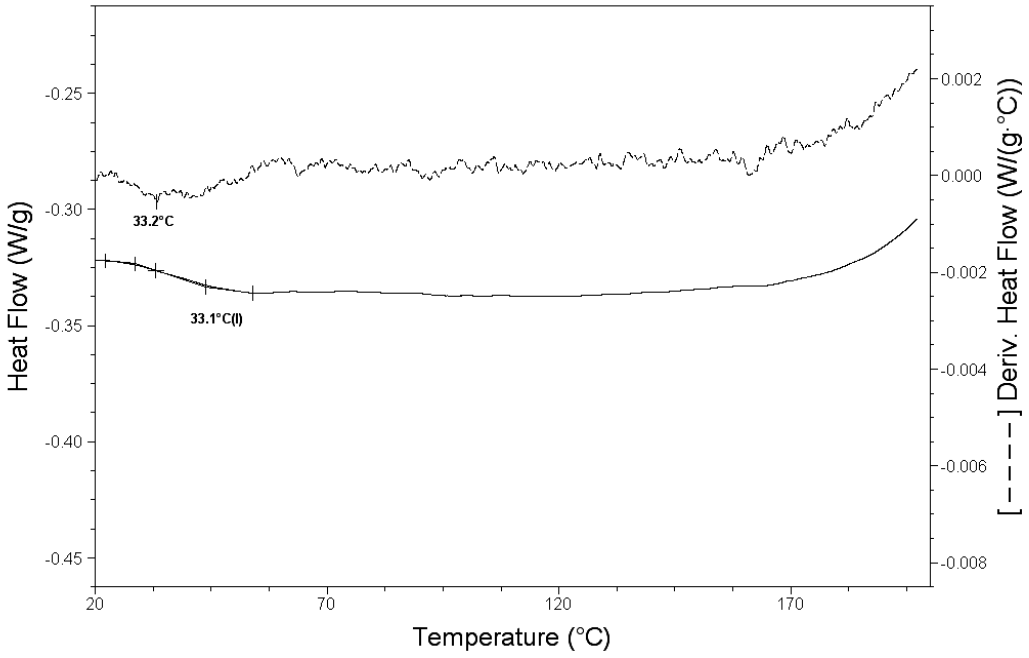

Figure 4.48 : DSC thermodiagram of T_g of PAM.

4.2.3 The synthesis of donor-acceptor side chain containing copolymer

4.2.3.1 Synthesis of poly(CzMS-*r*-AM)

AM and CzMS were copolymerized by using AIBN as an initiator in cyclohexanone (Figure 4.49). The presence of some aromatic protons of carbazole at 8.02-8.00 (2H) and naphalimide 8.36-8.34 (3H) were seen in the ^{1}H NMR (Figure 4.50). The broad peaks and the absence of protons of vinyl group in the ^{1}H NMR were an evidence for

the formation of poly(CzMS-*r*-AM) (Figure 4.50). Copolymer fractions of AM and CzMS calculated by ^{1}H NMR using equation **(4.1)**,

$$F_1 = \frac{I_1/3H}{(I_1/3H)+(I_2/2H)} \quad \textbf{(4.1)}$$

F_2= 1-F_1, where F_1 and F_2 are the contents of AM and CzMS units, respectively, in the copolymer chain, I_1 the peak area of proton in aromatic -CH=CH- (δ=8.36-8.34, 3H) characteristic for AM units and I_2 the peak area of protons in aromatic -CH=CH- (δ=8.02-8.0 ppm, 2H) for CzMS units. Although (n_{AM})/(n_{CzMS}) ratio was 0.33 in theoretical, the copolymer fraction was found as F1= 0.177 and F_2= 0.823 according to the equation (**4.1**).

The calculated T_g value from Fox equations **(4.2)** is compared with observed T_g value from DSC curves, where w_1 and w_2 are the weight fractions of AM and CzMS in the copolymer, respectively. T_{g1} and T_{g2} are the glass transition temperatures of homopolymer of AM (T_g=33.1 ^{o}C) and CzMS (T_g=155 ^{o}C), respectively. The observed T_g value is 128.3 ^{o}C for poly(CzMS-*r*-AM) (Figure 4.53) which has quite good matching with theoretical one calculated from Fox equations as 126.8 ^{o}C.

Fox's equation is:

$$\frac{1}{T_g} = \frac{w_1}{T_{g1}} + \frac{w_2}{T_{g2}} \quad \textbf{(4.2)}$$

The observed peak of ester carbonyl stretching at 1729 cm^{-1}, the peak of -CO-N-CO- at 1693 and 1653 cm^{-1} of AM and the absence of peaks of vinyl group of at 977 cm^{-1} and of CzMS at 904 cm^{-1}, the signal at 748-722 cm^{-1} belong to CzMS in FT-IR spectrum were proved that copolymer formation (Figure 4.51). The numberaverage molecular weights and polydispersity were measured by GPC against PS standarts and found as M_n=2674 g/mol and PDI=1.39 (Figure 4.52). Unseen the melting points signal of CzMS and AM (175.3 and 47 ^{o}C, respectively) in DSC thermogram was proved the absence of unreacted monomers in the copolymer (Figure 4.53). In addition that, the glass transition temperature (T_g) of poly(CzMS-*r*-AM) as 128.3 ^{o}C is different than the glass transition temperature of PCzMS (T_g = 155 ^{o}C) and PAM (T_g = 33.1 ^{o}C) (Figure 4.54).

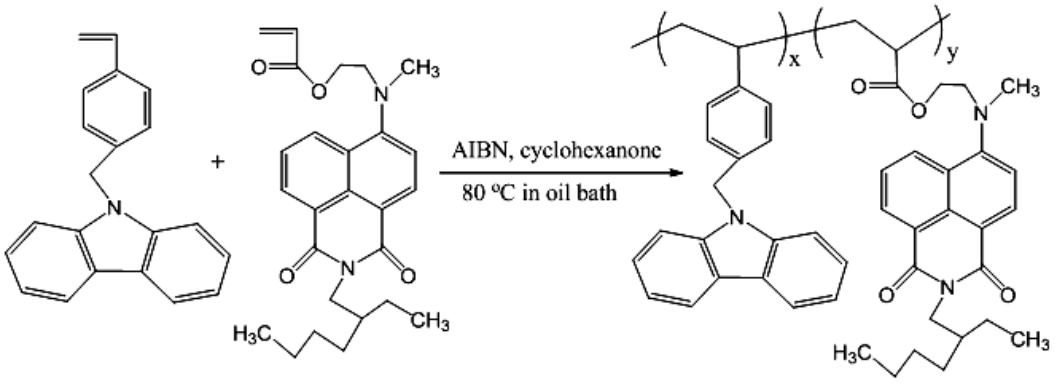

Figure 4.49 : Synthesis of poly(CzMS-*r*-AM).

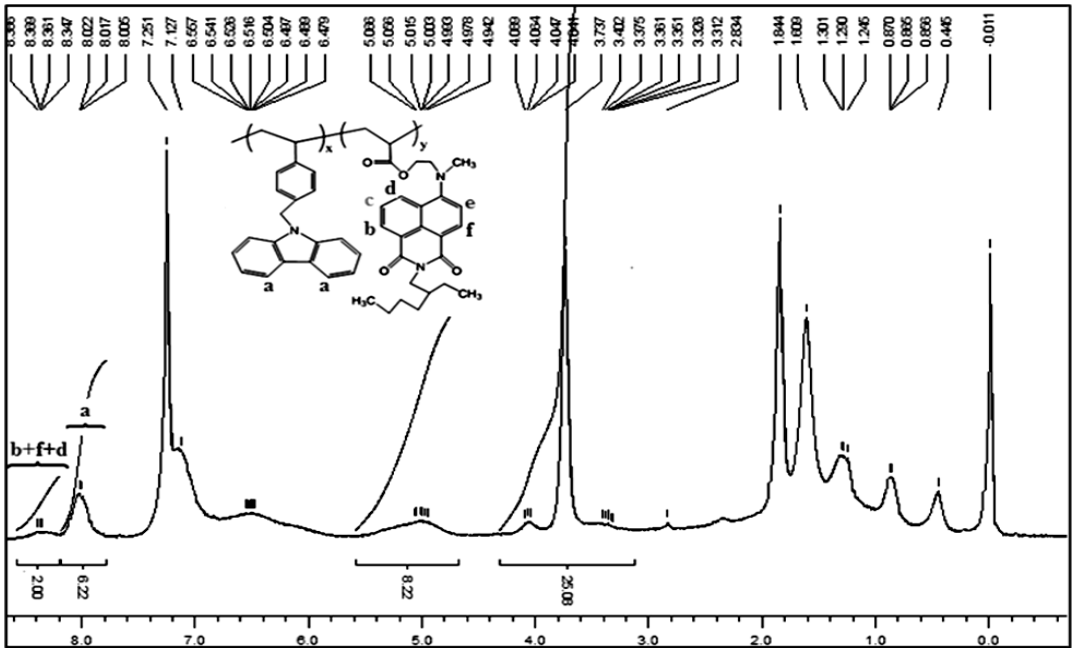

Figure 4.50 : ^{1}H NMR spectrum of poly(CzMS-*r*-AM).

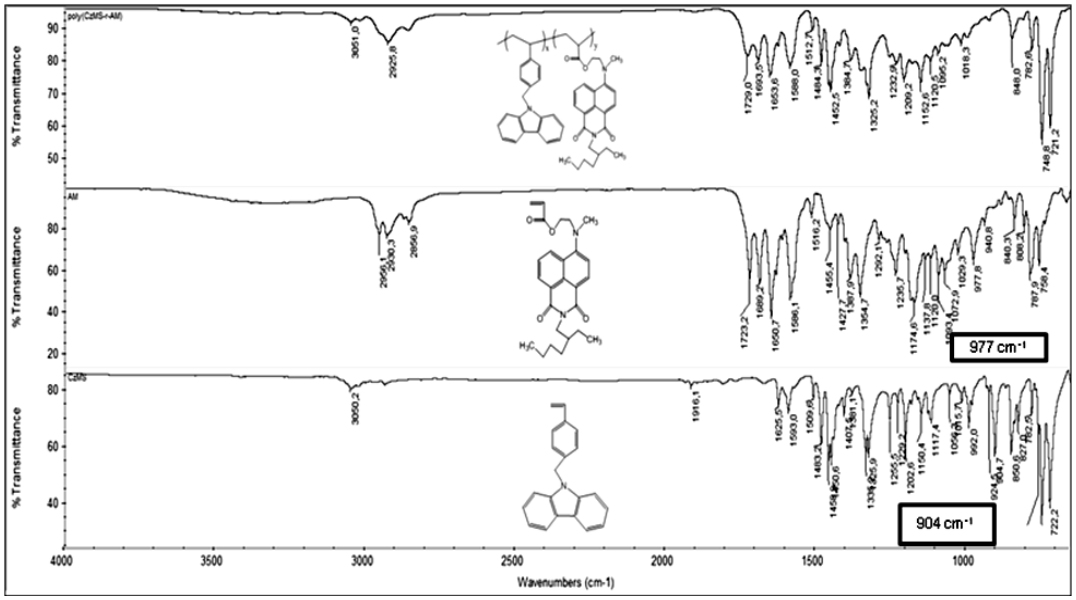

Figure 4.51 : FT-IR spectrum of poly(CzMS-*r*-AM), AM and CzMS.

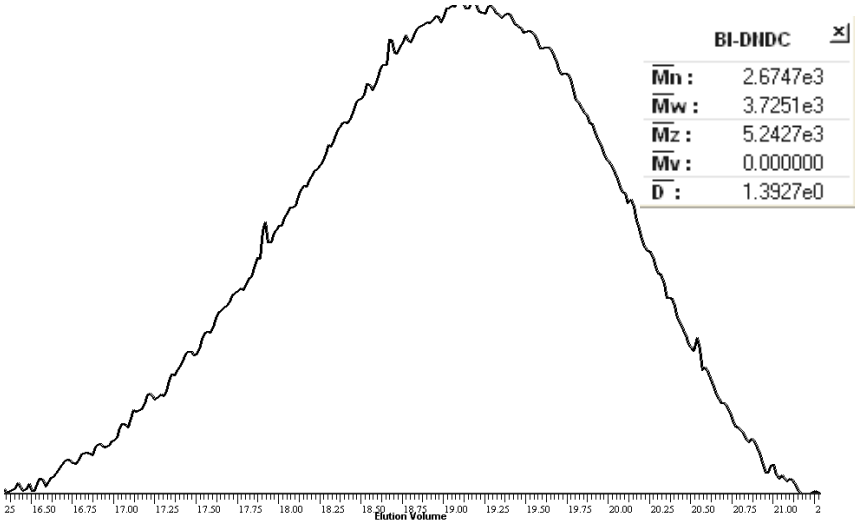

Figure 4.52 : GPC trace of poly(CzMS-*r*-AM)

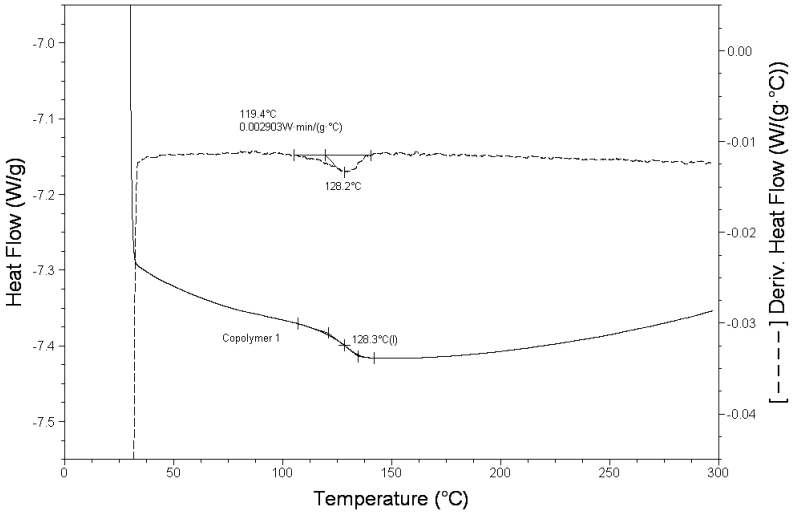

Figure 4.53 : DSC thermodiagram of T_g of poly(CzMS-*r*-AM).

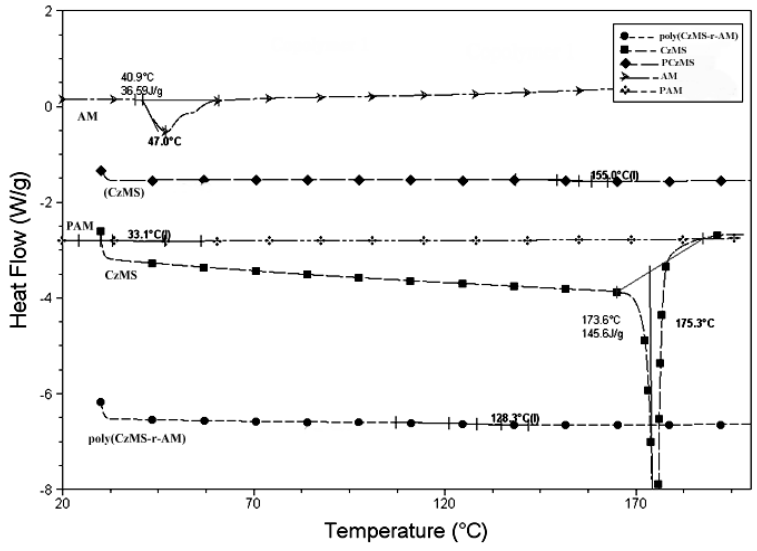

Figure 4.54 : DSC thermogram of poly(CzMS-*r*-AM), PCzMS, PAM, CzMS and AM.

4.2.3.2 Synthesis of poly(VBEC-*r*-AM)

VBEC and AM were copolymerized by using AIBN as an initiator in cyclohexanone (Figure 4.55). The presence of some aromatic protons of carbazole at 8.02-7.95 (2H) and naphalimide at 8.47-8.43 (3H) were seen in the ^{1}H NMR (Figure 4.56). Although, some small peaks of vinyl protons were seen in the ^{1}H NMR, the melting points of VBEC and AM (94.9 and 47 ^{o}C, respectively) were not seen in DSC thermogram which proves that the copolymer do not contain monomers (Figure 4.59). In addition that, the observed broad peaks in ^{1}H NMR were also one of evidence for the formation of poly(VBEC-*r*-III) (Figure 4.56). Copolymer fractions of AM and VBEC calculated by ^{1}H NMR using equation **(4.3)**.

$$F_1 = \frac{I_1/3H}{(I_1/3H)+(I_2/2H)} \qquad \textbf{(4.3)}$$

F_2= 1-F_1, where F_1 and F_2 are the contents of AM and VBEC units, respectively, in the copolymer chain, I_1 represents the peak area of proton in aromatic for AM units at δ=8.47–8.43 ppm (3H) and I_2 represents the peak area of aromatic protons for VBEC unit at δ=8.02-7.95 ppm (2H) for VBEC units. Although (n_{AM})/(n_{VBEC}) ratio was 1 in theoretical, the copolymer fraction was found as F_1= 0.39 and F_2= 0.61 according to the equation **(4.3)**.

The observed peak of ester carbonyl stretching at 1726 cm^{-1}, the peak of -CO-N-CO- at 1689 and 1651 cm^{-1} and the aromatic peak at 784 cm^{-1} of AM and the absence of peaks of vinyl group of acceptor at 977 cm^{-1} and of VBEC at 893 cm^{-1}, the asymmetrical ether stretching at 1153 cm^{-1} (-C-O-C-) and aromatic peak at 723 cm^{-1} belong to VBEC in FT-IR spectrum were proved that copolymer formation (Figure 4.57). The numberaverage molecular weights and polydispersity were measured by GPC against PS standarts and found as M_n=3630 g.mol^{-1} and PDI=1.5 (Figure 4.58).

The calculated T_g value from Fox equations **(4.2)** is compared with observed T_g value from DSC curves, where w_1 and w_2 are the weight fractions of acceptor and VBEC in the copolymer, respectively. T_{g1} and T_{g2} are the glass transition temperatures of homopolymer of AM (T_g=33.1 ^{o}C) and VBEC (T_g=74.8 ^{o}C), respectively. The observed T_g value is 55.4 ^{o}C (Figure 4.59) for poly(VBEC-*r*-AM) which has quite good matching with theoretical one calculated from Fox equations as 57.3 ^{o}C. In addition that, the glass transition temperature (T_g=55.4 ^{o}C) of poly(VBEC-*r*-AM)

was seen different from the glass transition temperature (T_g) of PVBEC (74.8 ^oC) and PAM (33.1 ^oC) (Figure 4.60). Unseen the melting points signal of VBEC and AM (94.9 and 47 ^oC, respectively) in DSC thermogram was proved the absence of unreacted monomers (Figure 4.60).

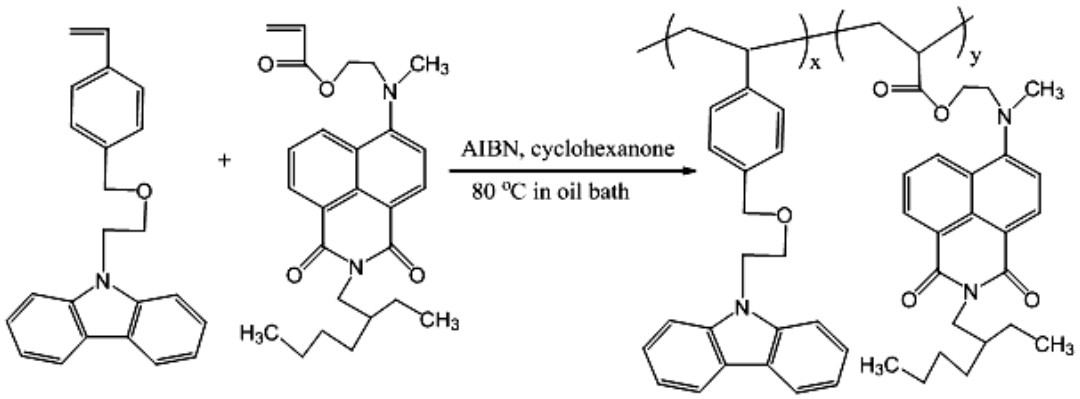

Figure 4.55 : Synthesis of poly(VBEC-*r*-AM).

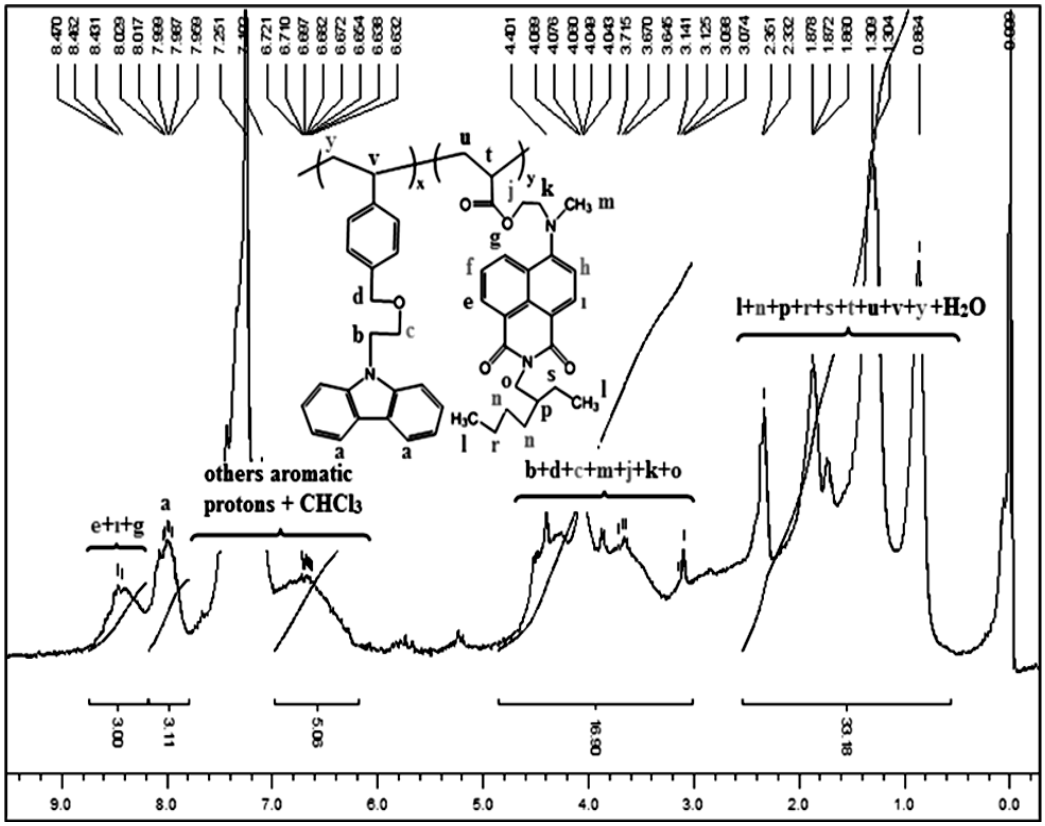

Figure 4.56 : ^1H NMR spectrum of poly(VBEC-*r*-AM).

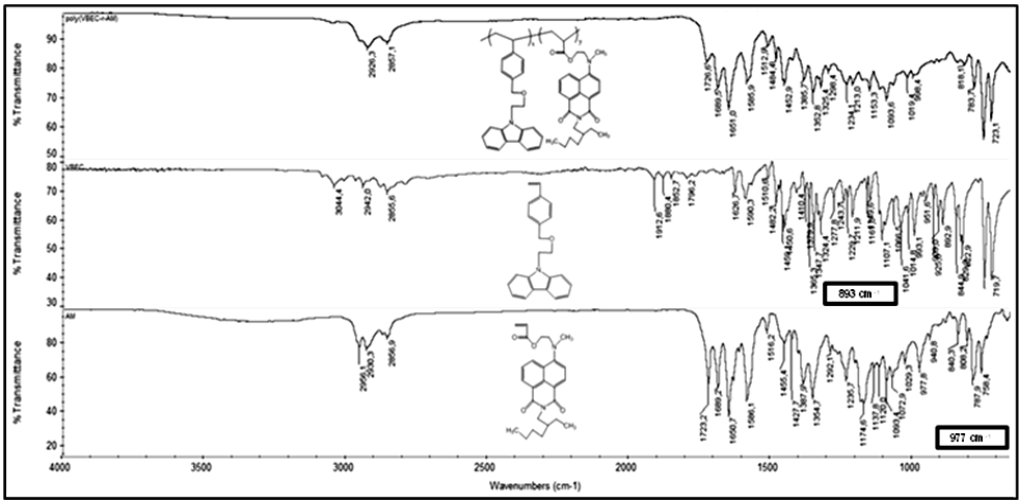

Figure 4.57 : FT-IR spectrum of poly(VBEC-*r*-AM), AM and VBEC.

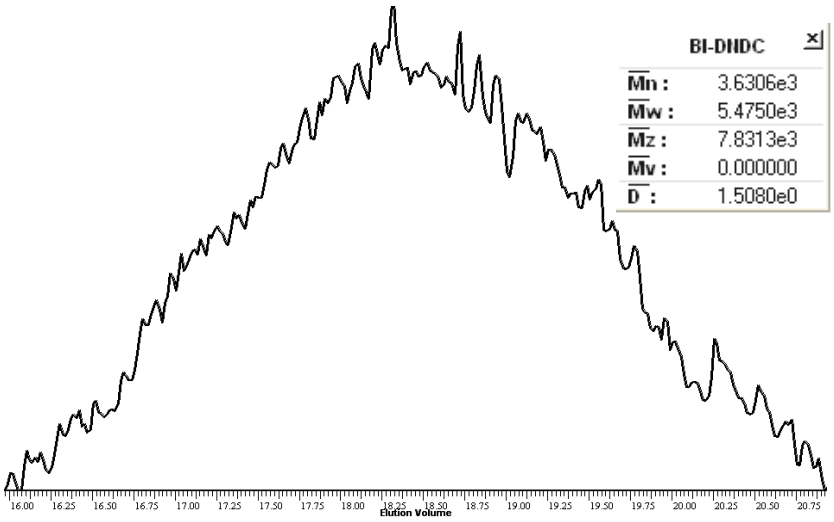

Figure 4.58 : GPC trace of poly(VBEC-*r*-AM).

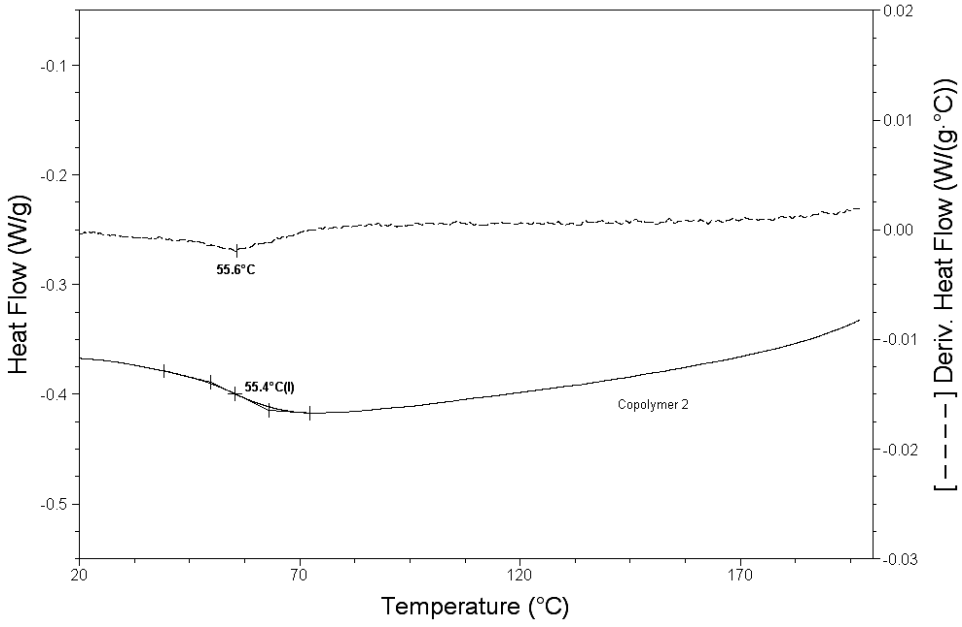

Figure 4.59 : DSC thermodiagram of T_g of poly(VBEC-*r*-AM).

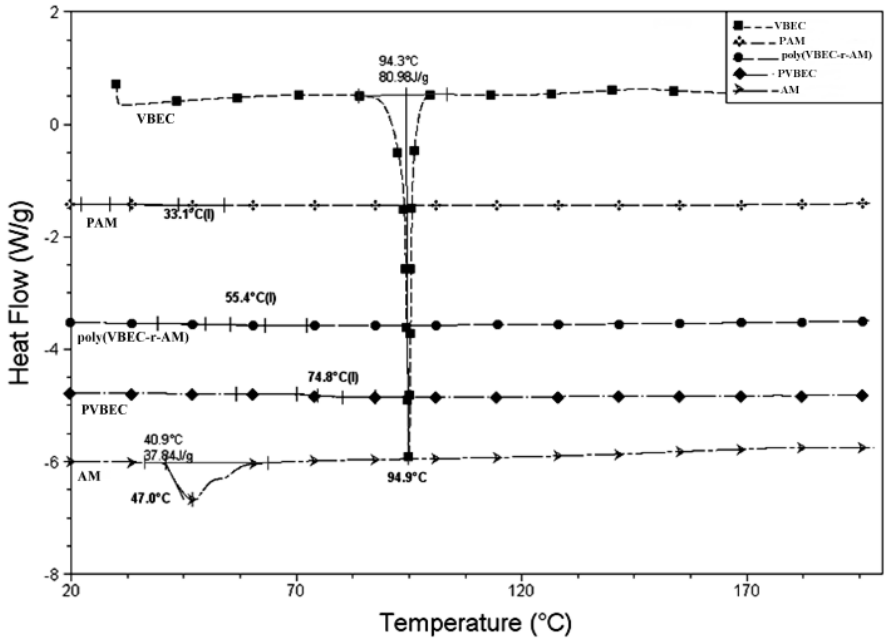

Figure 4.60 : Illustration of T_g of poly(VBEC-*r*-AM).

4.3 Electrochemical properties of carbazol side chain polymers

The electrochemical properties of carbazole side chain donor polymers were investigated by cyclic voltammetry (CV). An explicit difference in redox behavior of the PCzMS, PCEA and PVBEC can be deduced from the CV which was depicted in Figure 4.61. During CV scan in the anodic regime of carbazole side chain donor polymer with different spacer moiety, semi reversible oxidation peaks were exhibited at $E^{ox}_{m,a}$ =+1.30V and $E^{ox}_{m,c}$ =+0.96 V; $E^{ox}_{m,1/2}$ =+1.13V for PCzMS, $E^{ox}_{m,a}$ = +1.19V and $E^{ox}_{m,c}$ =+0.75V; $E^{ox}_{m,1/2}$ =+0.97V for PCEA, $E^{ox}_{m,a}$ = +1.19V and $E^{ox}_{m,c}$ = +0.73V; $E^{ox}_{m,1/2}$ = +0.96V for PVBEC during an anodic scan.

Electrochemical crosslinking was carried out in a reaction medium containing 2.0 × 10^{-3} M carbazole side chain donor polymers and 0.1 M $TBAPF_6$/DCM via repetitive cycling at a scan rate of 100 mV s^{-1}. The electroactive polymers were directly coated onto the working electrode (platinum disc or ITO/glass surface). Potentiodynamic electrochemical crosslinking of PCzMS was carried out repetitive cycling at a potential between 0 and 1.65 V exhibited two new redox couple at $E^{ox1}_{m,a}$ = +1.14V and $E^{ox1}_{m,c}$ = +0.94V and $E^{ox2}_{m,a}$ = +1.43V and $E^{ox2}_{m,c}$ = +0.21V (Figure 4.61). Due to presence of electron rich etoxy spacer group, electrochemical polymerization of PCEA and

PVBEC requires higher potentials compared with PCzMS standard molecule. Because of this effect, PCEA and PVBEC was scanned more narrow range for crosslinking process. All peaks were increased current density after each successive cycle clearly indicated the formation of crosslinked polymer deposited onto the surface of the working electrode. Prepared polymer films on ITO/glass surface was dedoped electrochemically in monomer free-electrolyte solution to equilibrate the redox behavior after washing with CH_3CN to remove dopand agents.

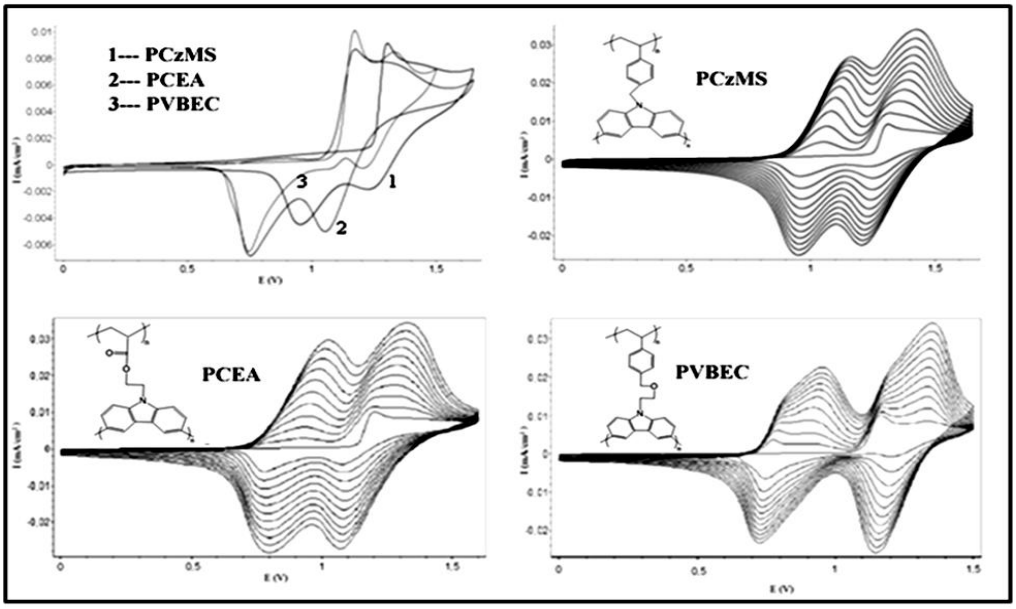

Figure 4.61 : CV voltammogram of PCzMS, PCEA and PVBEC.

In the cathodic scan regime of the cyclic voltammogram of acceptor homopolymer (PAM), it exhibits a characteristic reversible reduction peak with a half wave potential ($E^{red}_{m,c}$) of -1.55V, respectively, and this observation is attributed to one-electron stepwise reduction process of naphthalimide-carbonyl moiety. Similarly, the reversible reduction peaks with half wave potential of −1.54V were observed for stable radical anion formation of poly(VBEC-*r*-AM) (Figure 4.62). In comparison to PAM, the reduction potential of poly(CzMS-*r*-AM) and poly(VBEC-*r*-AM) was observed at the almost same value because of having not connection between donor-carbazole and acceptor-napthalimide parts at the ground state. In the positive regime, poly(CzMS-*r*-AM) exhibits one irreversible oxidation peak ($E^{ox}_{m,a}$) at 1.21V emanating from tertiary amine moiety (Figure 4.62). As expected, oxidation peak of poly(VBEC-*r*-AM) ($E^{ox}_{m,a}$ = 1.30 V) was observed at higher potential due to strongly oxidize of aliphatic tertiary amine moiety than that of carbazole (Figure 4.62).

Furthermore, due to content of naphtalimide moiety (AM) is lower than carbazole moiety (VBEC) in poly(VBEC-*r*-AM) (contents of AM and VBEC units, F_1= 0.39 and F_2= 0.61, respectively), the oxidation peak of carbazole is concealed the oxidation peak of tertiary amine. The oxidation onset potentials of both compounds are observed around 1.02 V as shown in the Figure 4.62.

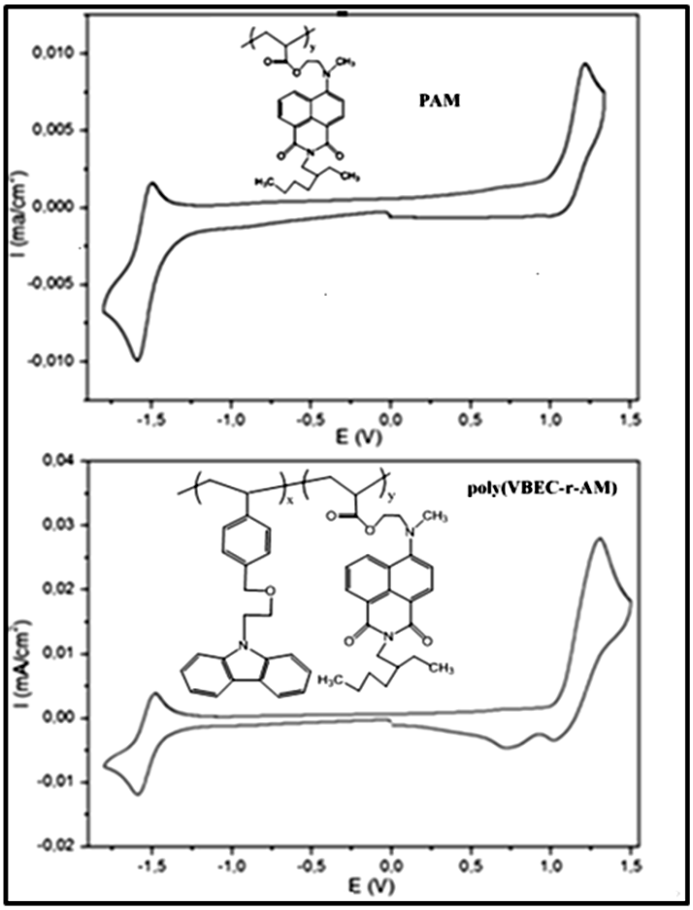

Figure 4.62 : CV voltammogram of PAM and poly(VBEC-*r*-AM).

4.4 Optical properties of carbazol side chain polymers

The absorption spectra of PCzMS, PCEA and PVBEC were recorded in the solution phase using dichloromethane (Figure 4.63). The electronic absorption spectrum of carbazole based polymers exhibited an absorption band with maxima at 292 nm attributed to π-π* transition of carbazole moieties. In addition, the maximum absorption wavelength (λ_{max}) with lower intesity at 328 and 346 nm attributed to n-π* transition of carbazole moieties. According to these results, the optical band gap values of all carbazole side chain donor polymers were found to be 3.52 eV. On the other hand, fluorescence spectra were recorded in the same condition. The excitation

of all carbazole side chain donor monomers at the absorption maxima (λ_{max}=292 nm) resulted in two distinct emission band at about 350 and 365 nm, respectively. As a result of differentiated in the spacer moiety between polymer chain and photoactive carbazole group, the emission intensity of PCEA was observed as about two times grater than that of the others.

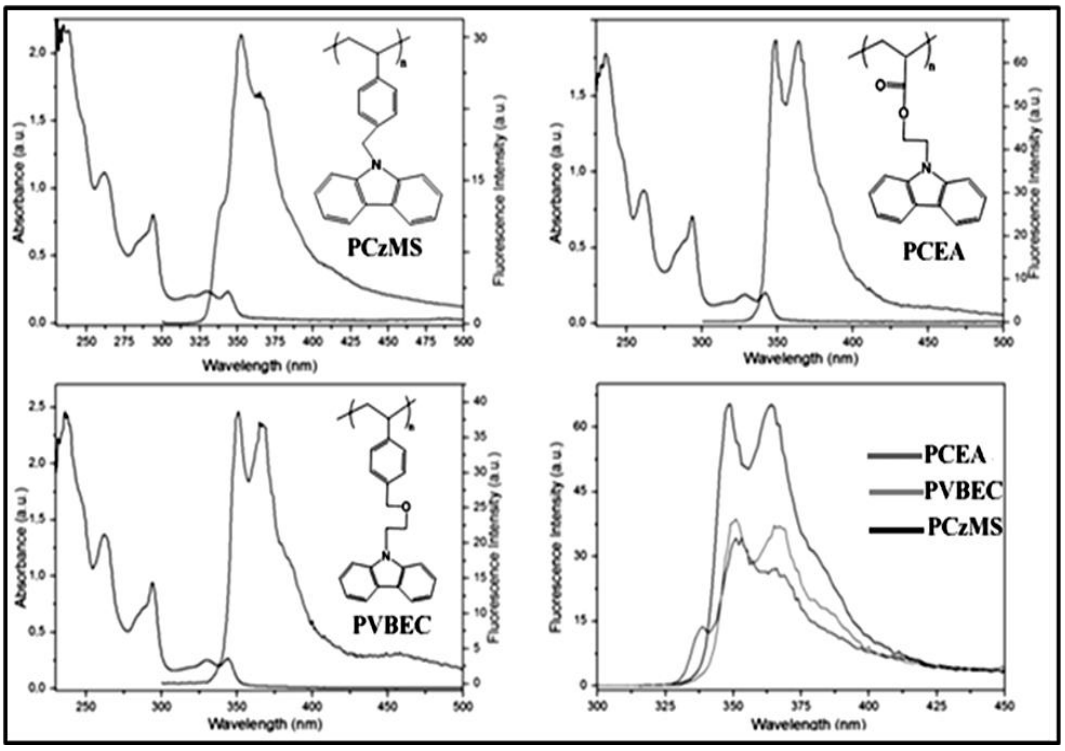

Figure 4.63 : UV-Vis and fluorescence of PCzMS, PCEA and PVBEC.

On the other hand, acceptor polymers bearing napthalimide moiety exhibits two main absorption peaks at about 273, 398 nm attributed to naphthalimide moietie. Napthalimide chromophore containing electron donating substitutents (i.e, -OR or -N-R_2) typically have charge transfer band in the UV-vis absorption spectra that are red shifted in liquid phase. Due to tert-amine moiety is directly attached onto acceptor-napthalimide chromophore, the charge transfer band was observed at about 398 nm. The energy transfer ability of this system on the basis of the absorption spectra by comparing with the photo-luminescence spectra of PVBEC, PAM and their copolymer (poly(VBEC-*r*-AM)) was investigated (Figure 4.64). The excitation of PVBEC at its absorption maxima (max= 292 nm) resulted in two distinct emission bands at 351 and 362 nm. Besides, when PAM was excited at the absorption maxima (λ_{max} =399 nm), it exhibited a strong emission band at 504 nm that is a Stokes' shift of 105 nm. When poly(VBEC-*r*-AM) is excited at the same wavelengths, a band at

504 nm was observed in the photo-luminescence spectra. On the other hand, upon the excitation of poly(VBEC-*r*-AM) at 292 nm (carbazole absorbtion), two distinct emission bands were observed at 358 and 504 nm and these distinct bands are attributed to carbazole and napthalimide moiety. When the excitation of poly(VBEC-*r*-AM) bathochromically shifted (i.e. 328, 346 and 399), these bands are almost completely quenched when compared to 292 nm excitation-emission band. The exitation overall, these intensified band proved that energy transfer from donor moiety (carbazole) to acceptor part (napthalimide) on the copolymer structure.

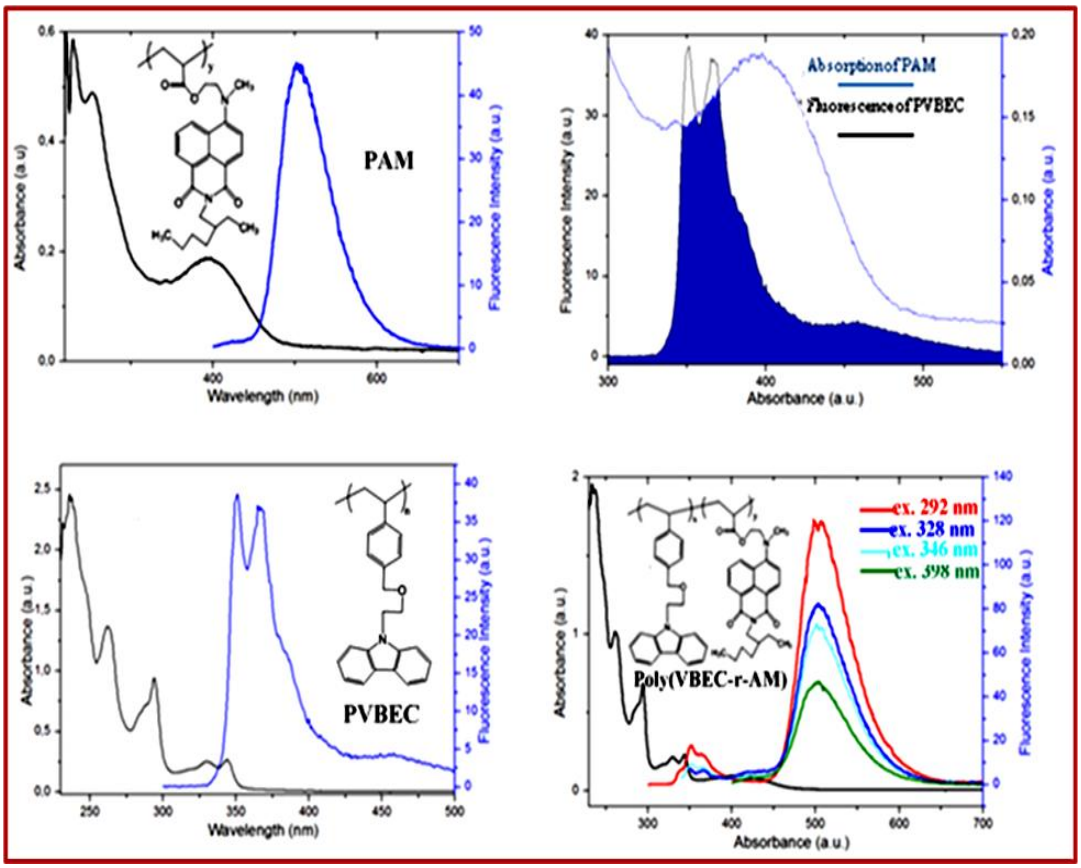

Figure 4.64 : UV-Vis and fluorescence of PAM, PVBEC and poly(VBEC-*r*-AM).

Overall these results, the electrochemical and optical HOMO-LUMO band gap of all polymers calculated from the onset of oxidation/reduction peaks potentials and absorbtion onset values were presented in Table 4.1.

Table 4.1 : HOMO and LUMO energy levels, electrochemical ($E_g^{'}$) and optical band gaps (E_g) values of donor and acceptor polymers.

Molecule	Peak potentials (V) Reduced group 1,8-Napthalimide (C=O)	Peak potentials (V) Oxidized group Carbazole (Ring)	HOMO (eV)	LUMO (eV)	$E_g^{'}$, Electrochemical Band Gap (eV)	E_g, Optical Band Gap (eV)
PCzMS	-	1.34	-5.62	-2.07[a]	-	3.55
PCEA	-	1.16	-5.43	-1.88[a]	-	3.55
PVBEC	-	1.17	-5.46	-1.91[a]	-	3.55
PAM	-1.50 and -1.60 *Reversible*	1.23[b]	-5.39	-3.07	2.32	2.54
Poly(VBEC-*r*-AM)	-1.48 and -1.60 *Reversible*	1.30	-5.41	-2.97	2.44	2.87
Poly(CzMS-*r*-AM)	-1.49 and 1.57 *Reversible*	1.34	-5.46	-2.97	2.49	2.72

[a]Calculated by the subtraction of the optical band gap from the HOMO level of (PCzMS, PCEA, PVBEC)
[b] This peak attributed to tert-amine moiety

4.5 Spectroelectrochemical properties of carbazol side chain donor polymers

Owing to spectro-electrochemical measurements, both the electronic structure and optical behavior of carbazole based carbazol side chain donor polymers coated ITO/glass surface via electrochemical process upon p-doping process can be explained. It observed that all carbazol side chain donor polymers polymers have similar electrochromic behavious because of containing carbazole pending units on the polymer main chain. Upon incremental oxidative scans from 0 to 2.0 V, the valence-conduction band (π–π* transition) at about 448 nm is initially intensified (<1.2 V) and then dramatically bleached at higher potentials (> 1.2 V). Furthermore, at low doping levels, an increase in the absorbance at 972 nm (0-1.2 V) was observed corresponding to the formation of polaron. At higher oxidation levels (1.2-1.7 V), a new broad absorption band started to intensify, which indicates the formation of bipolaronic states on the polymer film at 690 nm that extends into the IR region (Figure 4.65). The observed colors during *p*-doping of the polymer film at neutral (0 V), intermediate (1.2 V) and the over-oxidized (1.7 V) states were indexed according to Commision Internationale de I'Eclairage (CIE) and the colors with their

parameters were transparent (Luminance L = 91, hue a = –8, and saturation b = 5), yellowish green (L: 87; a: –59; b: 83), green *(L:45; a: –46; b:42)* and dark blue *(L:16; a: –21; b:11)*, respectively (Tablo 4.2).

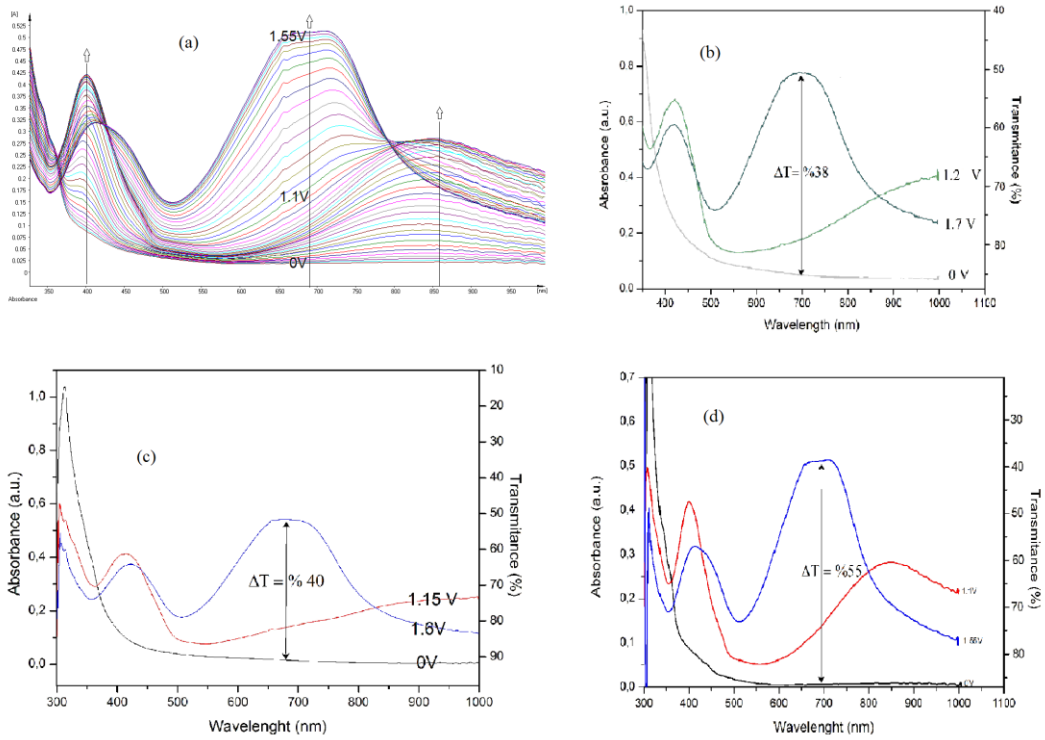

Figure 4.65 : a) Absorbtion band chances of PVBEC upon applient potential b) spectroelectrochemical behaviour of PCzMS c) spectroelectrochemical behaviour of PCEA d) spectroelectrochemical behaviour of PVBEC.

Double step chronoamperometry technique was used to monitor the changes in the electro-optical responses during switching (kinetic study). Electrochromic parameters of the polymer film was analyzed by changes that occurred in the transmittance (increments of the absorption band at 690 nm with respect to time) while switching the potential step wisely between neutral and oxidized states with a residence time of 10 s. Although carbazol side chain donor polymers have similar electrochemical and optical properties, all electrochromic parameters (ie. Response time, contrast change …) were effected by the differentiated to the spacer groups between carbazole-electroactive moiety and polymer chain (Table 4.1).

Table 4.2 : Electrochromic parameters PCzMS, PCEA and PVBEC.

Molecules	Optical Contrast Change (ΔT%)			Responce time (s)	Optical activity after 1000 cycles (%)	CIE color parameters *Luminance (L), hue (a), saturation (b)*	Coloration efficiency, (cm^2 C^{-1})
	420 nm	**700 nm**	**950 nm**				
X-PCzMS	ΔT : 23% T_{neut} : 78% T_{oxi} : 55%	ΔT : 38% T_{neut} : 90% T_{oxi} : 52%	ΔT : 21% T_{neut} : 92% T_{oxi} : 71%	*Oxidation* 3.4 *Reduction* 4.1	32.2	Neutral state *L: 92.5; a:-1; b:11.6* Intermediate state *L:82.6; a:-16.1; b:31* Oxidized state *L:69.6; a:-26.3; b:7.8*	210
	415 nm	**700 nm**	**930 nm**				
X-PCEA	ΔT : 28% T_{neut} : 89% T_{oxi} : 61%	ΔT : 40% T_{neut} : 91% T_{oxi} : 51%	ΔT : 19% T_{neut} : 92% T_{oxi} :73%	*Oxidation* 4.8 *Reduction* 6.2	41.1	Neutral state *L:97.3; a:-0.57; b:4.6* Intermediate state *L:91.7; a:-10.5;b:23.65* Oxidized state *L:78.5; a:-22.3; b:4.4*	218
	400 nm	**690 nm**	**850 nm**				
X-PVBEC	ΔT : 35% T_{neut} : 80% T_{oxi} : 45%	ΔT : 55% T_{neut} : 94% T_{oxi} : 39%	ΔT : 34% T_{neut} : 94% T_{oxi} : 60%	*Oxidation* 2.1 *Reduction* 2.6	64.3	Neutral state *L:97.8; a:-0.5; b:3.5* Intermediate state *L:94.3; a:-8.1; b:17.9* Oxidized state *L:81.2; a:-21.3; b:4.2*	331

5. CONCLUSION

First of all, carbazole and napthlamide side chain containing styrenic and acrylate type monomers with different chain lengths (CzMS, CEA, VBEC, AM) were synthesized according to the literature and characterized by ^{1}H NMR, FT-IR, DSC.

The polymerizations of 4-(9-carbazolyl) methylstyrene (CzMS) were carried out via ATRP. However, according to ^{1}H NMR and GPC results, the polymer were not obtained. Then the iniferter method was applied but again the polymerization is not proceeded. Due to unsuccessfull result were obtained by the application of controlled radical polymerization, CzMS and the other monomers (CEA, VBEC and AM) were polymerized via free radical polymerization. Polymers were characterized by ^{1}H NMR, FT-IR, GPC and DSC.

Copolymer (poly(CzMS-*r*-AM)) of AM with CzMS was synthesized via free radical polymerization and characterized by ^{1}H NMR, FT-IR, DSC, GPC. Copolymer fractions of AM and CzMS calculated by ^{1}H NMR. Although $(n_{AM})/(n_{CzMS})$ ratio was 0.33 in theoretical, the copolymer fraction was found as F1= 0.177 and F_2= 0.823, where F_1 and F_2 are the contents of AM and CzMS units, respectively, in the copolymer chain. The calculated T_g value from Fox equations is compared with observed T_g value from DSC curves. The observed T_g value is 128.3 ^{o}C for poly(CzMS-*r*-AM which has quite good matching with theoretical one calculated from Fox equations as 126.8 ^{o}C.

Copolymer (poly(VBEC-*r*-AM)) of AM with VBEC was synthesized via free radical polymerization and characterized by ^{1}H NMR, FT-IR, DSC, GPC. Copolymer fractions of AM and VBEC calculated by ^{1}H NMR. Although $(n_{AM})/(n_{VBEC})$ ratio was 1 in theoretical, the copolymer fraction was found as F_1= 0.39 and F_2= 0.61, where F_1 and F_2 are the contents of AM and VBEC units, respectively, in the copolymer chain. The calculated T_g value from Fox equations is compared with observed T_g value from DSC curves. The observed T_g value is 55.4 ^{o}C for poly(VBEC-*r*-AM) which has quite good matching with theoretical one calculated from Fox equations as 57.3 ^{o}C.

The electrochemical properties of carbazole side chain donor polymers were investigated by cyclic voltammetry (CV). PCzMS exhibited an semi reversible oxidation peak at $E^{ox}_{m,a}$ = +1.30V and $E^{ox}_{m,c}$ = +0.96 V; $E^{ox}_{m,1/2}$ = +1.13V during an anodic scan, and this oxidation potential is higher than that of PCEA and PVBEC (semi reversible; $E^{ox}_{m,a}$ = +1.19V and $E^{ox}_{m,c}$ = +0.75V; $E^{ox}_{m,1/2}$ = +0.97V for PCEA and semi reversible; $E^{ox}_{m,a}$ = +1.19V and $E^{ox}_{m,c}$ = +0.73V; $E^{ox}_{m,1/2}$ = +0.96V for PVBEC). As expected, this result indicated that PCEA and PVBEC has a more electron rich nature than PCzMS when including the etoxy based spacer moiety in a similar system.

The absorption spectra of PCzMS, PCEA and PVBEC were recorded in the solution phase using dichloromethane. As a result of differentiated in the spacer moiety between polymer chain and photoactive carbazole group, the emission intensity of PCEA was observed as about two times grater than that of the others two.

Furthermore, although carbazol containing polymers have similar electrochemical and optical properties, all electrochromic parameters (ie. Response time, contrast change …) were effected by the differentiated to the spacer groups between carbazole-electroactive moiety and polymer chain.

The energy transfer ability of this system on the basis of the absorption spectra by comparing with the photo-luminescence spectra of PVBEC, PAM and their copolymer (poly(VBEC-*r*-AM)) was shown that the energy transfer from donor moiety (carbazole) to acceptor part (napthalimide) on the copolymer structure (poly(VBEC-*r*-AM)) was proved with the all exitation and intensified band.

X-PVBEC was shown shorter response time than X-PCzMS and X-PCEA. X-PVBEC was shown higher optical contrast changes than X-PCzMS and X-PCEA (at around 410, 700 and 910 nm). PVBEC was shown lower oxidation potantial of than PCzMS and PCEA. Higher fluorescence intensity for Poly(VBEC-r-AM) was observed at 292 nm. Both copolymers were shown moderately lower band gaps.

REFERENCES

[1] **Valeur, B.**, 2002. *Molecular Fluorescence Principles and Applications*. WILEY-VCH: Weinheim, p 3-123.

[2] **Wardle, B.**, 2009. *Principles and Applications of Photochemistry*. John Wiley & Sons, Ltd: Cornwall, p 29-117.

[3] **Jiun-Haw Lee, D. N. L., Shin-Tson Wu**, 2008. *Introduction to Flat Panel Displays*. JohnWiley & Sons Ltd: p 177-187.

[4] **Fritz Vögtle, G. R. a. N. W.**, 2009. *Dendrimer Chemistry*. WILEY-VCH Verlag GmbH & Co.: Weinheim, p 169-192.

[5] **Neuteboom, E. E.; van Hal, P. A.; Janssen, R. A. J.**, 2004. Donor-Acceptor Polymers: A Conjugated Oligo(P-Phenylene Vinylene) Main Chain with Dangling Perylene Bisimides. *Chemistry-a European Journal,* **10**, (16), 3907-3918.

[6] **Tzong-Liu Wang, A.-C. Y., Chien-Hsin Yang, Yeong-Tarng Shieh, Wen-Janq Chen, Tsung-Han Ho**, 2011. Synthesis and Photovoltaic Properties of a Low Band Gap Donor–Acceptor Alternating Copolymer with Benzothiadiazole Unit. *Solar Energy Materials & SolarCells,* **95**, 3295-3302.

[7] **Shuang Lia, Z. H., Aoshu Zhonga, Jian Yua, Hongbin Wub, Yue Zhoua, Su'an Chena, Cheng Zhonga,; Jingui Qina, Z. L.**, 2011. New Alternating Copolymers of Fluorene and Triphenylamine Bearing Terthiophene and Acceptor Groups in the Side Chains: Synthesis and Photovoltaic Properties. *Polymer,* **52**, 5302-5311.

[8] **Lihui Guo, J. D., Lirong Zhang, Qian Xiu, Gaojun Wen, Chaofan Zhong**, 2012. Synthesis and Applications of 3,6-Carbazole-Based Conjugated Side-Chain Copolymers Containing Complexes of 1,10-Phenanthroline with Zn(Ii), Cd(Ii) and Ni(Ii) for Dye-Sensitized Solar Cells. *Dyes and Pigments,* **92**, 1062-1068.

[9] **Taranekar, P.; Fulghum, T.; Baba, A.; Patton, D.; Advincula, R.**, 2007. Quantitative Electrochemical and Electrochromic Behavior of Terthiophene and Carbazole Containing Conjugated Polymer Network Film Precursors: Ec-Qcm and Ec-Spr. *Langmuir,* **23**, (2), 908-917.

[10] **Fang, Y.-K.; Liu, C.-L.; Chen, W.-C.**, 2011. New Random Copolymers with Pendant Carbazole Donor and 1,3,4-Oxadiazole Acceptor for High Performance Memory Device Applications. *Journal of Materials Chemistry,* **21**, (13), 4778-4786.

[11] **Bagheri, M.; Entezami, A.**, 2002. Synthesis of Polymers Containing Donor-Acceptor Schiff Base in Side Chain for Nonlinear Optics. *European Polymer Journal,* **38**, (2), 317-326.

[12] **Haridharan, N.; Dhamodharan, R.**, 2011. Controlled Polymerization of Carbazole-Based Vinyl and Methacrylate Monomers at Ambient Temperature: A Comparative Study through Atrp, Set, and Set-Raft Polymerizations. *Journal of Polymer Science Part a-Polymer Chemistry,* **49**, (4), 1021-1032.

[13] **Mori, H.; Nakano, S.; Endo, T.**, 2005. Controlled Synthesis of Poly(N-Ethyl-3-Vinylcarbazole) and Block Copolymers Via Raft Polymerization. *Macromolecules,* **38**, (20), 8192-8201.

[14] **Simionescu, C. I.; Percec, V.**, 1979. New Carbazole-Containing Monomers and Polymers. *Journal of Polymer Science Part a-Polymer Chemistry,* **17**, (8), 2287-2297.

[15] **Bottle, S.; Busfield, W. K.; Jenkins, I. D.; Thang, S.; Rizzardo, E.; Solomon, D. H.**, 1989. The Mechanism of Initiation in the Free-Radical Polymerization of N-Vinylcarbazole and N-Vinylpyrrolidone. *European Polymer Journal,* **25**, (7-8), 671-676.

[16] **Brar, A. S.; Kaur, S.**, 2006. Atom Transfer Radical Polymerization of N-Vinyl Carbazole: Optimization to Characterization. *Journal of Polymer Science Part a-Polymer Chemistry,* **44**, (5), 1745-1757.

[17] **Babazadeh, M.**, 2006. Thermal Stability and High Glass Transition Temperature of 4-Chloromethyl Styrene Polymers Bearing Carbazolyl Moieties. *Polymer Degradation and Stability,* **91**, (12), 3245-3251.

[18] **Zhang, W.; Yan, Y.; Zhou, N.; Cheng, Z.; Zhu, J.; Xia, C.; Zhu, X.**, 2008. Controlled Synthesis and Fluorescent Properties of Poly(9-(4-Vinylbenzyl)-9h-Carbazole) Via Nitroxide-Mediated Living Free-Radical Polymerization. *European Polymer Journal,* **44**, (10), 3300-3305.

[19] **Uryu, T.; Ohkawa, H.; Oshima, R.**, 1987. Synthesis and High Hole Mobility of Isotactic Poly(2-N-Carbazolylethyl Acrylate). *Macromolecules,* **20**, (4), 712-716.

[20] **Keyanpourrad, M.; Ledwith, A.; Hallam, A.; North, A. M.; Breton, M.; Hoyle, C.; Guillet, J. E.**, 1978. Some Photophysical Properties of 5 New Carbazole-Containing Methacrylate Polymers. *Macromolecules,* **11**, (6), 1114-1118.

[21] **Grazulevicius, J. V.; Strohriegl, P.; Pielichowski, J.; Pielichowski, K.**, 2003. Carbazole-Containing Polymers: Synthesis, Properties and Applications. *Progress in Polymer Science,* **28**, (9), 1297-1353.

[22] **Sato, M.; Kawata, A.; Morito, S.; Sato, Y.; Yamaguchi, I.**, 2008. Preparation and Properties of Polymer/Zinc Oxide Nanocomposites Using Functionalized Zinc Oxide Quantum Dots. *European Polymer Journal,* **44**, (11), 3430-3438.

[23] **Wei, Y.; Gao, D.; Li, L.; Shang, S.**, 2011. Memory Effect in Polymer Brushes Containing Pendant Carbazole Groups. *Polymer,* **52**, (6), 1385-1390.

[24] **Bardajee, G. R.; Li, A. Y.; Haley, J. C.; Winnik, M. A.**, 2008. The Synthesis and Spectroscopic Properties Fluorescent Naphthalimide of Novel, Functional Dyes. *Dyes and Pigments,* **79**, (1), 24-32.

[25] **Bouche, C. M.; Le Barny, P.; Facoetti, H.; Soyer, F.; Robin, P.**, 1998. Electroluminescent Properties of Side-Chain Naphthalimide-Derivated Polymers. *Journal De Chimie Physique Et De Physico-Chimie Biologique,* **95**, (6), 1351-1354.

[26] **Tian, H.; Zhu, W. H.; Elschner, A.**, 2000. Single-Layer Electroluminescence Device Made with Novel Copolymers Containing Electron- and Hole-Transporting Moieties. *Synthetic Metals,* **111**, 481-483.

[27] **Kukhta, A.; Kolesnik, E.; Grabchev, I.; Sali, S.**, 2006. Spectral and Luminescent Properties and Electroluminescence of Polyvinylcarbazole with 1,8-Naphthalimide in the Side Chain. *Journal of Fluorescence,* **16**, (3), 375-378.

[28] **Chen, B. J.; Liu, Y. Q.; Lee, C. S.; Yu, G.; Lee, S. T.; Li, H. Y.; Gambling, W. A.; Zhu, D. B.; Tian, H.; Zhu, W. H.**, 2000. Carrier Transport and High-Efficiency Electroluminescence Properties of Copolymer Thin Films. *Thin Solid Films,* **363**, (1-2), 173-177.

[29] **Hu, C.; Zhu, W. H.; Lin, W. Q.; Tian, H.**, 1999. Synthesis and Luminescence of Novel Emitting Copolymers. *Synthetic Metals,* **102**, (1-3), 1129-1130.

[30] **Vijay K. Varadan, K. J. V., S. Gopalakrishnan**, 2006. *Smart Material Systems and Mems: Design and Development Methodologies*. England, p 1-40.

[31] **Mikhail A. Vorotyntsev, V. A. Z., and Dmitry V. Konev**, 2010. Mechanisms of Electropolymerization and Redox Activity: Fundamental Aspects, In *Electropolymerization Concepts, Materials and Applications*, pp.51-70, Eds. Karyakin, S. C. a. A., WILEY-VCH Verlag & Co. KGaA, Weinheim.

[32] **Farah, A. A.; Pietro, W. J.**, 2005. Synthesis and Characterization of Multifunctional Polymers Via Atom Transfer Radical Polymerization of N-(Omega '-Alkylcarbazolyl) Methacrylates Initiated by Ru(Ii) Polypyridyl Chromophores. *Journal of Polymer Science Part a-Polymer Chemistry,* **43**, (23), 6057-6072.

[33] **Evanoff, D. D., Jr.; Carroll, J. B.; Roeder, R. D.; Hunt, Z. J.; Lawrence, J. R.; Foulger, S. H.**, 2008. Poly(Methyl Methacrylate) Copolymers Containing Pendant Carbazole and Oxadiazole Moieties for Applications in Single-Layer Organic Light Emitting Devices. *Journal of Polymer Science Part a-Polymer Chemistry,* **46**, (23), 7882-7897.

[34] **Liu, Y.; Li, N.; Xia, X.; Xu, Q.; Ge, J.; Lu, J.**, 2010. Worm Memory Devices Based on Conformation Change of a Pvk Derivative with a Rigid Spacer in Side Chain. *Materials Chemistry and Physics,* **123**, (2-3), 685-689.

[35] **Amamoto, Y.; Kikuchi, M.; Masunaga, H.; Sasaki, S.; Otsuka, H.; Takahara, A.**, 2009. Reorganizable Chemical Polymer Gels Based on Dynamic Covalent Exchange and Controlled Monomer Insertion. *Macromolecules,* **42**, (22), 8733-8738.

CURRICULUM VITAE

Name Surname: Damla GÜLFİDAN

Place and Date of Birth: İstanbul, 29.12.1985

Address: Mevlanakapı Mah. Selamağası Sok. Yiğit Apt. No:32/1 Şehremini/İST

E-Mail: damlagulfidan@hotmail.com

B.Sc.: Chemist, Çanakkale Onsekiz Mart University

Professional Experience and Rewards:

- MPOL (Start-up company in ITU-KOSGEB, Researcher, (02.12.2010-...)
- ITU (Student assistant) (28.09.2009-01.01.2010)
- Organizing Committe Member, "2nd International Symposium Controlled/Living Polimerization: From Synthesis to Applicatons, CLP'11, April 12-16, 2011, Antalya, Turkey.

PUBLICATIONS/PRESENTATIONS ON THE THESIS

▪ Damla Gulfidan, Emre Sefer, Ayhan Oral, Sermet Koyuncu, Metin Hayri Acar, 2011: Synthesis of Donor/Acceptor Containing Monomers. *2nd International Symposium Controlled/Living Polimerization: From Synthesis to Applicatons*, April 12-16, 2011, Antalya, Turkey.

▪ Damla Gulfidan, Emre Sefer, Ayhan Oral, Sermet Koyuncu, Metin Hayri Acar, 2012: Donör-Akseptör İçeren Polimerler Sentezi. *1.ARGE Proje Pazarı,* January 27-28, 2012, İstanbul, Turkey.